Reactive transport modelling within the bentonite backfill of a deep nuclear waste repository

Comparing the migration of radionuclides through FEBEX (Spain) and MX-80 (Switzerland) bentonite taking into account sorption competition effects

A thesis submitted to

Escola Tècnica Superior d'Enginyeria Industrial de Barcelona

Universitat Politècnica de Catalunya

performed at

Laboratory for Waste Management

Nuclear Energy and Safety Research Department

Paul Scherrer Institut, Switzerland

supervised by

Dr. Wilfried Pfingsten, Paul Scherrer Institut

Dr. Javier Dies, Universitat Politècnica de Catalunya

presented by

Albert Riera Boadas

Barcelona, March 2014

"Will there be anybody around to check the

validity of our safety assessments?"

Hummel, W., November 2013 during a lecture of the Master of Science in Nuclear Engineering at ETH Zurich

Models, results and conclusions will be presented at the **III TrePro workshop** about Reactive Transport Modeling organized by the **Karlsruhe Institut of Technology** from 5th to 7th March 2014 in Karlsruhe, Germany.

Abstract

The geological repository is, by international consensus, the final destination for radioactive waste that cannot be permanently stored on the surface for a period of time during which security and stability can be ensured. A first aim of this thesis is to get closer to the radioactive waste management policy in Switzerland, as an example of an advanced policy worldwide in which long-term storage in deep geological formations is close to become a reality. With it, the foreseen design of this repository will be detailed, where the engineered barrier of bentonite will start playing a major role.

For safety assessments of high level waste repositories, the understanding of radionuclide sorption is essential. This sorption is directly related to the transport media, which leads to the second aim of this project: comparing FEBEX to MX-80, the foreseen bentonite types that will be used, respectively, in the Spanish and Swiss geological repositories. After a number of calculations, FEBEX eventually turned out to have a better capacity to retain radionuclides, so it would be more recommendable for a repository.

For these calculations reactive transport models are used. MCOTAC is a state-of-the-art code developed at PSI, which couples chemical reactions and transport processes. For performing consistently this calculations, robust FEBEX and MX-80 bentonite models are necessary. An important part of this thesis consist on the setup of these models, at real-scale dimensions, whose robustness is a prior aim. This models will be afterwards available for further research projects.

Moreover, for reactive transport calculations, data coming from the Linear Free Energy Relationships (Bradbury & Baeyens, [19]) is usually used. These relationships are accompanied by an uncertainty for values of the surface complexation constants. Therefore, an analysis about the propagation of this uncertainty is necessary and demonstrated in this thesis, although apparently would not be very significant for safety assessments of a nuclear waste repository (it could become important for other applications).

Eventually, the results from batch sorption experiments on Montmorillonite have demonstrated that bivalent transition metals compete for sorption sites. For safety assessments of geological repositories with compacted bentonite near fields, competitive sorption of radionuclides has to be assessed, which is another aim of this thesis. Significant influence of this competition has been found, more relevant for FEBEX than for MX-80 due to their intrinsic characteristics. Ni(II) is used as tracer for all calculations, as an example of bivalent metal (with radioactive isotopes) leaching from the canister competing for sorption sites with the saturated concentration of Fe(II) in bentonite.

Table of contents

List of figures

List of tables

Notation

For the reader, these writing abbreviations and linking resources have been frequently used along the thesis:

Fig. : Figure.

[Reference number]: Reference or source detailed at the references section in the end of the thesis.

i.e.: that is

e.g.: for example

In addition, technical notation is also used:

≡: Surface complexation reactions are usually written with a "site ligand" **≡**

≡SOH: Surface Hydroxyl group as site ligand, to write surface complexation reactions (or ≡OH)

[A]: Concentration of element/species A

{A} :Activity of element/species A

CEC: Cation Exchange Capacity

NPP: Nuclear Power Plant

PWR: Pressurized Water Reactor

BWR: Boiling Water Reactor

HLW: High Level Waste

ILW: Intermediate Level Waste

LLW: Low Level Waste

SF: Spent Fuel

PSI: Paul Scherrer Institut

LES: Laboratory for Radioactive Waste

wt.% Percentage of weight

Nagra: Swiss National Cooperative for the Disposal of Radioactive Waste

Enresa: Empresa Nacional de Residuos Radiactivos S.A.

ATC: Almacén Temporal Centralizado

RTI: Radiotoxicity Index

1 Preface

1.1 Project origin

From February to August 2013 the author was enrolled in the Master of Science in Nuclear Engineering, at ETH Zurich, as Erasmus exchange student. One of the most general courses was "Nuclear Energy Systems", in which radioactive waste management was addressed as part of the fuel cycle. Moreover, Switzerland is quite active in research regarding radioactive waste management.

After he showed his interest for the radioactive waste management field, came up the possibility to perform the Final Project (PFC) in Industrial Engineering (author's studies) supporting the research line of Dr. Wilfried Pfingsten, supervisor of this thesis, at the Laboratory for Waste Management of the Paul Scherrer Institut.

1.2 Motivation

A first motivation was to get familiarized with the advanced radioactive waste management policy in Switzerland compared to the different policies worldwide, and with the corresponding necessary criteria and calculations involved in the safety assessments for the Swiss concept of radioactive waste repository in deep geological formations.

Furthermore, a precise prediction of the transport of radionuclides through the multiple barriers of the geological repository is a determinant factor of these safety assessments, and the PSI is quite active in research to improve predictions of this issue, working closely with Nagra.

Off-topic motivations were to get in touch with a research working environment in such an important institute like the PSI, and to live and work abroad for personal and professional growing.

2 Introduction

Switzerland has currently five nuclear reactors in operation. Spain, 7. Therefore, both countries have to manage with the radioactive waste. Despite they currently have different radioactive waste management policies, both recognize that the repository in deep geological formations will become at some point necessary. Actually, the geological repository is, by international consensus, the final destination for radioactive waste that cannot be stored permanently on the surface for a period of time during which the security and stability required by the regulatory bodies can be ensured.

At the moment Switzerland is more active in research and has more advanced policies in this direction, led by Nagra and working together with the Paul Scherrer Institut –where this thesis was developed–. Spain, with Enresa in front, also developed research projects related with the deep geological repository (even at Swiss laboratories, like the FEBEX project), although they currently do not continue, since the "General Plan of Radioactive Waste" [21] gathers its efforts in the centralized interim storage (ATC).

A first aim of this thesis is to introduce the reader to the current radioactive waste management concept and policy in Switzerland, also with references to the Spanish, as representative stages of policies worldwide. After, the attention is zoomed in the geological repository concept of Switzerland, to focus the thesis on the study of the migration of radionuclides through the barriers containing the High Level Waste and the Spent Fuel – specifically, the bentonite buffer. The understanding of the migration processes of radionuclides in bentonite is necessary as part of the safety assessments, since after 10000 years of containment in steel canisters, the radionuclides will leach out of the waste matrix.

In Nagra's publications (e.g. [1]) it is specified that a called MX-80 bentonite will be used for the Swiss repository concept. In Spain, Enresa revealed in previous work ([2]) that the chosen bentonite for its repository concept is the called FEBEX bentonite. These bentonites have different constitutional features that will affect differently to the migration of radionuclides and will make them more or less suitable for the geological repository.

For safety assessments, due to the impossibility to carry out real time scale experiments, considerable amount of work has been carried out over the past several years to develop sorption models capable of predicting the sorption of radionuclides on clay minerals (e.g. bentonite): the Kd model is the most popular method and will be explained and used for the calculations. However it has some important drawbacks and therefore it is supported by much more complex models called reactive transport. For this thesis a reactive transport code called MCOTAC, developed at the PSI (Pfingsten, W., 1996 [3], 2002 [4], 2010 [5]) and which couples chemical equilibrium and transport processes according to the 2SPNE SC/CE formalism (Bradbury, M. & Baeyens, B.; [3], [4]) for radionuclides and major ions, will be used for the comparison of MX-80 against FEBEX. An important part of the thesis consist on the setup of these bentonite models, with the pertinent calibration and at real-scale dimensions.

With these models already prepared, MCOTAC will run a set of calculations. Each calculations lasts about 6 hours. The results of these calculations will be used firstly to compare the Swiss and the Spanish bentonites foreseen for the deep repository.

Besides, an analysis that may concern the reactive transport modelers' community worldwide is carried out. It is the study of the propagation of the Linear Free Energy Relationships (Bradbury & Baeyens, [19]) uncertainty to reactive transport calculations (section 6). The reason of this actually very necessary analysis is to support the research line of Dr. Pfingsten, W., and by extension the Laboratory for Radioactive Waste at the PSI, in their aim to improve and support the safety assessments of the geological repository made by Nagra.

Another purpose of this project is the assessment of competition phenomena for sorption sites that the high Fe(II) concentrations in bentonite have to the sorption of Ni(II), as an example of a bivalent transition metal leaching from the waste into the bentonite backfill. The one dimensional calculations were performed with MCOTAC at different Ni(II) equilibrium concentrations at the boundary and in different conditions.

3 Overview: radioactive waste management

3.1 Classification of radioactive waste and disposal

According to the International Atomic Energy Agency (IAEA) [5] the radioactive waste can be classified following in 6 categories ([5]).

Exempt waste

Waste that meets the criteria of exemption, clearance or exclusion as described in Ref. [6].

Very short lived waste (VSLW)

Can be stored for decay over a limited period of up to a few years and then cleared for uncontrolled disposal, use or discharge. Waste with short half-live radionuclides used for research and medical purposes would be included.

Very low level waste (VLLW)

Waste that does not need a high level of containment and isolation and, therefore, can be disposed in near surface landfill facilities with limited regulatory control. For example, soil or rubble with low activities would be VLLW.

Low level waste (LLW)

Waste that is above clearance levels with limited number of long lived radionuclides. It requires robust containment for periods of a few hundreds of years and is suitable for disposal in engineered near surface facilities. This class covers a very broad range of waste. LLW may include not only short lived radionuclides at high activities but also long lived radionuclides at relatively low activity levels.

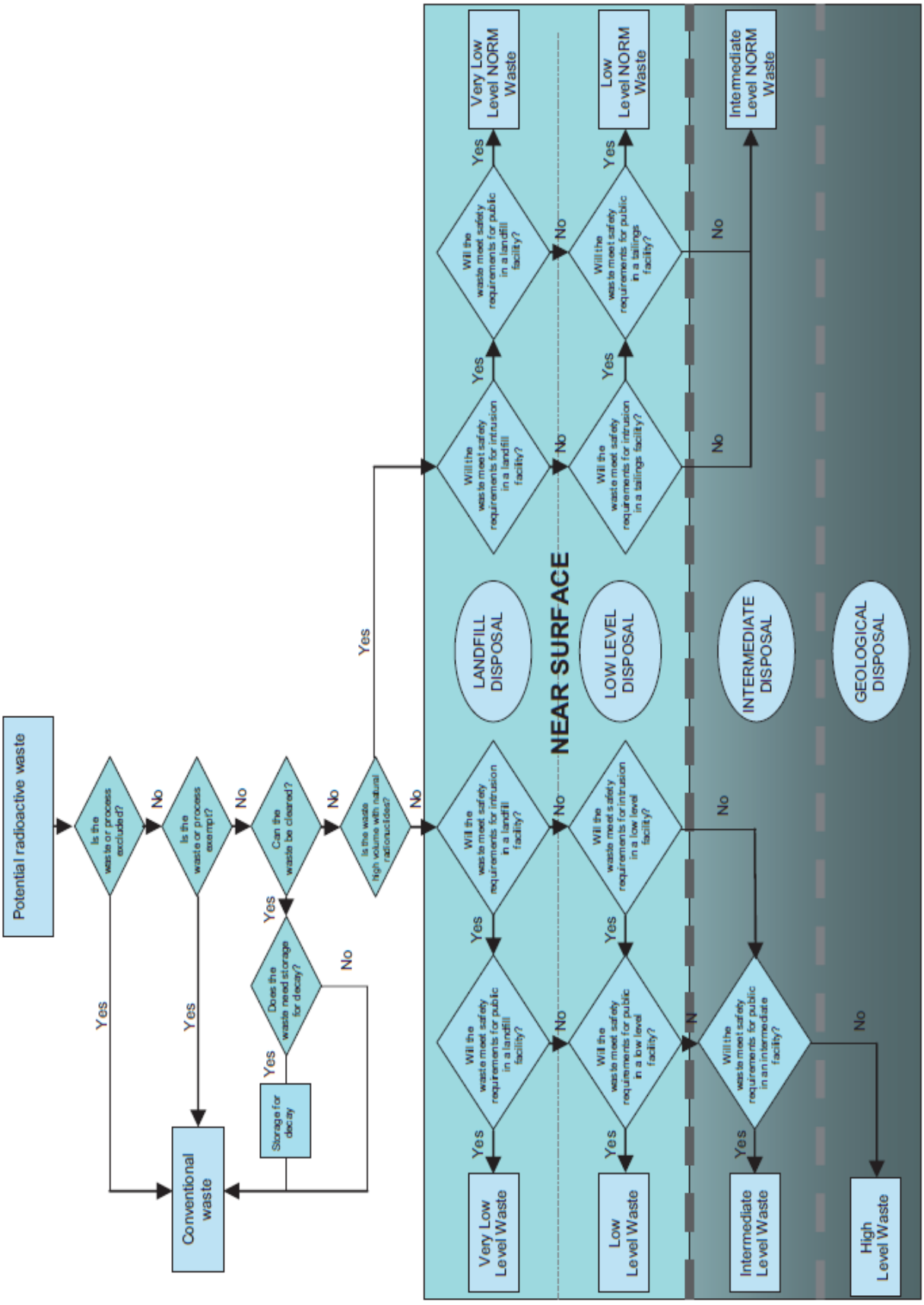

Fig. 1 Classification criteria of the radioactive waste, related to its disposal. [5]

Intermediate level waste (ILW)

This waste consist on long lived radionuclides, so it requires a higher level of containment and isolation than a near surface disposal. Nevertheless, ILW does not need any provision (or only limited) for heat dissipation during its storage and disposal. ILW may contain long lived radionuclides (alpha emitting) that will not reach a level of activity concentration as low as to be acceptable for near surface disposal during the time that "reliable control" will be managed. Therefore, waste in this class requires disposal at higher depths (tens of meters to a few hundreds)

High level waste (HLW)

This waste has levels of activity concentration high enough to produce significant quantities of heat by the radioactive decay or has large quantities of long lived radionuclides. Disposal in deep (several hundreds of meters) and stable geological repositories is the disposal option for this class.

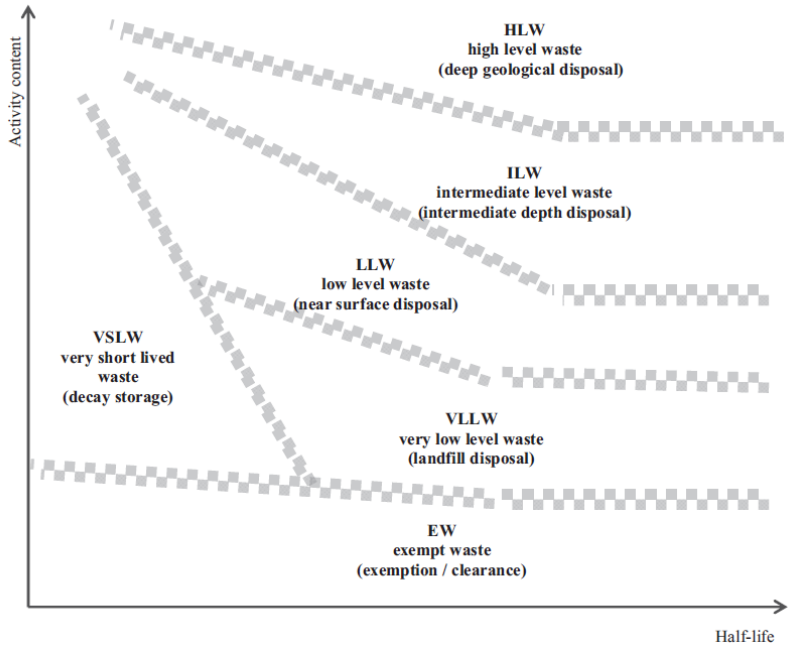

Fig. 2 Qualitative classification of the radioactive waste. [5]

For more details about this classification, please see reference [5] and related.

3.2 Radioactive waste management in Switzerland

In Switzerland, the producers of radioactive waste are responsible for its safe disposal. The Swiss disposal concept sees the final solution as the long-term storage of radioactive waste in repositories located in suitable rock formations. To figure out other current and future national policies like reprocessing or direct disposal, in [20] a useful comparison table is available.

3.2.1 Categorization of radioactive waste for its waste management in Switzerland

Spent fuel (HLW)

During the operation of a NPP, highly radioactive substances are generated in the fuel elements. The so-called spent fuel has to be replaced after a period of three to five years in the reactor. Then, it can either be reprocessed or disposed. In any case, it is considered HLW.

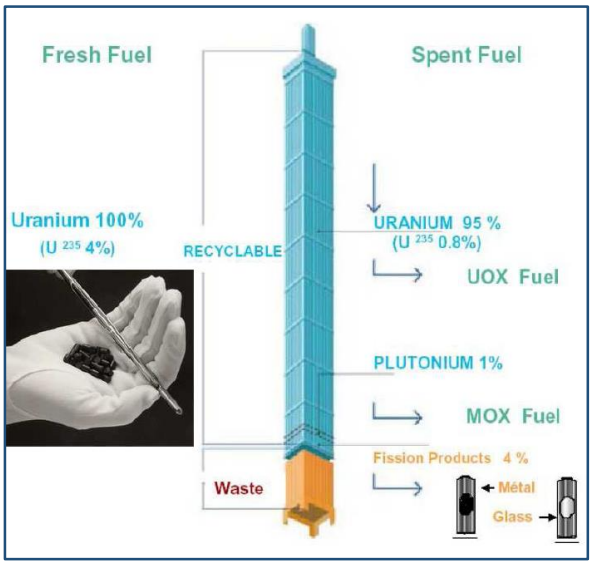

Fig. 4 Spent fuel element after three years in a PWR. [7]

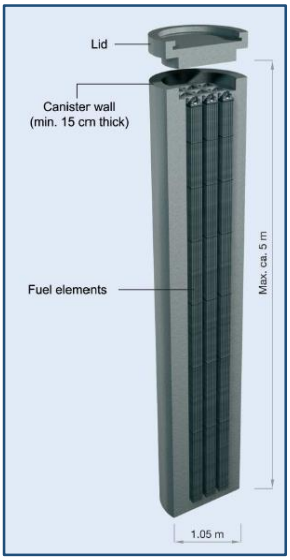

Fig. 3 Canister for spent fuel. [7]

Actinides and fission products from reprocessing (HLW)

During reprocessing, U and Pu are extracted from the fuel and are re-used. The actinides (An) and fission products (FP), which are highly active residues, are separated and melted together with additives to form a glass. This resulting borosilicate glass, solidified in steel containers, has to be disposed as high-level waste (HLW).

Currently, Switzerland does not perform reprocessing with its spent fuel, but the waste from the reprocessing from foreign countries (like France or United Kingdom) is managed.

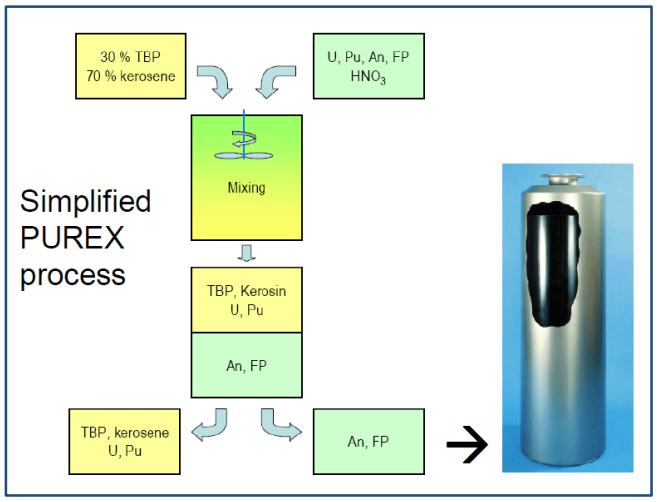

Fig. 5 Simplified PUREX process. Actinides and Fission products are vitrified and classified as high-level waste. [7]

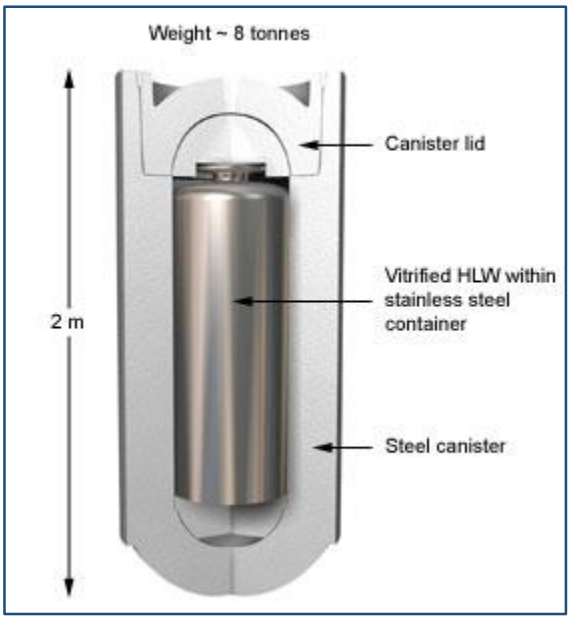

Fig. 6 HLW canister design. [8]

Operational waste (I/LLW)

The NPP also produce intermediate and low-level waste during operation. It can be compacted or incinerated, but anyway the resulting waste has to be treated as radioactive. This includes, for example:

- Contaminated protective clothing,
- Shoes, cleaning materials

- Tools & machine components
- Ion-exchange resins
- Filters from cleaning systems
- Activated reactor components.

Fig. 7 Operational waste [1]

There is a conditioning step to bring the waste in a form that it can be safely stored in a repository. In Switzerland, Zwilag use a state-of-the-art method for the incineration of radioactive waste. It is melted at high temperatures by a high-output plasma burner. The product is a "lava-like" solid.

Fig. 8 "Lava-like" solid for operational waste after the plasma burner. [1]

Decommissioning waste (I/LLW)

The components surrounding the reactor can be either activated or contaminated during the operation of the reactor, so they have to be treated also as intermediate and low-level waste.

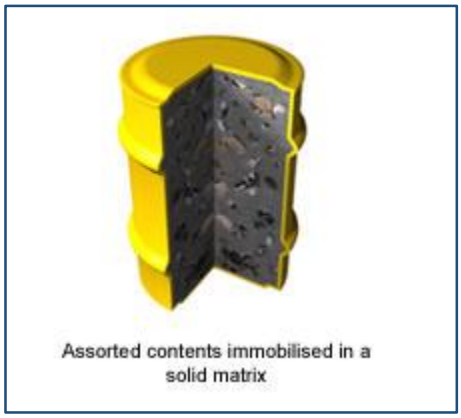

Fig. 9 L/ILW Drum of 200 liters. [8]

MIR waste (I/LLW)

The waste coming from Medicine, Industry and Research, is also classified and disposed. This includes, for example:

- Radioactive sources (60Co, 137Cs) used in radiation therapy (mainly recycled)
- Medical tracers (very short half-lives).
- Tritium waste (3H) from luminous paints in the watch industry.
- Radioactive substances (241Am) from measuring cells in old smoke detectors.
- Radioactive chemicals.
- Waste from accelerator facilities.

Alpha toxic waste (ATW)

ATW is a waste with a content of alpha-emitters exceeding a value of 20.000 Bq per gram of conditioned waste.

A preliminary allocation of the alpha-toxic waste (ATW) to the HLW or L/ILW repository is made, with the final decision being based on the results of the safety analyses for the planned sites.

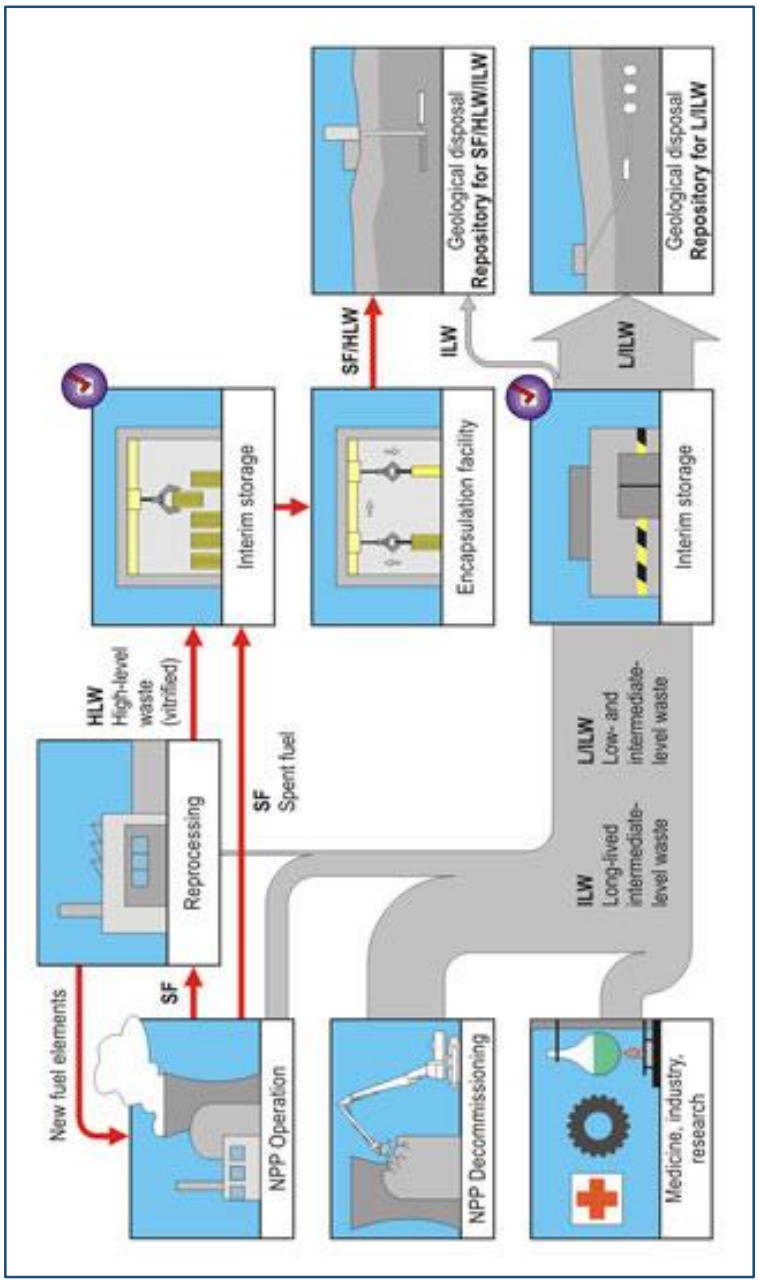

Fig. 10 Radioactive waste management and sources in Switzerland. [8]

3.2.2 The geological repository

3.2.2.1 Why?

Nuclear fuel can be used as resource or simply as a waste. Nuclear power takes full responsibility for all its wastes and includes the waste management costs into the product price. Safe methods for the final disposal of high-level radioactive waste are technologically proven, and the internationally consensus is that this should be geological disposal. The idea of shooting HLW

to the space has too risk of accident, because the waste would fall to the earth's surface with no possibility of control.

It is recognized worldwide that, for high-level and long-lived intermediate-level waste, disposal in stable geological formations is the only way to ensure safety over the necessary long time spans. This principle is anchored in the Nuclear Energy Act of 2003 and also applies in Switzerland to low- and intermediate-level waste.

In facilities at the surface, the waste can be directly controlled and monitored and is easily retrievable. However, such facilities require continuous supervision and maintenance. An absolute prerequisite for this is stable social conditions over the necessary long timescales. In contrast to geological conditions and the evolution of the engineered safety barriers, social and climatic changes cannot be reliably predicted. Geological repositories are therefore preferable.

3.2.2.2 Types of geological repository

In the Swiss geological repository concept two types of repository are foreseen, regarding the classification of the waste.

Deep geological repository for HLW/SF for spent fuel and vitrified fission product solutions from reprocessing. For this kind of waste, deep geological disposal is the only viable option. Even if transmutation technology were to function at some time in the future, a deep geological repository would still be required for the remaining waste. Consisting of a tunnel system for SF and HLW and separated tunnels for ILW, vertically accessible.

Deep geological repository for low- and intermediate-level waste (L/ILW): disposal at the surface exists and is already practiced in France and Spain. In Switzerland, however, deep geological disposal is also legally prescribed. Consisting of caverns mined under a mountain, horizontally accessible. As the for this thesis the interest is focused in the developing of reactive transport modelling calculations within the bentonite buffer specifically in the HLW and SF repositories, in the next section the features of this type of repository are detailed.

For waste with short half-lives no deep geological disposal is necessary (containing nuclides with half-lives shorter than 60 days or wastes that decay to below clearance level within 30 years of their production).

Radioactive waste must be stored in interim storage for 30 to 40 years until it emits no heat. Then, it can be finally stored underground. For low and medium-level waste, an interim storage facility can fill the time gap until there is a deep geological repository. The treatment plants for preparing the waste for final disposal are available.

Zwilag facility, which was visited by the author during his stay at the PSI, is the link between the generation of waste and its long-term storage in deep geological repositories. All categories of radioactive waste generated in Switzerland are processed and temporarily stored in the Zwilag facility and the neighbouring Federal interim storage facility.

Fig. 11 Cask storage hall of the Zwilag facility in Würenlingen (next to PSI), Switzerland. [6]

3.2.2.3 Facility and barriers of the HLW and SF repository

In all geological repository concepts a multiple safety barrier system is considered. This system is composed of engineered barriers and geological barriers. Here, the safety barriers for of the SF, HLW and long-lived ILW are briefly explained. There are three engineered barriers, which are:

Waste matrix: the spent fuel assemblies, the glass (HLW), the cement, etc. Contains the radionuclides.

Canister: prevents inflow and release of radionuclides from waste for several thousand years.

The candidates for the canister material were:

- **Steel**: complete inclusion of radioactive waste and prevention of inflow water for 10.000 years. Then it is expected to be breached and the instant release fraction starts migrating. The corrosion of the matrix will start.
  It is cheaper than cooper. Considered in Switzerland, for now, as material of the canisters.
- **Copper**: complete inclusion of radioactive waste for 100.000 years. More expensive than steel. Sweden decided to use this material for its repository in granite.

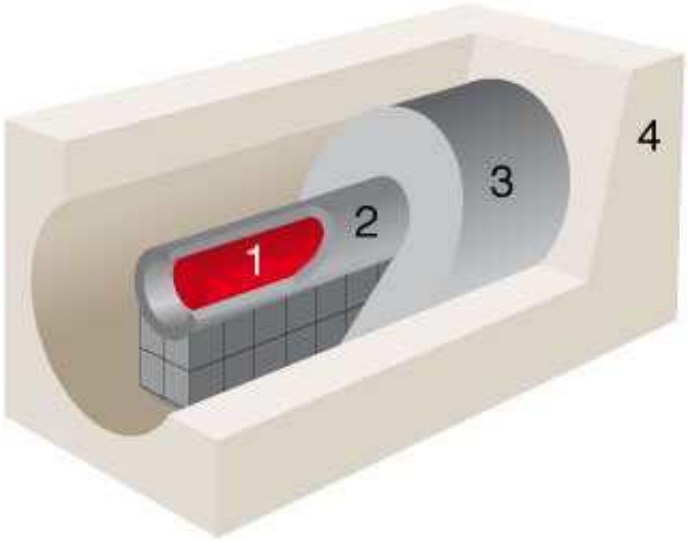

Fig. 12 Barriers within the geological repository. [7]

Backfill: bentonite

Although there are some other options,like cement, salt, or nothing, in many radioactive waste repository concepts compacted bentonite is proposed as a backfill surrounding the canisters. Its main aim is the retardation of radionuclides. Moreover, bentonite provides a number of advantatges:

- Long resaturation time
- Plasticity (self-sealing following physical disturbance)
- Low solute transport rates (diffusion)
- Retardation of radionuclide transport
- Low radionuclide solubility in pore water
- Swelling
- Is generated frequently from the alteration of volcanic ash.

The host rock

The host rock in which the repository is excavated is generally selected to be adequately stable for the construction and operation of the facility and, most importantly, to provide a stable environment where groundwater fluxes through the repository zone are small, and other natural geological and geochemical processes are slow and predictable.

The need for predictability arises from the requirement to make scientifically evaluations of the long-term radiological safety of a disposal facility.

The pillars of safety related to the radionuclides transport through the host rock are:

- the limited concentration of radionuclides in aqueous solution by **Solubility**
- retardation of radionuclides by **Sorption**

The main candidates for becoming the host rock of the repository are, together with their advantages and shortcomings:

	Advantatges	Disadvantatges
Clay	Diffusive contaminant transport Strong retardation by sorption Low water flow	Difficult mechanical engineering properties Generation of H2 gas by canister corrosion -> Fractures?
Granite	Excellent mechanical engineering properties.	Advective contaminant transport through Fractures -> Difficult to assess
Salt	No water flow under normal conditions High thermal conductivity	High solubility & strong corrosion effects

Table 1 Advantages and disadvantages of candidates for material of the host rock

In Switzerland, **clay** is the chosen candidate and a lot of research is involved In the areas of laboratory studies and modelling, Nagra works together with partners from Switzerland (e.g. the Paul Scherrer Institut and the University of Bern) and abroad (e.g. through participation in EU research programmes).

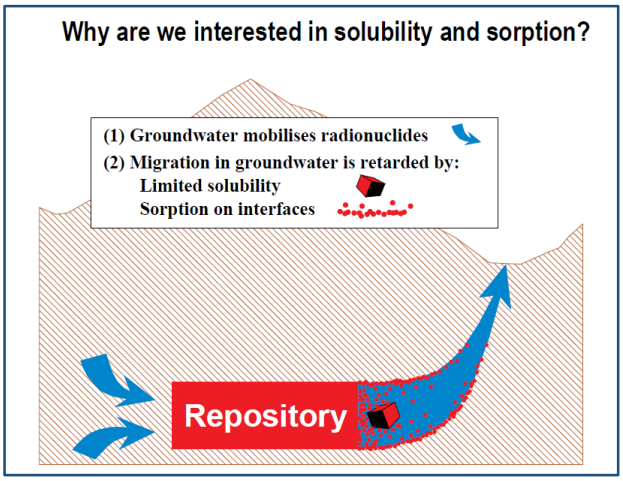

Fig. 13 Simplified sketch of a geological repository showing the main geochemical processes concerning radionuclide mobilization and retardation. [7]

Fig. 14 Nagra works closely with the Paul Scherrer Institut (PSI). The Laboratory for Waste Management is responsible for these research activities.

Rock laboratories provide researchers the opportunity to carry out large scale experiments. There, the behaviour of the rock is investigated under relevant conditions, while technical methodologies are also tested. Nagra has its own rock laboratory: Grimsel Pass, in Canton Bern; and is involved in the programme at the Mont Terri Rock Laboratory in Canton Jura; which is managed by the Federal Government of Switzerland.

Fig. 15 Experiments at the Grimsel facility [8].

Fig. 16 One of the tunnels inside the Grimsel facility [8]

3.2.3 Safety assessments

In order to demonstrate that a repository will comply with safety regulations, performance assessments or safety assessments are carried out. To demonstrate the long-term the long-term safety of any radiactive waste repository in deep geological formations, the timescales of three main processes must be predicted and compared:

- Radioactive decay times. Many isotopes in radioactive waste decay relatively rapidly and, although highly active decay products may he formed, there is a steady decrease in the overall activity of the wastes with time. A number of the more radioactive radionuclides are sufficiently short-lived that they are expected to decay to insignificant levels before there is any possibility of their release from the repository near-field. However, other radionuclides decay very slowly and, consequently, it is much harder to conceive of containing them in the engineered barriers before they decay to reasonable values.
- Progressive degradation of the engineered barriers
- Posterior release and transport times of the radionuclide through the host rock.

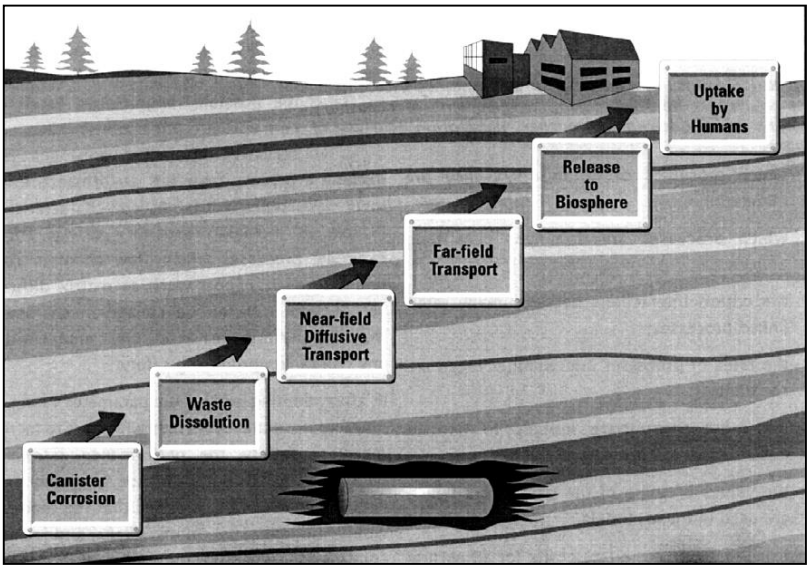

Fig. 17 Scheme of a performance assessment model chain. This thesis is involved in the Near-field Diffusive Transport step. The final step is predicting the radiological dose and risk to humans living in the vicinity of the repository. [7]

3.2.4 Evolution of the Inventory of radionuclides in the waste. Interest for Ni

Ni would not be the first radionuclide that a nuclear engineer would consider, regarding its radiotoxicity (RTI). There quite a lot of radionuclides within the waste like Pu, U, Po, Cs, Am, etc. that would be candidates in terms of studying its sorption behavior within clay materials. Nevertheless, a lot of them still have important lacks of reliable experimental data regarding its transport behavior within the barrier materials of the repository, in such a way that Ni becomes an interesting radionuclide (isotopes Ni-59 and Ni-63) for modelling.

Moreover, nickel (Ni(II)) is a bivalent metal, which makes it also interesting to study its competition for sorption sites against the also bivalent metal iron Fe(II), which is an aim of this thesis.

The next **Table 2** shows some of the inventory of radionuclides of a canister containing 4 PWR UO_2 fuel assemblies with a burnup of 48 GWd/t_{HM}, after 40 years, 1000 years, and 10000 years decay. The complete inventory is detailed in [1].

As can be appreciated, Ni-59 is the seventh most active radionuclide after 10000 years.

Radionuclide	Half-life T1/2 [years]	Fuel [Bq]	Structural materials [Bq]	TOTAL Activity after 40y decay [Bq]	Activity after 1000 y decay [Bq]	Activity after 10000 y decay [Bq]
Pu-239	2.41E+04	2.20E+13	1.40E+08	2.20E+13	2.14E+13	1.65E+13
Pu-240	6.56E+03	3.60E+13	2.00E+08	3.60E+13	3.25E+13	1.26E+13
Tc-99	2.11E+05	1.10E+12	1.90E+08	1.10E+12	1.10E+12	1.06E+12
Am-243	7.37E+03	2.00E+12	2.30E+07	2.00E+12	1.83E+12	7.84E+11
Pu-242	3.73E+05	1.70E+11	1.70E+06	1.70E+11	1.70E+11	1.67E+11
Zr-93	1.53E+06	1.50E+11	1.00E+10	1.60E+11	1.60E+11	1.59E+11
Ni-59	7.60E+04	8.40E+08	1.20E+11	1.21E+11	1.20E+11	1.10E+11
U-234	2.46E+05	1.00E+11	5.40E+04	1.00E+11	9.97E+10	9.72E+10

Table 2 Inventory of the most radioactive radionuclides after 40, 1000 and 10000 years decay (4 PWR UO_2 fuel assemblies with a burnup of 48 GWd/t_{HM}) [1]

4 Migration of contaminant models

A partial differential equation describes the migration of a contaminant, considering advection, dispersion, diffusion and first-order decay:

$$R\frac{\partial C}{\partial t} = D\frac{\partial^2 C}{\partial x^2} - v\frac{\partial C}{\partial x} - \Lambda C$$

Although it can be formulated in three dimensions, this one-dimension formulation is simpler and is applicable in many practical problems.

$\boldsymbol{C}$: Contaminant concentration in the porewater [mol·dm^{-3}]

$\boldsymbol{t}$: Migration time [s]

$\boldsymbol{x}$: Migration distance [m]

$\boldsymbol{v}$: Average groundwater flow velocity [m·s^{-1}]

$\boldsymbol{D}$: Dispersion – diffusion coefficient [m^2·s^{-1}]

$\boldsymbol{R}$: Retardation factor [-] (defined in 4.1.1)

$\boldsymbol{\Lambda} = \lambda \cdot R$, where λ is the decay constant for first-order decay of the contaminant [s^{-1}], also, $\lambda = \ln(2)\ /T_{1/2}$ where $T_{1/2}$ is the half-life of the species [s].

Advection: The water flow carries dissolved substances. This is the dominant process in high flow rate media.

Dispersion: Mass spreading out from the path followed by advection due to heterogeneities in the flow field.

Diffusion: Mass transport due to concentration gradients, i.e. contaminants moves from high concentration areas to low concentration areas. Diffusion is the dominant process in low flow rate media.

First-order decay: Decay of radioactive species or decay of organic compounds, e.g. due to hydrolysis reactions.

The numerical solution is, in general, the only one useful to solve this equation. Nevertheless, an analytical solution can be derived for a limited number of problems. The most important one for contaminant transport in the subsurface is the "**Movement of a contaminant in a semi-infinite column"**

For this specific case, the assumption is that a column (x > 0), at the beginning with individual contaminant concentration C = 0, is connected to a reservoir containing a contaminant solution of constant concentration C_0 (flow in +x direction).

The initial and boundary conditions are

$$t \leq 0 \; and \; x \geq 0: \; C = 0$$

$$t > 0 \; and \; x = 0: \; C = C_0$$

$$t > 0 \; and \; x = \infty: \; C = 0$$

The solution then is

$$C(x,t) = \frac{C_0}{2} \exp\left(\frac{vx}{2D}\right) \left\{ \left(\exp\left(x \sqrt{\frac{v^2}{4D^2} + \frac{\lambda R}{D}} \right) \cdot erfc \frac{Rx - \sqrt{v^2 + 4\lambda RDt}}{2\sqrt{RDt}} \right) + \left(\exp\left(x \sqrt{\frac{v^2}{4D^2} + \frac{\lambda R}{D}} \right) \cdot erfc \frac{Rx + \sqrt{v^2 + 4\lambda RDt}}{2\sqrt{RDt}} \right) \right\}$$

Where erfc is the complementary error function, $erfc(x) = 1 - \mathrm{erf}(x) = \frac{2}{\sqrt{\pi}} \int_x^\infty e^{-\alpha^2} d\alpha$

If radioactive decay or any other first-order chemical decay in transport modelling is not explicitly considered, i.e. assuming infinite half-life for any compound in the model calculations (which means setting $\lambda = 0$) , a much simpler equation results:

$$R \frac{\partial C}{\partial t} = D \frac{\partial^2 C}{\partial x^2} - v \frac{\partial C}{\partial x} \qquad \textbf{(Hydrodynamic Dispersion Equation)}$$

And its solution:

$$C(x,t) = \frac{C_0}{2} \left\{ erfc \frac{Rx - vt}{2\sqrt{RDt}} + \exp\left(\frac{vx}{D}\right) \cdot erfc \frac{Rx + vt}{2\sqrt{RDt}} \right\}$$

Which can be simplified even further for special cases, like the low flow rate media, where the migration of a contaminant is dominated essentially by diffusion and there is no advection (no groundwater flow, $v \to 0$):

$$C(x,t) = \frac{C_0}{2} \left\{ erfc \frac{Rx}{2\sqrt{RDt}} \right\}$$

4.1.1 The Kd model

The most common and simplest way of estimating contaminant retardation is based on the element-dependent, equilibrium sorption, linear Kd coefficient. It is a factor that relates the partitioning of a contaminant between the solid (soil) and aqueous phases (porewater). It is an empirical unit of measurement that attempts to account for many retardation mechanisms (chemical and physical). It is the simplest, but least robust model available. Nagra is still using this model to predict the transport mechanism for solutes in the bentonite buffer [1].

The retardation factor R is related to the Kd as:

$$R = 1 + K_d \cdot \rho_b / \varepsilon$$

where

$\boldsymbol{\rho_b}$ is the bulk dry density ρ_d of the soil $[kg \cdot m^{-3}]$

$\boldsymbol{\varepsilon}$ is the accessible porosity

$\boldsymbol{K_d}$ is the sorption value $[m^3 \cdot kg^{-1}]$

The Kd is the ratio between the quantity of adsorbate adsorbed per unit of mass of solid, to the amount of adsorbate in solution at equilibrium:

$$K_d = \frac{Mass\ of\ adsorbate\ sorbed}{Mass\ of\ adsorbate\ in\ solution} = \frac{\frac{mols\ of\ adsorbte}{kg\ of\ soil}}{\frac{mols\ of\ adsorbate}{l\ of\ liquid}} = [l/kg]$$

The Kd data comes from experimental experiences. That means that it depends particularly on each contaminant and on the different chemical conditions in which it was measured. Ideally, thinking in the radioactive geological repository, Kd values should be experimentally measured for the repository conditions.

The Kd approaches are successfully supported by much more sophisticated sorption models that include several sorption reactions on mineral surfaces, ion exchange reactions, etc.

4.1.2 The 2SPNE SC/CE sorption model

One of those alternative models is the two site protolysis non electrostatic surface complexation/cation exchange sorption model (2SPNE SC/CE), created by Bradbury and Baeyens (1997, 2006). Because of the importance of bentonite as a backfill material in the Swiss concept for a high level radioactive waste repository, Na-Montmorillonite was selected as a first medium for the

developing of the model. This is the sorption model incorporated to the reactive transport code MCOTAC, used afterwards for the calculations of this project.

As this is a consolidated model coming from extensive research developed during several years at the PSI, a few explanatory remarks focused on its application for this project are provided. More details have been described on numerous publications by Bradbury and Baeyens (e.g., [3] and [4]).

Clay minerals, as it is the case of Montmorillonite, carry a permanent negative surface charge. In the next **Fig. 18** this negative charges on the surface are illustrated. The total permanent negative surface charge is known as cation exchange capacity. Ion exchange is a reversible chemical reaction wherein an ion (an atom or molecule that has lost or gained an electron and thus acquired an electrical charge) from solution is exchanged for a similarly charged ion attached to an immobile solid particle.

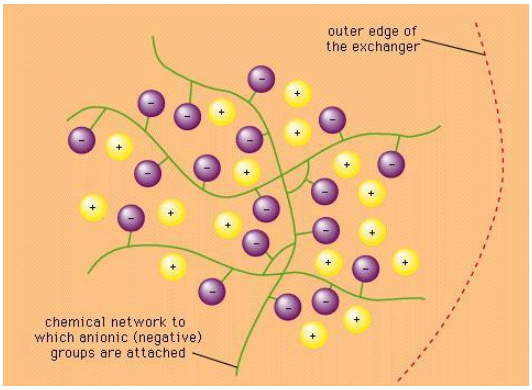

Fig. 18 Chemical structure of cation exchanger. [9]

This negative charge on the clay surfaces is neutralized by the presence of an excess of electrostatically bound cations held close to the surface which can exchange with cations in solution.

After finding non-linear relations of the sorption isotherms of their experiments, Bradbury and Baeyens indicated that at least two different ≡SOH type sites were contributing to the overall sorption on Na-Montmorillonite. A set of sorption sites are conceived to be located at the edges of clay platelets, considered surface hydroxyl groups (≡SOH) which can protonate, deprotonate and interact with metal species in solution. For the protonation/deprotonation reactions, two weak sites: ≡Sw1OH, ≡Sw2OH. And for the sorption edges and sorption isotherms modelling, strong and weak sites: ≡Sw1OH, ≡SSOH. The model does not need electrostatic terms in the mass action relations of protolysis and surface complexation reactions. The strong sites have a low capacity and a high sorption affinity and dominate the uptake of radionuclides at low concentrations. The second type of sites, the weak ones, have a larger capacity but a much lower sorption affinity.

The surface complexation reactions are described in section 5.7 of the setting up of the specific models used for this thesis. An assumption for the models of this project will be that only free cations and hydrolysed species are sorbing.

Finally, the 2SPNE SC/CE sorption model can be used in reactive transport models allowing the calculation of radionuclide migration under spatially and temporally changing conditions.

4.1.3 Reactive transport modelling: MCOTAC

The following intends to be a summary of what is behind the user interface of the MCOTAC program. That is, a conceptual explanation of the calculations, the transport and chemical phenomena considered and the methods used to develop the calculations. More specific explanations are found in references [10], [11]and [12].

The intention of MCOTAC is to get efficient modelling to calculate reactive transport phenomena by a multispecies random walk coupled to chemical equilibrium. That means, an alternative way to solve the contaminant transport problem that the one of the Kd model.

MCOTAC is a sequentially coupled code. It couples one-dimensional transport of particles described by random walk and the chemical equilibrium complexation reactions between the species of the system and precipitation/dissolution reactions. These species have assigned initial concentrations (that is why, for this project, the porewater composition of the bentonites is necessary), and they can be basis, complexes, and solid.

The input information required by the code is, as a summary:

- System description and numerical parameters: total distance, total real time of calculation, number of cells, number of particles
- Chemical composition of porewater and solids, equilibrium constants and stoichiometry of the reactions
- Decay information for the depleting species
- Porosity, diffusion coefficient
- Boundary conditions

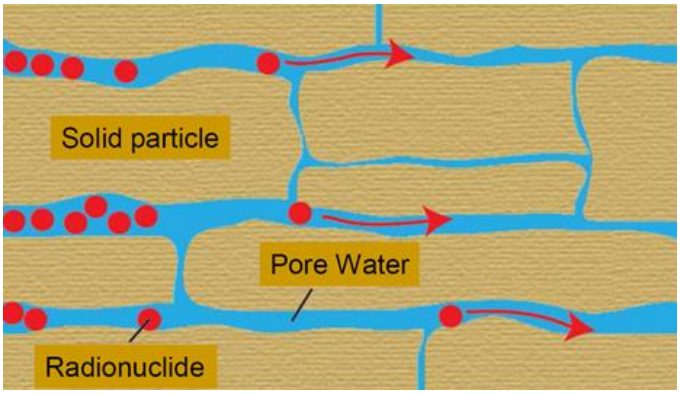

Fig. 19 Illustrative sketch of part of the system to be modelled. [7]

As assumptions, the flow field is considered to not change significantly during the calculation (for clays, the water velocity is zero) and the total mass is conserved.

The notation used in the next equations is:

- $X_j = basis\ species\ concentrations\ \left(j = 1, \dots, N_j\right)\ (\frac{mol}{l})$
- $C_i = complexes\ concentrations\ (i = 1, \dots, N_c)\ \left(\frac{mol}{l}\right)$
- $U_j = total\ aqueous\ concentrations\ \left(j = 1, \dots, N_j\right)\ \left(\frac{mol}{l}\right)$
- $P_k = immobile\ solid\ phases\ concentrations\ (k = 1, \dots, N_k)\ \left(\frac{mol}{l\ fluid}\right)$
- A_{ij} , B_{jk} :stoichoiometric matrixes to form complexes and solids from basis species
- $t = time\ (s)$
- $x = coordinate\ in\ x\ direction$
- $D = dispersion\ coefficient\ (\frac{m^2}{s})$
- $v = effective\ flow\ velocity\ \left(\frac{m}{s}\right)$

The complexation reactions are described by: $\{C_i\} = K_i \cdot \prod_j^{N_j}\{X_j\}^{A_{ij}}$, with $\{X_j\} = \gamma_j \cdot X_j$, $K_i = equilibrium\ constant$, $\gamma_j = activity\ coefficient$

The precipitation / dissolution reactions, by: $K_{so}^k = \prod_{j=1}^{N_j}\{X_j\}^{B_{jk}}$, $with\ K_{so}^k = solubility\ product$

And the transport equation for advective-dispersive/diffusive transport must be solved:

$$\frac{\partial U_j}{\partial t} + v\frac{\partial U_j}{\partial x} - \frac{\partial}{\partial x}D\frac{\partial U_j}{\partial x} = -\sum_{k=1}^{N_k} B_{jk}\frac{\partial P_k}{\partial t}$$

with total aquous concentrations: $U_j = X_j + \sum_{i=1}^{N_c} A_{ij}C_i$

During a tranport step, no interaction between solid and liquid phases is assumed, and so the transport equation is simplified:

- $\frac{\partial U_j}{\partial t} + v\frac{\partial U_j}{\partial x} - \frac{\partial}{\partial x}D\frac{\partial U_j}{\partial x} = 0$

Then, to get the coupling after each transport step, the chemical equilibrium calculation takes place, with mass transfer between solid and liquid phases (set of Nj + Nc+ Nk non-linear equations for Nj independent and Nc+ Nk dependent variables):

- $\frac{\partial}{\partial t}(U_j + \sum_{k=1}^{N_k} B_{jk}P_k) = 0$

A finite number of cells, acting as elementary volumes, distributed all along the 1D system are used for the chemical equilibrium calculation. For each cell,

- $w_{j\,total|m} = [U_j + \sum_{k=1}^{N_k} B_{jk}P_k]_m$ *is the total concentration of basis species*

And the Newton-Raphson procedure is used to solve the set of nonlinear equations.

Independent particles, each associated with a set of masses of chemical substances, are moved within a flow field in a statistical manner. Mass vector approach: the transport step is done for all solutes in one step. Each particle n is related to a particle mass vector n to characterize the particle properties

- The vector n has $N_j + N_c + 2$ components:
  - $n = \left(m_1, m_2, \ldots, m_{N_j}, m_{N_j+1}, m_{N_j+2}, \ \ldots, m_{N_j+N_c}, x_n, \ t\right)$
- Where m are species masses per particle, location, and time:
  - $m_{j|cell\ m} = \frac{X_j \cdot V}{nb\ (m)(number\ of\ particles\ in\ cell\ m)}$
- And finally, for each time step, new particle positions are calculated depending on the transport processes.
  - $x_n = x_{n,old} + v \cdot \Delta t + Z_n \cdot (2D \cdot \Delta t)^{1/2}$,

  where Z_n is as normally distributed random number.

4.1.4 Competition for sorption sites

Bradbury and Baeyens already warned that "*...background impurity cations can, depending on the circumstances, be competitive for the available sorption sites...*" [3]. This effect has not been extensively studied yet and it is an important aspect influencing the sorption of any dissolved radioactive metal. Currently, these competitive sorption effects are not explicitly included in safety assessments, and are therefore issues which need to be addressed.

5 Bentonite models setup

5.1 Introduction

In this section the models of the two bentonite systems analysed are described, i.e. porewater composition, sorption model, calculation conditions and numerical parameters. This setting up was carried out carefully, since it is the part of the project that is necessary for the consistency of the results, but at the same time would be enough for the non-consistency of them.

The geochemical system setup consists of a water-saturated Na-Montmorillonite with porewater composition according to [1] and [2], where on side at x=0 m Ni(II) leaches into the Na-montmorillonite at constant (solubility limited) concentration. Ni(II) breakthrough will be calculated at different time instants and distances.

The water-saturated Na-Montmorillonite bentonite systems studied are the MX-80 barrier designed in Switzerland for the real repository concept and the FEBEX barrier used in the experiments made up to now by Spain. The idea is that the calculations carried out for this project are full-scale models with the expected characteristics of the future real deep repositories.

References used are provided during all the project. However, as it is absolutely relevant for the consistence of the models, the main references used to get the models parameters are listed below, to encourage the reader to have a look to them:

1. M. García-Gutiérrez, J.L. Cormenzana, T. Missana, M. Mingarro, J. Molinero. Overview of laboratory methods employed for obtaining diffusion coefficients in **FEBEX** compacted bentonite. J. Iberian Geology, 32 (1) (2006), pp. 37–53

2. Huertas F., Fuentes-Cantillana J.L., Jullien F., Rivas P., Linares J., Fariña P., Ghoreychi M., Jockwer N., Kickmaier W., Martínez M.A., Samper J., Alonso E., Elorza F.J. (2000). Full-scale engineered barriers experiment for a deep geological repository for high-level radioactive waste in crystalline host rock (**FEBEX** project). Nuclear Science and Technology, EUR 19147.

3. Nagra (2002c): Project Opalinus Clay. Safety Report. Demonstration of disposal feasibility for spent fuel, vitrified high-level waste and long-lived intermediate-level waste (Entsor gungsnachweis). Nagra Tech. Rep. NTB 02-05. Nagra, Wettingen, Switzerland.

Obviously, data provided by Enresa and Nagra (and related institutions) in their official publications was highly taken into account, as well as the references mentioned in their multiple publications about the geological repository.

For the FEBEX case, as the main parameters come from the two first listed references, a proper explanation of how this is matched is necessary: from the first reference mentioned above, porosity, dry density and diffusion coefficients are used. Using this data, the s:l ratio is calculated (detailed calculation following in this section), which coincides with the s:l value given in the second reference, whose porewater composition is there detailed.

For the Swiss case, the data comes mainly from a Nagra's safety report, which involves a lot of published and non-published papers.

5.2 Calibration of calculation parameters

A calibration previous to the setup of the models was necessary to find the best configuration of the program and the system, for optimizing both the calculation time and the precision of the results. Fixing all the system features and modifying only parameters of interest, one can figure out the influence of the modified parameter to the calculation and its best configuration.

For the calibration, MX-80 bentonite and a Ni injection of 10^{-5} M were used.

5.2.1 Number of cells

Results for different cell numbers along the column were compared. As it can be appreciated in **Fig. 20**, the number of cells has a high influence to the calculation time. Obviously, the more cells, the more calculation time, because each transport and chemical equilibrium step is carried out in each cell until it converges.

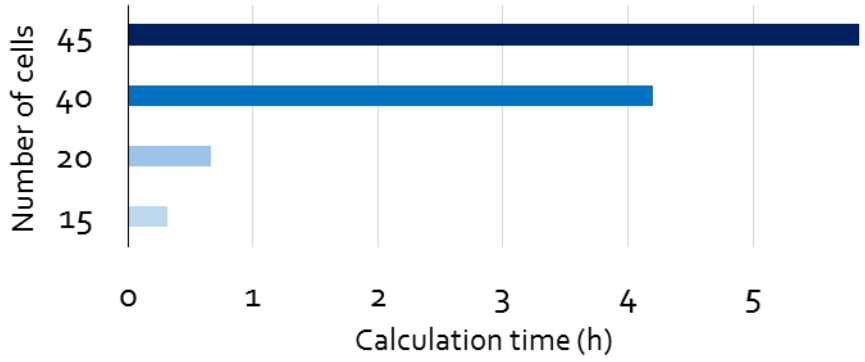

Fig. 20 Calculation times depending on the number of cells along the 1D column.

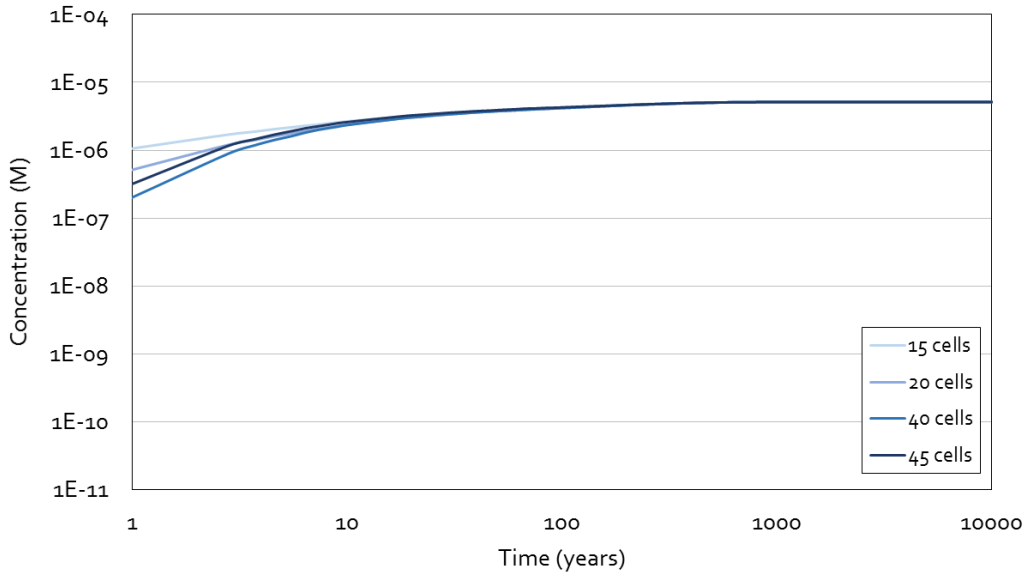

Fig. 21 Ni (II) breakthrough curves at x≈0.10 m into the MX-80 bentonite, depending on the number of cells.

As can be observed in **Fig. 21** and **Fig. 22** (different distances), differences between the calculations with different number of cells exist.

An important effect is the numerical dispersion, which increase with lower number of cells, as the cell length increase due to the fixed total length of the system. When mainly diffusion transport processes are assumed to happen in the real system, as it is in the bentonite buffer, dispersion transport processes induce also dispersivity in the results. Mathematically, diffusion and dispersion are coupled, i.e. described by the same transport equation term (D coefficient, see section 4). The longer the cell length is, the more important becomes the dispersivity, since it has longer times and space to appear and become important within each cell.

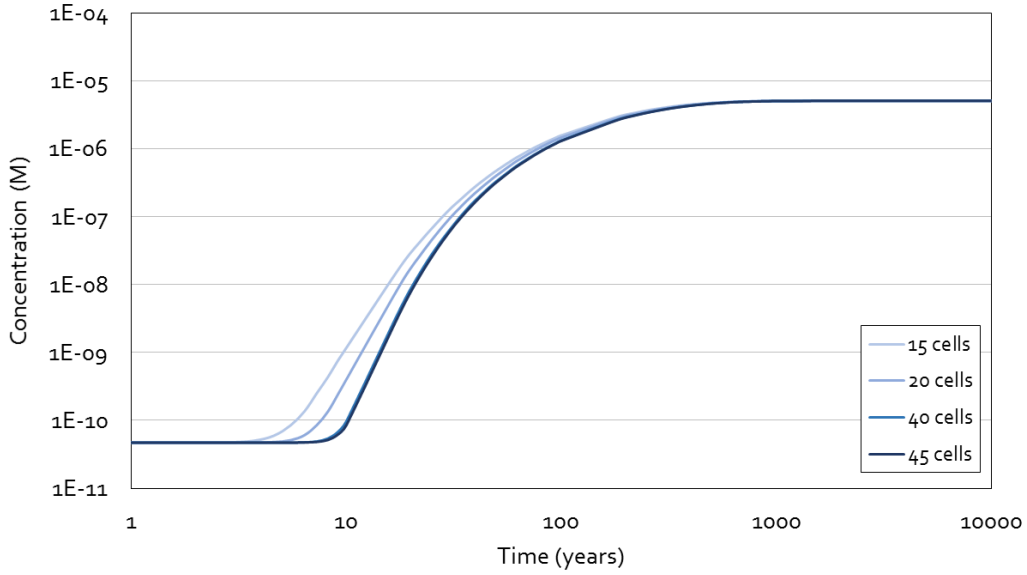

Fig. 22 Ni (II) breakthrough curves at x≈0.65 m into the MX-80 bentonite, depending on the number of cells.

For further calculations, models with 45 cells will be used, to avoid the dispersivity effect taking into account that the calculation time is not much higher than the 40 cells case.

5.2.2 Number of particles

The total number of particles determines the number of particles distributed per cell, which is the number of particles used for the transport calculation in each cell. **Fig. 23** shows the differences in calculation time between calculations with different number of particles. The more particles, the more calculation time.

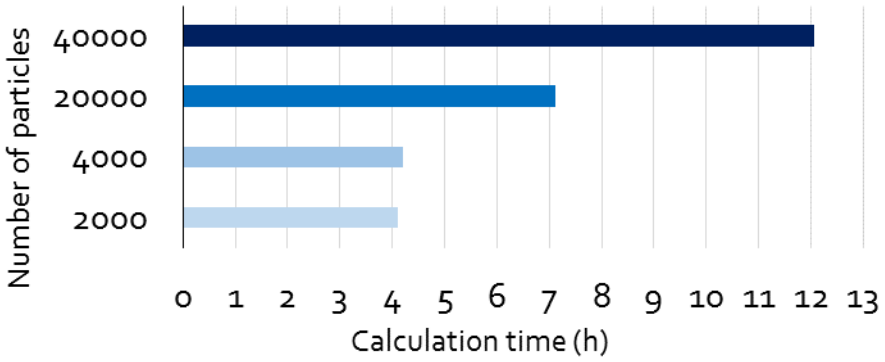

Fig. 23 Calculation times depending on the number of particles.

Fig. 24 indicates that there are not big differences between configurations with different number of particles, regarding the breakthrough curves. However, a number lower than 100 particles per cell is not recommended by the MCOTAC code developers.

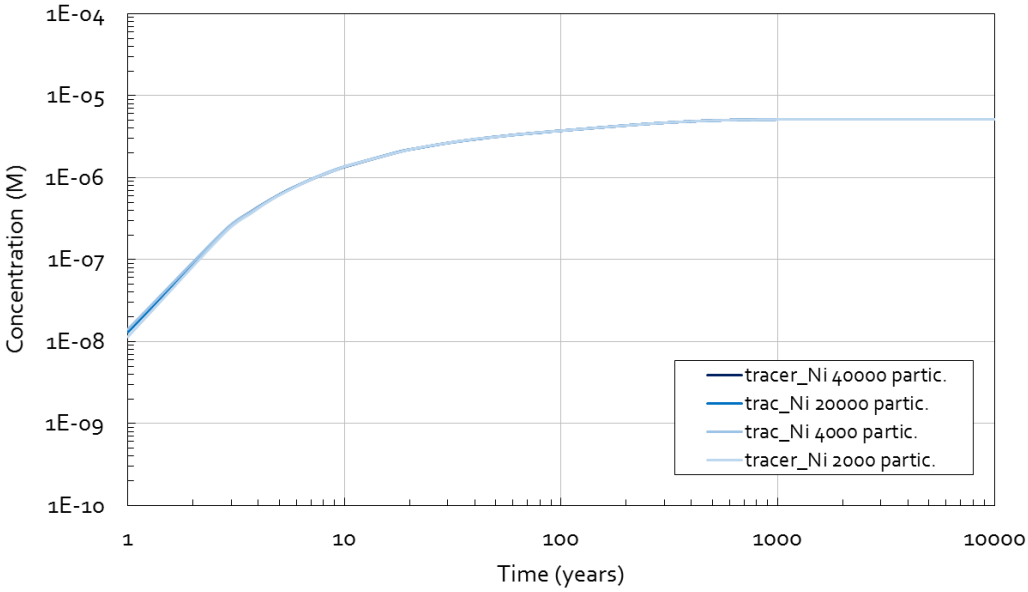

Fig. 24 Ni (II) breakthrough curves at x=0.1575 m into the MX-80 bentonite, depending on the number of particles.

5.2.3 Convergence error

Convergence errors of 10^{-8} and 10^{-10} were compared. The calculation times needed are shown in figure **Fig. 25** and results (Ni breakthrough curves for x=0.6125) for both cases are compared in figure **Fig. 26**.

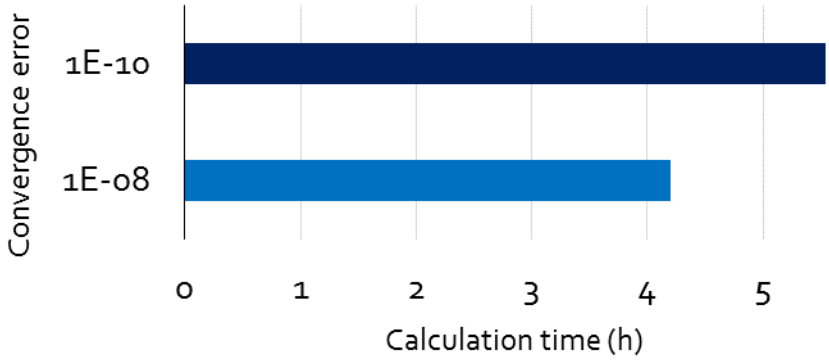

Fig. 25 Calculation times depending on the convergence error.

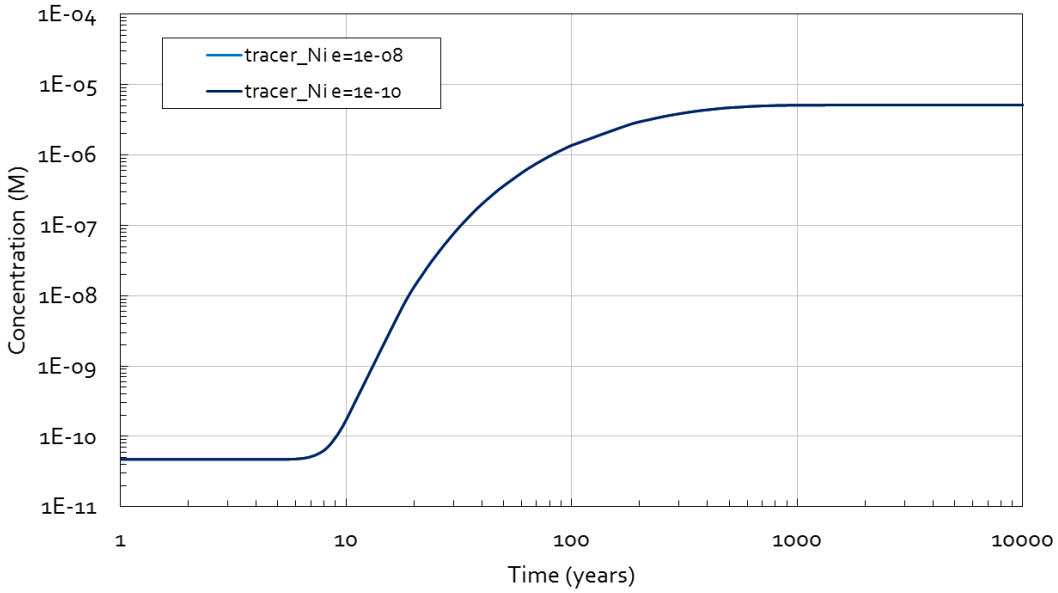

Fig. 26 Ni (II) breakthrough curves at x=0.1575 m into the MX-80 bentonite, depending on convergence error.

5.2.4 Smooth/ not smooth options

MCOTAC has an option that allows the user getting smoother results, i.e. smoother breakthrough curves when using a low number of particles for a calculation. The next figures show that the calculation times are very different and the results are certainly smoother for the smooth option, whilst still similar. The reason is that low number of particles means less calculation time, and therefore smooth concentration distributions yield to fast convergence of the geochemical module.

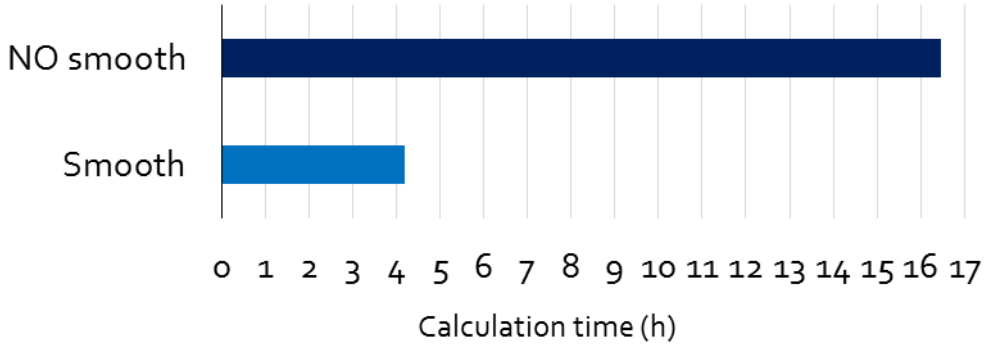

Fig. 27 Calculation times depending on the smooth option active or not.

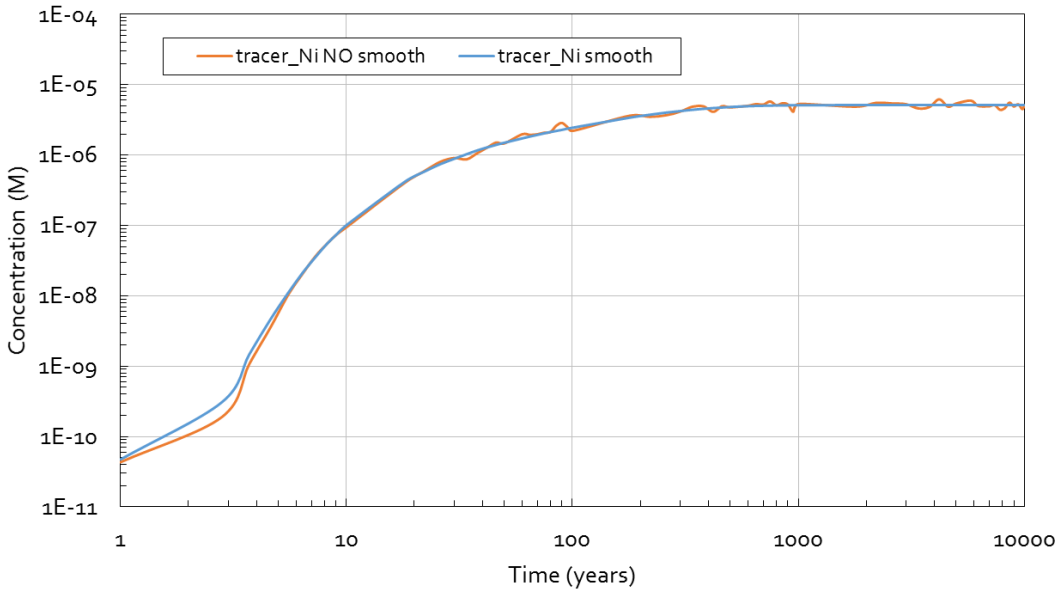

Fig. 28 Ni (II) breakthrough curves at x=0.3325 m into the MX-80 bentonite, depending on the smooth option active or not.

5.3 Numerical parameters

Numerical parameters are adjusted to the calculation with the previous calibration. Maximum time step, number of particles, number of cells and convergence error (**Table 3**) are adjusted to avoid numerical calculation dispersivity or coarse discretization, and intending to get good results with reasonable calculation times.

The 70 cm thickness is discretized in 40 cells of 1.75 cm. with 4000 particles distributed along the column. The convergence error used is 10^{-8}, and the smooth option is chosen for all the following calculations. The maximum time step is calculated according to [10]:

$$\Delta t_{max} \leq \frac{\Delta x^2}{2D} = \frac{0.0175^2}{2 \cdot D}$$

Maximum time step FEBEX/MX-80	$1.028 \cdot 10^6$ / $2.756 \cdot 10^5$ sec.
Number of particles	4000
Number of cells	40
Cell length	0.0175 m
Convergence error	10^{-8}
Molecular diff. coef. (D) FEBEX/MX-80	$1.49 \cdot 10^{-10}$/$5.56 \cdot 10^{-10}$ $m^2 s^{-1}$

Table 3 Numerical parameters of the models.

5.4 Model dimensions

The calculations with MCOTAC were performed for 1D geometry to get reasonable calculation times, so the main dimension of interest is the foreseen thickness of bentonite buffer around steel containers in a high level waste repository.

70 cm is exactly the bentonite radius used in the FEBEX experiment and a thickness very close to the Swiss repository design.

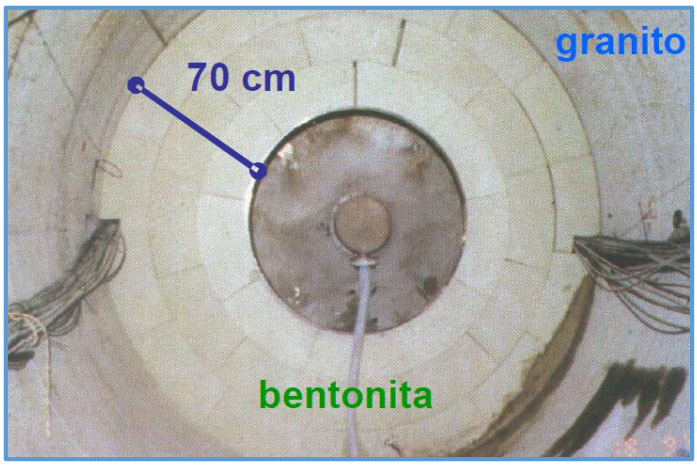

Fig. 29 Picture of the FEBEX experiment at the Grimsel facility. [13]

The thickness of the Swiss MX-80 bentonite backfill will be 68 cm for the HLW repository, according to Nagra:

$$Outer\ bentonite\ radius - Inner\ bentonite\ radius = 1.15m - 0.47m = 0.68m$$

Parameter	Reference value	Variations / Comments
Time of canister failure	10^4 a	10^3 a (Johnson & King 2003)
Glass corrosion rate		
MW glass (WA-BNF-1)	5.5×10^{-4} kg m^{-2} a^{-1}	4.0×10^{-2} kg m^{-2} a^{-1} (Curti 2003)
SON-68 glass (WA-COG-1)	7.3×10^{-5} kg m^{-2} a^{-1}	4.0×10^{-2} kg m^{-2} a^{-1} (Curti 2003)
Number of canisters, n_{COG} n_{BNFL}	460 270	McGinnes (2002)
Length of glass blocks, h	752 m (1.03 m for each block, 730 blocks)	McGinnes (2002)
Initial diameter of glass blocks, d_0	0.43 m	McGinnes (2002)
Glass density	2750 kg m^{-3}	McGinnes (2002)
Factor of glass surface area increase due to fracturing	15	Pessimistic assumption, adjusted upwards from value of 12.5 used in Nagra (1994a)
Volume for dissolution, V_R (thickness, d^f, of reservoir)	d = 2.5 cm 24.6 m^3 (0.037 m^3 for each block)	$V_R = h*(d_0/2+d/2)*2\pi*d$
Canister radius	0.47 m	Steag & Motor Columbus (1985)
Inner bentonite radius	0.47 m	0.81 m (half-thickness, assuming alteration)
Outer bentonite radius	1.15 m	Radius after convergence (Section 5.3.3.1)
Bentonite porosity	0.36	(Section 5.3.3.1)
Bentonite solid density	2760 kg m^{-3}	Nagra (1994a)

Fig. 30 Information of the HLW bentonite backfill according to Nagra [1].

5.5 Timescale of concern

The calculations run as long as the user needs, and MCOTAC generates output files, i.e. saving concentrations all along the bentonite column, in as many time points as wished. In this case, another previous calibration is made to get an idea of how long it is the necessary time for the tracer to reach the last points of the column, and to know which time instants would be representative for the interpretation of the results. The chosen times are:

$$1, 10, 50, 100, 500, 1000, 5000 \text{ and } 10000 \text{ years.}$$

This means that the program calculates the transport of radionuclides and its influence to the porewater chemistry during 10000 real years. The time reference (t=0) corresponds to that when the waste starts leaching from the canister. That is between 10000 and 20000 years after the waste emplacement in the repository.

But, as only individual radionuclides are defined as "tracers" diffusing along the bentonite thickness for simplicity and understanding of the MCOTAC models, and this thesis is focused in Ni transport , the questions that if this time range is proper for Ni or not appears. Therefore, **Fig. 31** and **Fig. 32** indicate that the analysis of the diffusion of Ni through the bentonite buffer is relevant, because it loses a high part of its radiotoxicity during its retardation in the bentonite.

Fig. 31 shows that around the 30% of the radiotoxicity of ^{59}Ni is lost in the bentonite buffer. And **Fig. 32** that the bentonite is such an important layer retarding this element (isotope, but considered the most as the most important one of the whole Ni, for conservative analysis).

Nuclide	Proportion of radionuclide inventory originating in spent fuel that decays in:				
	waste matrix	waste matrix + immediate surroundings + precipitates	waste matrix + immediate surroundings + precipitates + the buffer	waste matrix + immediate surroundings + precipitates + the buffer + the Opalinus Clay	outside the Opalinus Clay
^{14}C (organic)	0.88	0.88	0.90	1.00	4.5×10^{-5}
^{36}Cl	0.41	0.41	0.41	0.89	0.11
^{59}Ni	0.22	0.56	0.95	1.00	0.00
^{79}Se	0.89	0.99	0.99	0.99	6.8×10^{-3}
^{99}Tc	0.96	0.96	1.00	1.00	0.00
^{129}I	0.69	0.69	0.69	0.72	0.27
Nuclide	**Proportion of radionuclide inventory originating in HLW that decays in:**				
	waste matrix	waste matrix + immediate surroundings + precipitates	waste matrix + immediate surroundings + precipitates + the buffer	waste matrix + immediate surroundings + precipitates + the buffer + the Opalinus Clay	outside the Opalinus Clay
^{59}Ni	0.62	0.62	0.91	1.00	0.00
^{79}Se	0.07	1.00	1.00	1.00	2.4×10^{-3}
^{99}Tc	0.28	0.93	1.00	1.00	0.00
^{129}I	0.01	0.01	0.01	0.10	0.89

Fig. 31 The proportions of the radiotoxicity index of key radionuclides that decay in every barrier of the multiple barrier safety system for SF and HLW. [1]

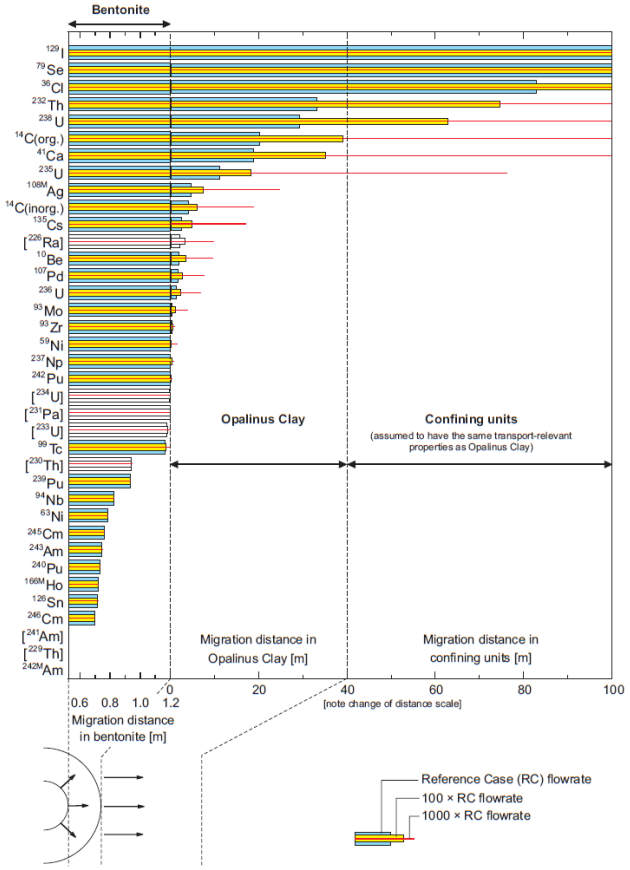

Fig. 32 Distance into the bentonite buffer and host rock at which radionuclide transport rates are attenuated by 99% due to decay. [5]

5.6 Bentonite conditions

5.6.1 Conceptualization of key phenomena in the Reference Case

As Nagra already does in his report [1], a first general conceptualization provide a first resource to the reader that facilitates the understanding of the bentonite system. In the next sections extended and detailed features of the system are provided.

- The bentonite is a well-mixed homogeneous volume of water, which inner boundary is assumed to receive the radionuclides released from the canister.
- The transport properties do not change within the bentonite, i.e. the bentonite is also homogeneous with its transport properties. Therefore, the thermally altered zone around the canister is assumed to be negligible.
- The media is assumed to have reducing conditions. The isotopes of the same elements are assumed to have the same solubility limits
- Precipitation only occurs when the sum of the concentrations of all isotopes of the same element overcomes the solubility limit.
- The background concentrations of isotopes in the bentonite are ignored, which is conservative.
- The transport of solutes in the bentonite occurs mainly by diffusion.
- Dissolved gas transport is considered negligible.
- Radionuclide -bearing colloids are considered immobile in the bentonite and are not taken into account.

5.6.2 Montmorillonite content

Montmorillonite, a member of the smectite minerals family, is the main constituent in bentonite and also the main responsible for sorption.

A ratio between the Montmorillonite content in both bentonites MX-80 and FEBEX is calculated and will be used afterwards. For MX-80, it is known that the Montmorillonite content is the 75% in weight [14]. For FEBEX, this is the 92% [2]. Then, the ratio between both values is calculated:

$$\frac{92\ wt\%\ Montmorillonite\ FEBEX}{75\ wt\%\ Montmorillonite\ MX80} = 1.23$$

5.6.3 Porosity

Porosity is considered to be homogeneous all along the thickness of bentonite and constant in time. It is not the same for the two models. The MX-80 used in the calculations has a porosity of 0.36 [1].

$$\varepsilon_{MX\text{-}80} = 36\%$$

The FEBEX porosity (**Table 4**), according to [15] for the "*Spanish concept of disposal, for the compacted bentonite*", is 0.389.

$$\varepsilon_{FEBEX} = 38.9\%$$

In this reference [15] is found part of a discussion that needs to be faced to prepare good models for later reactive transport calculation: the difference between porosity (ε) and accessible porosity (Φ). The definition of porosity is:

$$\varepsilon = \frac{V_{void}}{V_{total}}$$

Dry density (g/cm^3)	D_e (m^2/s)	D_a (m^2/s)	ϕ (%)	ε(%)
1.0			64.9±0.5	63.0
1.1	1.96±0.04E-10	3.3±0.1E-10		59.3
1.2			57.4±0.8	55.7
1.3	1.46±0.10E-10	3.1±0.1E-10		51.9
1.4			51.4±0.5	48.1
1.5	8.86±0.06E-11	2.6±0.1E-10		44.4
1.6			43.0±0.3	40.7
1.65	5.80±0.20E-11	1.6±0.5E-10		38.9
1.7	5.16±0.50E-11	2.6±0.1E-10		37.0

Table 4 [15] Experimental results for HTO at different bentonite clay densities Last column is the theoretical porosity.

For this thesis and for the repository concept, the bentonite is saturated with water. That means that

$$V_{void} = V_{water}, \text{ and then, } \varepsilon = \frac{V_{water}}{V_{total}}$$

Moreover, there is the concept of accessible porosity, which is an important parameter for describing the transport of radionuclides and is defined as the proportion of the total volume of a saturated porous material that is available for diffusion. For a better understanding, it is important to remember that diffusion is the main transport method in bentonite and clay, due to the low water flow rate.

The porosity really available for diffusion could be smaller than the normal porosity or total porosity, which is the concept of the values given above. Some pores of the bentonite microstructure may be not accessible, dead end or blind pores, which don't contribute to the transport of solute. Moreover, other processes like anion exclusion from the negatively charged surface vicinity may also reduce the porosity. As this effects depend on the charge and characteristics of each ion, different diffusion coefficients for each one should be considered, which would make the model much more complex.

In reference [15] the main conservative tracer studied was HTO, representative of neutral species. It is conservative because its accessible porosity is identical to the total porosity, which means that all the pores in compacted bentonite are available for diffusion of neutral species. However, for Cl^- and other anions, the accessible porosity is quite smaller than the total porosity.

Since for the models is not possible to introduce different accessible porosities for each specie, a conservative assumption is done and the accessible porosity is assumed to be the same as the total porosity, like it really happens for the neutral species.

5.6.4 Dry density

The dry density is defined as:

$$\rho_d = \frac{Mass\ of\ soil}{V_{TOTAL}}$$

For MX-80, according to [1], highly compacted bentonite blocks together with the backfill with granular bentonite (using a pneumatic system) upon emplacement is expected to have an average dry density of 1.5 kg/l. The consequent low thermal conductivity due to the high density and the low moisture must be taken into account for the safety assessment.

$$\rho_{d\ MX-80} = 1.5\ kg/l$$

For FEBEX, according to [15] (**Table 4**), its dry density is:

$$\rho_{d\ FEBEX} = 1.65\ kg/l$$

Dry density is related with porosity via the solid density:

$$\varepsilon = \frac{V_{void}}{V_{total}} = \frac{V_{total} - V_{soil}}{V_{total}} = 1 - \frac{V_{soil}}{V_{total}} = 1 - \frac{\frac{M_{soil}}{V_{total}}}{\frac{M_{soil}}{V_{soil}}} = 1 - \frac{\rho_d}{\rho_{soil}}$$

5.6.5 Solid to liquid ratio

This parameter gives an idea of the mass of soil per volume of porewater:

$$s{:}\,l = \frac{kg\ of\ soil}{l\ of\ water} = \frac{\frac{kg\ of\ soil}{l_{TOTAL}}}{\frac{l\ of\ water}{l_{TOTAL}}} = \frac{\rho_d}{\varepsilon}$$

So, for MX-80 it is

$$\frac{\rho_{d\ MX-80}}{\varepsilon_{MX-80}} = \frac{1.5\ kg/l}{0.36} = 4.17\ \frac{kg\ of soil}{l\ of\ water}$$

And for FEBEX:

$$\frac{\rho_{d\ FEBEX}}{\varepsilon_{FEBEX}} = \frac{1.65\ kg/l}{0.389} = 4.24\ \frac{kg\ of soil}{l\ of\ water}$$

5.6.6 Water velocity

As it is known, there is almost no water flowing through the bentonite, and this is an important reason explaining why this material is interesting as backfill for the canisters in waste repositories. The transport of radionuclides through bentonite is mainly due to diffusion and not to advection or dispersion, which induces the high interesting desired in a repository. The water velocity for the calculations is considered to be almost zero.

5.6.7 Diffusion coefficient

The compacted bentonite is treated as a homogenous porous medium in which all species are assumed to diffuse at the same rate. The MCOTAC input files require the molecular diffusion D_m coefficient, which is related to the effective diffusion D_e coefficient as follows:

$$D_e = \Phi \cdot D_m$$

Where o <Φ < 1 is the accessible porosity.

The effective diffusion coefficient contains all geometric and physical factors which reduce molecular mobility in the pore space compared to free water. For the MX-80 bentonite and taking the effective diffusion coefficient for Nickel reference, since it is a specie of direct interest for this thesis and it has the same diffusive coefficient as many other species according to [1]:

$$D_e = 2 \cdot 10^{-10}, \Phi = 0.36$$

$$D_e = \Phi \cdot D_m \rightarrow D_m = \frac{2 \cdot 10^{-10} m^2 s^{-1}}{0.36} = 5.56 \cdot 10^{-10} m^2 s^{-1}$$

For FEBEX, reference [15] (**Table 4**) provides the effective diffusion coefficient for HTO for the repository conditions. With it and the accessible porosity, the molecular diffusion coefficient is calculated:

$$D_e = \Phi \cdot D_m \rightarrow D_m = \frac{5.8 \cdot 10^{-11} m^2 s^{-1}}{0.389} = 1.49 \cdot 10^{-10}\ m^2 s^{-1}$$

5.6.8 Porewater composition

Table 1 details MX-80 and FEBEX bentonite compositions. The MX-80 composition comes from reference [16], i.e., a technical report form Nagra, and the FEBEX composition comes from reference [2] i.e., a final report from Enresa about the FEBEX experiment at the Grimsel facility.

The background concentration of Ni is very low compared to that of the Ni at the boundary, which is realistic in nature. Choosing different background concentrations but still very low compared to that at the boundary leads to no difference in the breakthrough curves.

Element	Concentration in MX-80 pw. [M]	Concentration in FEBEX pw. [M]
Na	$2.74 \cdot 10^{-1}$	$9.13 \cdot 10^{-2}$
K	$1.55 \cdot 10^{-3}$	$3.84 \cdot 10^{-4}$
Mg	$7.64 \cdot 10^{-3}$	$1.60 \cdot 10^{-2}$
Ca	$1.32 \cdot 10^{-2}$	$1.27 \cdot 10^{-2}$
Sr	$1.90 \cdot 10^{-5}$	$8.56 \cdot 10^{-5}$
Fe	$4.33 \cdot 10^{-5}$	$1.61 \cdot 10^{-6}$
Cl	$1.66 \cdot 10^{-1}$	$1.12 \cdot 10^{-1}$
SO_4	$6.16 \cdot 10^{-2}$	$1.31 \cdot 10^{-2}$
CO_3	$2.83 \cdot 10^{-3}$	$2.18 \cdot 10^{-3}$
Water type	Na-Cl	Na-Cl
pH	7.25	7.38
Ionic strength	0.32	0.19
s:l ratio	4.17:1	4.23:1

Table 5. MX-80 and FEBEX porewater composition used in the calculations

(As one can notice, in reference [2] the concentration units are [mg/l], so a previous unit conversion from mass to moles was necessary to get values in **Table 5**)

5.7 Chemical and sorption reactions

In total, 19 basis species and 55 complexes in solution and on surfaces were used for the reactive transport calculations. The thermodynamic data for all the reactions in solution taken into account in the reactive transport calculations are available in [17]. Moreover, in the appendices the MCOTAC input files used for the calculations are shown, where this thermodynamic data can be appreciated.

The sorption model used is the two sites protolysis non electrostatic surface complexation and cation exchange 2SPNE SC/CE model. The details of this model are described in a number of papers by Bradbury and Baeyens (1997, 2006) and in section 4.1.2.

The surfaces of Montmorillonite clay minerals carry a permanent negative surface charge, known as capacity of the clay. This charge is neutralised by the presence of an excess of bound cations near the surface, which can exchange with cations in solution. So, to simplify the models, a set of active sorption sites are conceived to be situated at the edges of clay platelets as hydroxyl groups (≡SOH) which can protonate and deprotonate and interact with aqueous metal species.

Three different sorption sites are considered: strong, weak 1 and weak 2. The ≡SSOH sites have a much smaller capacity, but form considerably stronger complexes with metals and dominate the sorption at trace concentrations. The sorption capacities for MX-80 are known [14] and for FEBEX are calculated with the Montmorillonite content ratio, as Montmorillonite is the responsible of sorption.

The surface complexation reactions considered are:

$$\equiv \mathrm{SOH} + \mathrm{Me}^{2+} \leftrightarrow \equiv \mathrm{SOMe}^{+} + \mathrm{H}^{+} \ (logK_0)$$

$$\equiv \mathrm{SOH} + \mathrm{Me}^{2+} + \mathrm{H_2O} \leftrightarrow \equiv \mathrm{SOMe}(OH)^{0} + 2\mathrm{H}^{+} \ (logK_1)$$

$$\equiv \mathrm{SOH} + \mathrm{Me}^{2+} + 2\mathrm{H_2O} \leftrightarrow \equiv \mathrm{SOMe}(OH)_2^{-} + 3\mathrm{H}^{+} \ (logK_2)$$

where Me^{2+} represents the Metal bivalent cations, like Ni^{2+} and Fe^{2+}. The reaction constants expressions are:

$$K_0 = \frac{[\equiv \mathrm{SOMe}^{+}]\cdot\{H^{+}\}}{[\equiv \mathrm{SOH}]\cdot\{Me^{2+}\}} \ ; \ K_0 = \frac{[\equiv \mathrm{SOMe}(OH)^{0}]\cdot\{H^{+}\}^2}{[\equiv \mathrm{SOH}]\cdot\{Me^{2+}\}} ; \ K_0 = \frac{[\equiv \mathrm{SOMe}(OH)_2^{-}]\cdot\{H^{+}\}^3}{[\equiv \mathrm{SOH}]\cdot\{Me^{2+}\}}$$

Only free cations and hydrolysed species are assumed as sorbates, and all other species are treated as being non-sorbing.

For the surface complexation reactions constants the Linear Free Energy Relationships (LFERs) is used [18]:

Strong sites:

$$log^{S}K_{x-1} = 8.1 \pm 0.3 + (0.90 \pm 0.02) log^{OH}K_x$$

Weak sites:

$$log^{W1}K_{x-1} = 6.2 \pm 0.8 + (0.98 \pm 0.09) log^{OH}K_x$$

Table 6 details the hydrolysis reaction constants [17].

Hydrolysis reactions	**$\log^{OH}K_x$**	
	Ni	**Fe**
$\mathrm{Me}^{2+} + \mathrm{H_2O} \leftrightarrow \ \mathrm{MeOH}^{+} \ + \mathrm{H}^{+}$	-9.86	-9.5
$\mathrm{Me}^{2+} + 2\mathrm{H_2O} \leftrightarrow \ \mathrm{Me(OH)}_2^{0} \ + 2\mathrm{H}^{+}$	-19.0	-20.6
$\mathrm{Me}^{2+} + 3\mathrm{H_2O} \leftrightarrow \ \mathrm{Me(OH)}_3^{-} \ + 3\mathrm{H}^{+}$	-30.0	-31.0

Table 6 Hydrolysis reactions constants

Furthermore, a charge balance correction is needed. As one can notice, despite these reactions are apparently charge balanced, they are non-charge balanced particularly on the surface and on the aqueous phase, which would be necessary because they are physically separated phases. Both surface and solution charges are neutralised with Na^+ or Cl^- ions, what is an assumption made because of the high concentration of NaCl in FEBEX and MX-80 bentonite porewaters relative to other components.

So the reactions finally are:

$$\equiv \mathrm{SOH} + \mathrm{Me}^{2+} + 2\mathrm{Cl}^- \leftrightarrow \equiv \mathrm{SOMe\_Cl} + \mathrm{H}^+ + Cl^- \ (\boldsymbol{logK_0'})$$

$$\equiv \mathrm{SOH} + \mathrm{Me}^{2+} + 2\mathrm{Cl}^- + \mathrm{H_2O} \leftrightarrow \equiv \mathrm{SOMe}OH + 2\mathrm{H}^+ + 2\mathrm{Cl}^- (\boldsymbol{logK_1'})$$

$$\equiv \mathrm{SOH} + \mathrm{Me}^{2+} + 2\mathrm{H_2O} + \mathrm{Na}^+ + 3\mathrm{Cl}^- \leftrightarrow \equiv \mathrm{SOMe(OH)_2\_}Na + 3\mathrm{H}^+ + 3Cl^- \ (\boldsymbol{logK_2'})$$

With new reaction constants defined, respectively:

$$K_0 = \frac{[\equiv \mathrm{SOMe\_Cl}]\cdot\{H^+\}}{[\equiv \mathrm{SOH}]\cdot\{Me^{2+}\}\cdot\{Cl^-\}};\ K_0 = \frac{[\equiv \mathrm{SOMe}OH]\cdot\{H^+\}^2}{[\equiv \mathrm{SOH}]\cdot\{Me^{2+}\}};\ K_0 = \frac{[\equiv \mathrm{SOMe(OH)_2\_}Na]\cdot\{H^+\}^3}{[\equiv \mathrm{SOH}]\cdot\{Me^{2+}\}\cdot\{\mathrm{Na}^+\}}$$

It may be convenient to remember that {} indicates activity, which is chemically defined as:

$$\{activity\} = \gamma \cdot [concentration]$$

where γ is the activity coefficient.

To get the corrected complexation constants, the non-charge balanced constants are calculated with the LFER relations and they are later corrected following the next relations:

$$logK_0' = logK_0 - \log\{Cl^-\}$$

$$logK_1' = logK_1$$

$$logK_2' = logK_2 - \log\{Na^+\}$$

Table 7 sum up surface complexation constants obtained for the 3 complexation reactions and for each site type, already charge balanced with either with Cl^- or Na^+. Protolysis constants are also indicated [14], corresponding to the next protolysis reactions:

$$\equiv \mathrm{SOH} + \mathrm{H}^+ + \mathrm{Cl}^- \leftrightarrow \equiv \mathrm{SOH_2}\_Cl \ (logK_{P1})$$

$$\equiv \mathrm{SOH} + \mathrm{Na}^+ + \mathrm{Cl}^- \leftrightarrow \equiv SO\_Na + \mathrm{H}^+ + \mathrm{Cl}^- \ (logK_{P2})$$

		MX-80			FEBEX		
		$\equiv S^{S}OH$	$\equiv S^{W1}OH$	$\equiv S^{W2}OH$	$\equiv S^{S}OH$	$\equiv S^{W1}OH$	$\equiv S^{W1}OH$
Protolysis	$logK_{P1}$	5.4	5.4	6.9	5.8	5.8	7.1
	$logK_{P2}$	-7.2	-7.2	-9.8	-6.3	-6.3	-9.3
Ni^{2+}	$logK'_0$	0.1	-2.6	-	0.3	-2.4	-
	$logK'_1$	-9.0	-12.4	-	-9.0	-12.4	-
	$logK'_2$	-18.2	-22.5	-	-17.7	-22.0	-
Fe^{2+}	$logK'_0$	0.5	-2.2	-	0.9	-2.0	-
	$logK'_1$	-10.4	-14.0	-	-10.4	-14.0	-
	$logK'_2$	- 19.1	-23.5	-	-18.2	-23.0	-

Table 7 Surface complexation constants and site capacities

Regarding the site capacities, the data for MX-80 reference from [14] and the FEBEX data, as no published data has this information, is directly obtained with the Montmorillonite contents relation.

Site types	Site capacities MX-80 [mol·kg^{-1}]	Site capacities FEBEX [mol·kg^{-1}]
$\equiv S^{S}OH$	$1.5 \cdot 10^{-3}$	$1.8 \cdot 10^{-3}$
$\equiv S^{w2}OH$	$3 \cdot 10^{-2}$	$3.7 \cdot 10^{-2}$
$\equiv S^{w2}OH$	$3 \cdot 10^{-2}$	$3.7 \cdot 10^{-2}$
Cation exchange capacity (CEC)	$8.1 \cdot 10^{-1}$	$9.7 \cdot 10^{-1}$

Table 8 Sorption sites capacities

5.8 Boundary conditions

A bentonite-canister left boundary (x=0 m) without flow, from where radionuclides (Ni as the representative radionuclide for this thesis) in the canister would enter to the bentonite, is assumed. During this injection there is no water flow inside the canister. The concentration of Ni is chosen to avoid precipitation occurring in the porewater (10^{-5} and 10^{-7} M for different analysis). At each time step, Ni is released into the porewater of the first bentonite control volume and it diffuses into the column.

On the other side (right), at x=0.7 meters, a free outflow boundary condition is used.

6 Propagation of the LFER uncertainty to reactive transport calculations

As experimental methodologies and techniques for obtaining complexation constants are very time consuming and therefore lacking for a lot of cations, when Bradbury & Baeyens [19] developed their complex sorption model, they delivered at the same time a Linear Free Energy Relationship (LFER) [18] to calculate surface complexation constants for cations on minerals, deduced from hydrolysis constants for cations, for which a lot of data is available from experiments. The derivation of the LFER from this data is accompanied by an uncertainty for values of the surface complexation constants, given by the following equations for strong and weak sites for Na-Montmorillonite [18]:

Strong sites:

$$log^{S}K_{x-1} = 8.1 \pm 0.3 + (0.90 \pm 0.02) log^{OH}K_{x}$$

Weak sites:

$$log^{W1}K_{x-1} = 6.2 \pm 0.8 + (0.98 \pm 0.09) log^{OH}K_{x}$$

Therefore, an analysis of the propagation of this uncertainty is necessary when using this data in reactive transport calculations (as, in fact, it is the case of this thesis). This analysis is carried out with the reactive transport code MCOTAC [12], for Ni(II) as an example of bivalent metal migrating through Na-Montmorillonite, the main mineral of bentonite.

Calculations were done using the MX-80 and FEBEX bentonite models described before, taking also into account sorption competition of Ni(II) and Fe(II), which increases the uncertainty space since in addition to Ni(II) surface complexation constants also surface complexation constants for Fe(II) are involved in the reactive transport calculation for the Ni(II) migration. Calculations were performed with and without taking into account weak sorption sites.

One has to keep in mind that LFER relationships include a bandwidth around a reference value and not an uncertainty distribution which would imply that the maximum and minimum values would be less likely than the reference value.

In the next figures Ni(II) breakthrough curves are shown using the maximum, reference and minimum values of the surface complexation constants calculated according to the LFER. The initial hypothesis is that the bandwidth of the surface complexation constants will transfer to a spreading between the breakthrough curves within a range of several hundreds of years, even thousands in some cases. This spreading is expected to increase with the incorporation of weak sites in addition to the strong sites and including Fe(II)-Ni(II) competition for sorption sites to the model.

In **Fig. 33** the breakthrough curves at x=0.33 m show already considerable differences between the three cases. Especially if the focus is on first arrival times then the spreading is from 20 years to 200 years at 0.33 cm within the bentonite. If the focus is on the 50% Ni(II) concentration level (**Fig. 34**) then the spreading of the breakthrough time is from 600 to 1200 years.

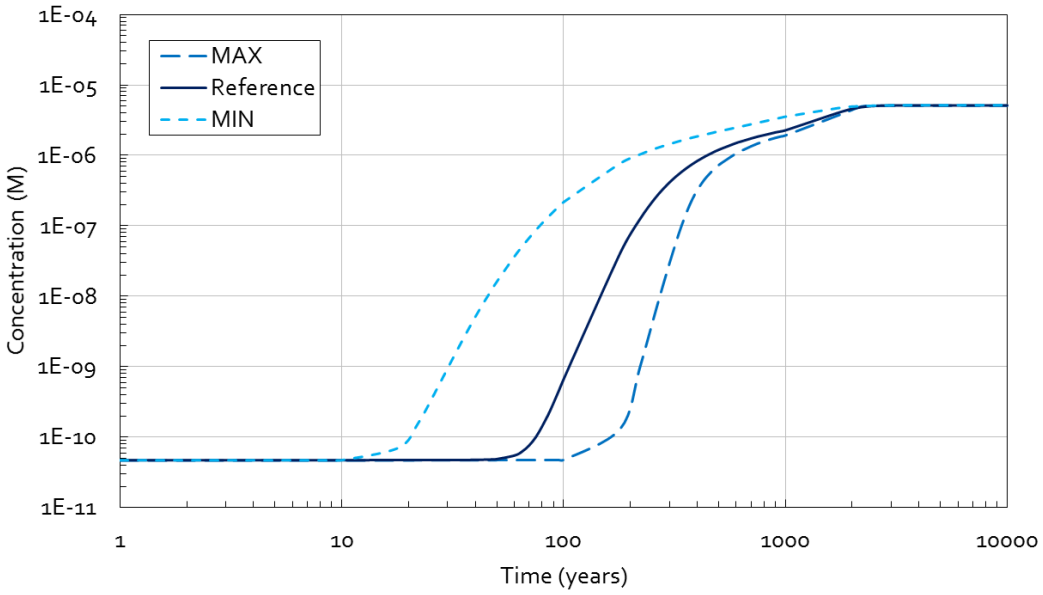

Fig. 33 Only strong sites. Ni (II) breakthrough curves at x=0.33 m into the MX-80 bentonite calculated for the LFER uncertainty range with MCOTAC.$(Ni(II)_{EQBM}$ level is 10-5 M; **NO sorption competition** with Fe (II) assumed)

From now on, in this section, only the calculated breakthrough curves near the outer radius of the bentonite buffer will be used for the analysis of the results, as this is the main distance of interest for the safety assessment of the repository.

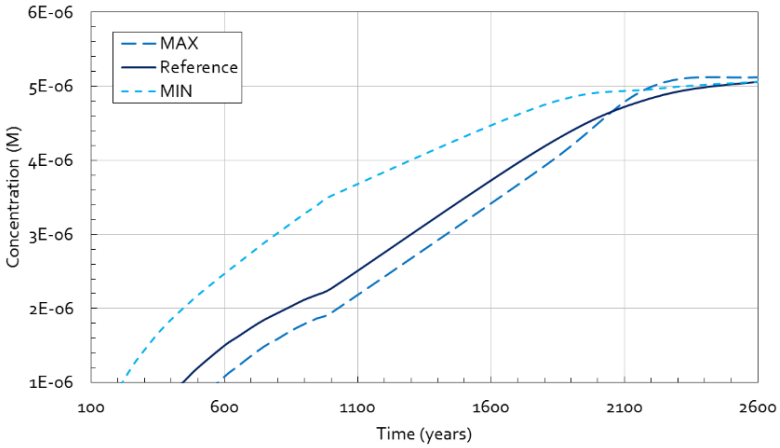

Fig. 34 Zoom to the breakthrough curves in Fig. 34, now linear scale. This figure allows better observation of the time differences mentioned at the 50% of the final Ni(II) concentration level.

With **Fig. 35** and **Fig. 36** the disagreement between including sorption competition with Fe(II) and not including it can be observed, at the moment only considering the presence of strong sites. Whilst the direct suspicion may be the contrary, the increase of the uncertainty space due to the incorporation of the Fe(II) surface complexation constants, for the case with sorption competition with Fe(II), does not lead to an increased spreading of the calculated Ni(II) breakthrough curves, due to the expected lower retardation of Ni(II). That means that Ni(II) sorption is not that important now, and therefore the propagated uncertainty becomes lower. Only about 5 to 50 years of difference are found in this case, while some hundreds years of disagreement are found in the case that sorption competition is not included in the model.

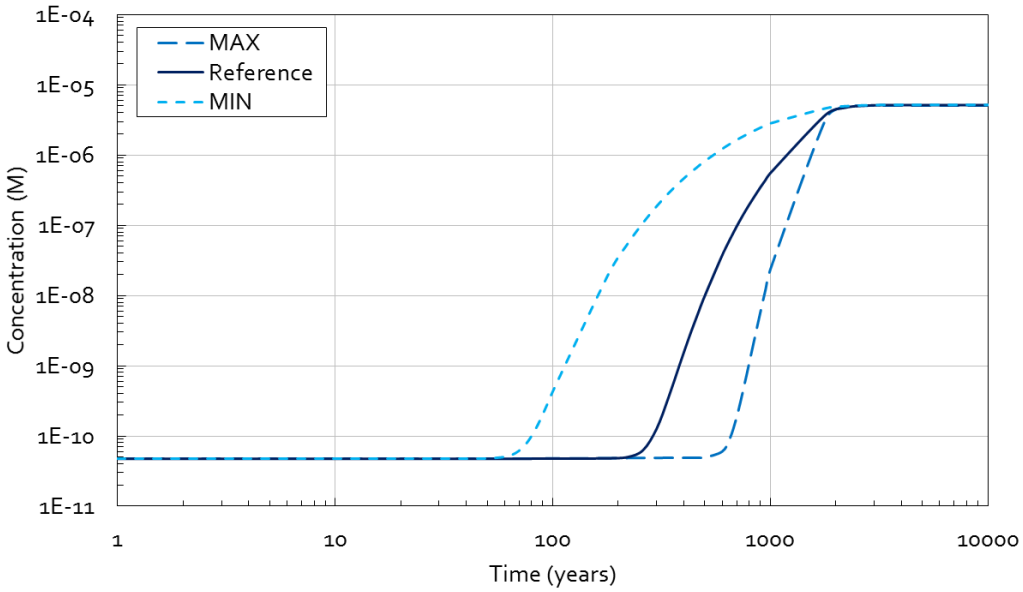

Fig. 35 Only strong sites Ni (II) breakthrough curves at x=0.61 m into the MX-80 bentonite calculated for the LFER uncertainty margin with MCOTAC. $(Ni(II)_{EQBM}$ level is 10^{-5} M; **NO sorption competition** with Fe (II) assumed).

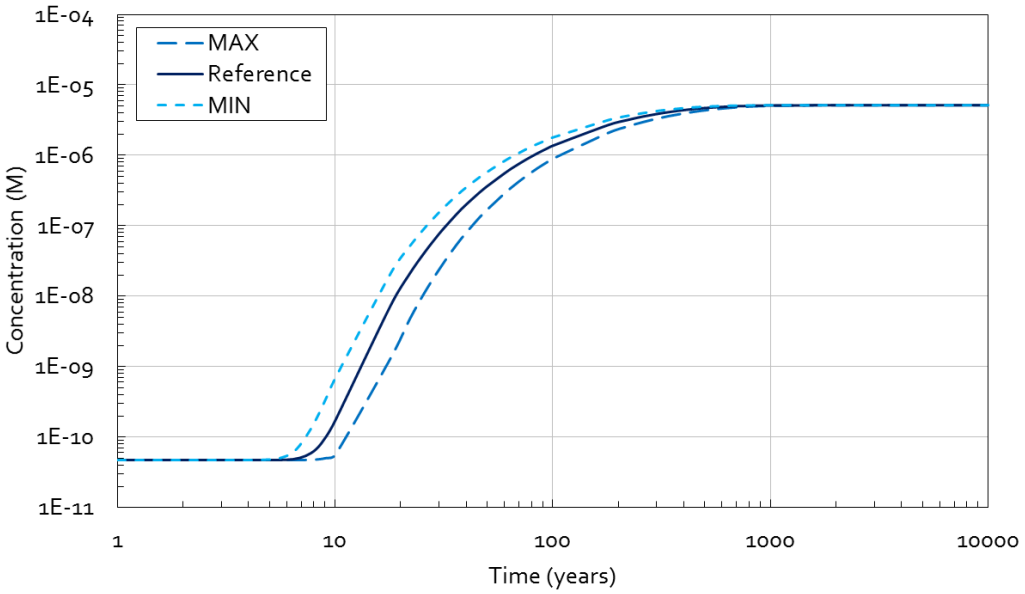

Fig. 36 Only strong sites. Ni (II) breakthrough curves at x=0.61 m into the MX-80 bentonite calculated for the LFER uncertainty margin with MCOTAC. ($Ni(II)_{EQBM}$ level is 10^{-5} M; **sorption competition** with Fe (II) assumed).

The same effects are observed for the FEBEX bentonite (**Fig. 37**); taking into account the later breakthrough times, similar results were calculated.

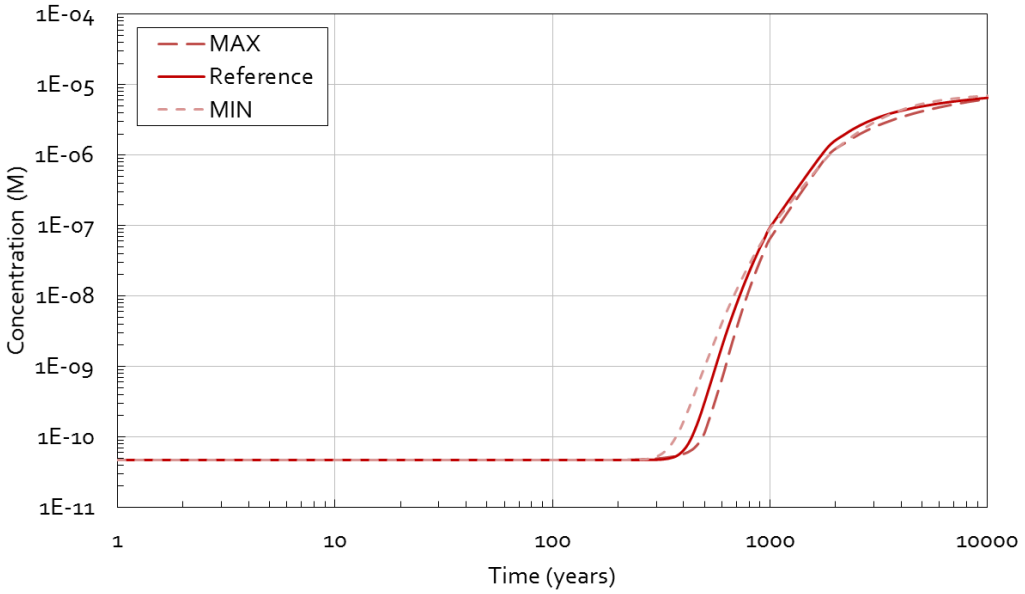

Fig. 37 Only strong sites. Ni (II) breakthrough curves at x=0.61 m into the FEBEX bentonite calculated for the LFER uncertainty margin with MCOTAC. ($Ni(II)_{EQBM}$ level is 10^{-5} M; **sorption competition** with Fe (II) assumed).

So far only the propagation of the uncertainty generated by the LFER equations for strong sites was evaluated. If weak sites are included to the models, the uncertainty bandwidth of their LFER relationships propagates also into the transport calculation, which makes the bandwidth between curves increase (**Fig. 38** and **Fig. 39**), as expected. **Fig. 39** and **Fig. 38** are compared to **Fig. 35** and **Fig. 36**, respectively, for the cases without and with competition.

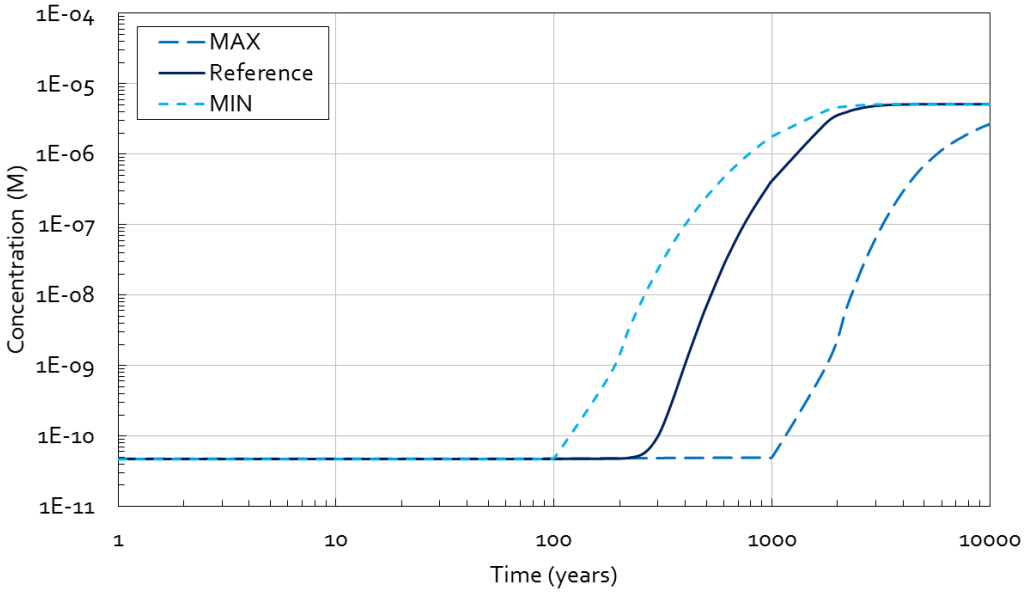

Fig. 38 Strong & Weak sites. Ni (II) breakthrough curves at x=0.61 m into the MX-80 bentonite calculated for the LFER uncertainty margin with MCOTAC. $(Ni(II)_{EQBM}$ level is 10^{-5} M; **NO sorption competition** with Fe (II) assumed).

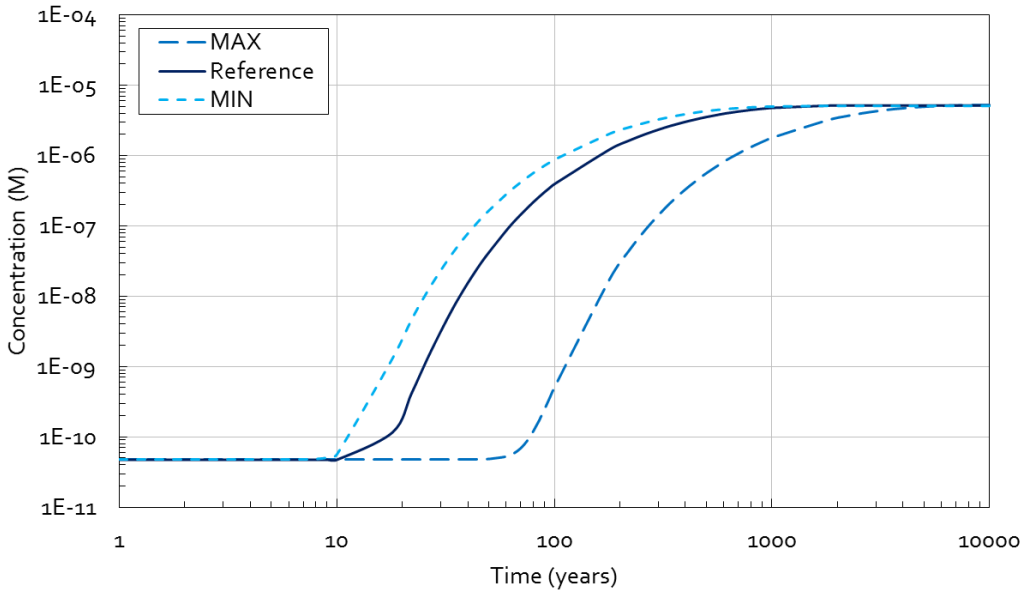

Fig. 39 Strong & Weak sites. Ni (II) breakthrough curves at x=0.61 m into the MX-80 bentonite calculated for the LFER uncertainty margin with MCOTAC. $(Ni(II)_{EQBM}$ level is 10^{-5} M; **sorption competition** with Fe (II) assumed).

Weak sites add an additional sorption process and if one maximizes the additional sorption process (maximum surface complexation constants) then the calculated breakthrough curves are strongly retarded. If this additional sorption effect is taken into account only minimal (minimum surface complexation constants) then the differences to not taking into account sorption on weak sides are less pronounced. This explains the wider difference of the curve on the right from the reference case than on the left side.

It is also appropriate to analyze the different propagation that the LFER bandwidth into the bentonites with different properties: MX-80 and FEBEX. It is difficult to predict how different these differences are, because of their dependence on many phenomena: logarithmic relationships, Fe concentration, Montmorillonite content, Cl^- and Na^+ concentrations, etc.

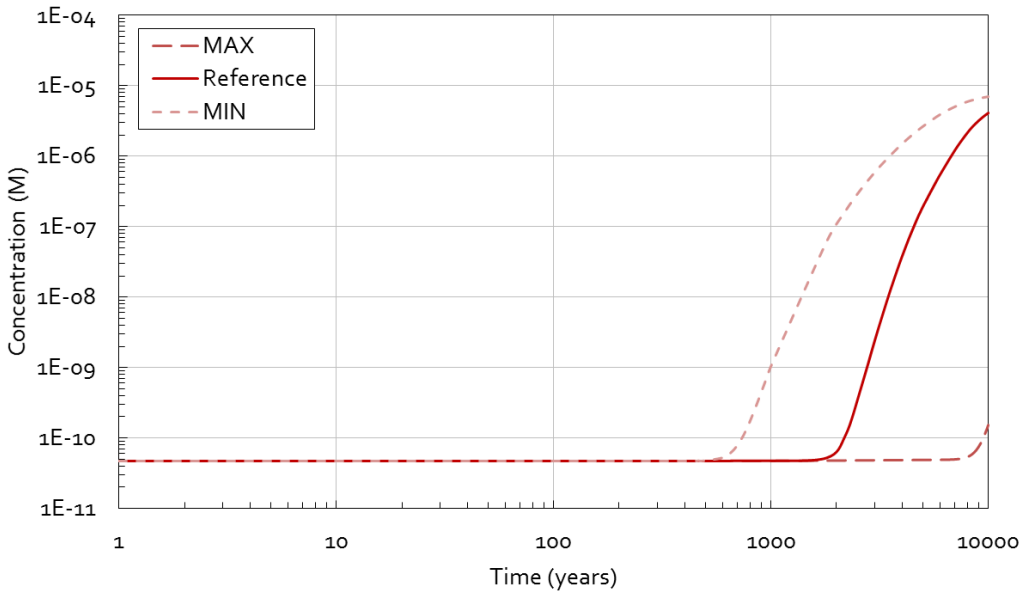

Fig. 40 Strong & Weak sites. Ni (II) breakthrough curves at x=0.61 m into the FEBEX bentonite calculated for the LFER uncertainty margin with MCOTAC. ($Ni(II)_{EQBM}$ level is 10^{-5} M; **NO sorption competition** with Fe(II) assumed).

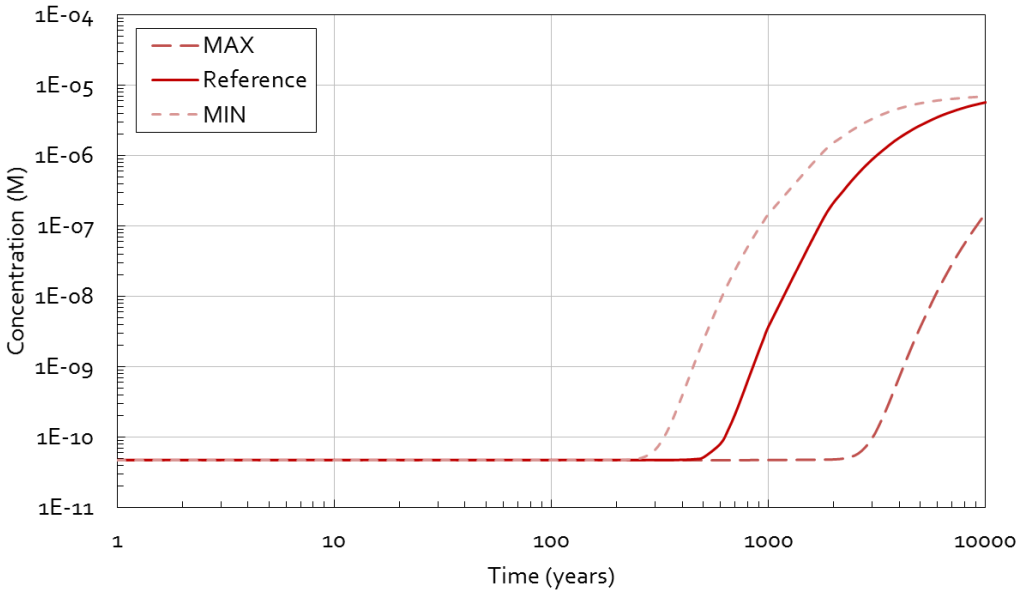

Fig. 41 Strong & Weak sites. Ni (II) breakthrough curves at x=0.61 m into the FEBEX bentonite calculated for the LFER uncertainty margin with MCOTAC. ($Ni(II)_{EQBM}$ level is 10^{-5} M; **sorption competition** with Fe (II) assumed).

In these last figures **Fig. 40** and **Fig. 41** is detected a wider bandwidth between breakthrough curves for FEBEX than for MX-80. The later breakthrough times induces these wider differences, pronounced also in the case of the maximization of the sorption parameter. Disagreements of several thousands of years between the two bentonites bandwidths are found, and this is an evidence of the LFER uncertainty propagation dependence on the conditions of the medium.

However, the differences are difficult to be quantified using the logarithmic representation. For a better inspection, plots with linear concentration and time scales are provided (**Fig. 42** and **Fig. 43**). One has to take into account the different concentration and time scales used to zoom the zones of interest. As reference, the 50% of the final concentration of free cation of Ni(II) is used for the comparison. This does not mean that the most significant differences are found at this concentrations, because they usually increase for higher concentrations. For FEBEX the total final equilibrium concentration is about $7.5 \cdot 10^{-6}$ M and for MX-80 it is $5 \cdot 10^{-6}$ M.

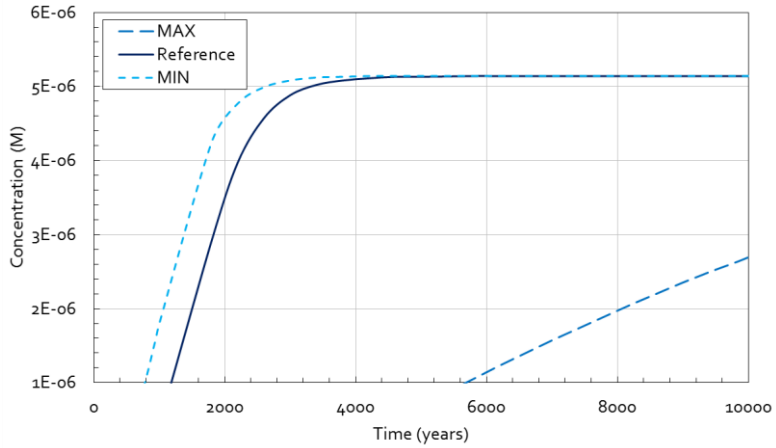

Fig. 42 Zoom to the breakthrough curves in **Fig. 38**

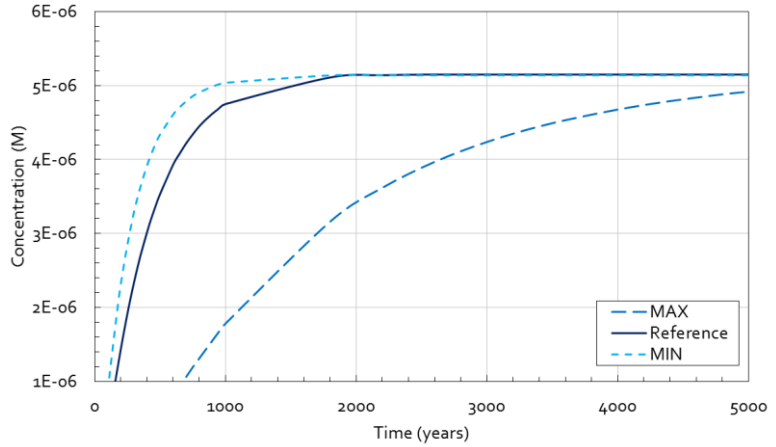

Fig. 43 Zoom to the breakthrough curves in **Fig. 39**.

For MX-80 there are differences of 9000 and 1200 years for the cases without and with competition, respectively, between the minimum and maximum calculated curves at the reference concentration of 50% of the final equilibrium concentration.

In the FEBEX case the calculation times are not long enough to cover the case of the maximum sorption parameters, and that is why a zoomed representation is not useful for a visual deduction of the time bandwidth at the 50% of final concentration. With **Fig. 40** and **Fig. 41** one can conclude that the bandwidths at this concentration are longer than 10000 years. However, for the case without competition this value is higher than for the case with competition.

Finally, **Table 9** summarizes quantitatively the differences found in all cases, as time bandwidths (years) between calculated curves corresponding to minimum and maximum surface complexation constants for a reference concentration of 50% of the final levels reached at x=0.61 for the free cation of Ni(II).

	NO Ni(II)-Fe(II) COMPETITION		Ni(II)-Fe(II) COMPETITION	
	Only strong sites	**Strong&Weak sites**	**Only strong sites**	**Strong&Weak sites**
MX-80	800 years	9000 years	80 years	1200 years
FEBEX	2200 years	>>10000 years	1000 years	>10000 years

Table 9 Time bandwidths at 50% of the final equilibrium concentration for different bentonite model configurations at x=0.61m.

As conclusion, it is clear that when more processes are taken into account in the modelling– "without" to "with" sorption competition with Fe(II) – the bandwidths decrease, although the wider uncertainty zone, due to the earlier breakthroughs. When weak sites are incorporated, the uncertainty zone increase, which generates an important increase of the bandwidths, as the breakthroughs occur begin at similar times. The bandwidths depend also on the system: FEBEX has always wider bandwidths, due to its higher retardation capacity. The order of magnitude of these bandwidths goes from 10^1 to 10^3 years, depending on the case.

This analysis, apparently straightforward, demonstrates the propagation of the uncertainty included in the LFER to reactive transport calculations, which should be kept in mind. For the bentonite backfill of a deep geological repository, the calculated differences for Ni(II) rise to several hundreds or even thousands of years, which apparently is not of high significance compared to the lifetime of a high level nuclear waste repository. More important is to take into account the appropriate processes as for example Ni(II) sorption competition with Fe(II) and the differences found when weak sorption sites uncertainties are incorporated.

In addition, the uncertainty of values for the surface complexation constants calculated using the LFER should be addressed when deducing for example diffusion coefficients for radionuclides from laboratory diffusion experiments, since the sorption parameter uncertainty transfers directly to the determination of the diffusion coefficient.

7 MX-80 vs FEBEX

7.1 Kd model

The first comparison between the two bentonites is carried out with the easiest and generally used Kd model. In section 4.1.1 there are the necessary theoretical remarks for the understanding of this model.

The particular interest for this model in this thesis arises from its use in the safety assessments made up to now by Nagra for the geological repository. However, reactive transport calculations are hypothetically much more complex and so more realistic.

On the other hand, Kd model will also work as a reference for later MCOTAC calculations, to check if the code is performing correctly.

The solution of the Kd model for this thesis is analytical, in contrast with the next numerical calculations performed with MCOTAC. Basically it consists on the solution of the next equation, demonstrated in section 4.1.1.

$$C(x,t) = \frac{C_0}{2}\left\{erfc\frac{Rx}{2\sqrt{RDt}}\right\}$$

with R related to Kd:

$$R = 1 + K_d \cdot \rho_b/\varepsilon$$

where

$\boldsymbol{\rho_b}$ is the bulk dry density ρ_d of the soil $[kg \cdot m^{-3}]$

$\boldsymbol{\varepsilon}$ is the accessible porosity

$\boldsymbol{K_d}$ is the sorption value $[m^3 \cdot kg^{-1}]$

$$K_d = \frac{Mass\ of\ adsorbate\ sorbed}{Mass\ of\ adsorbate\ in\ solution} = \frac{\frac{moles\ of\ adsorbte}{kg\ of\ soil}}{\frac{moles\ of\ adsorbate}{l\ of\ liquid}} = [l/kg]$$

These Kd are provided by experimental data for MX-80 bentonite [19] (**Fig. 52**).

$$K_{d,MX80} = 0.2 \frac{m^3}{kg}$$

The Kd value for the FEBEX bentonite, as it is not available, is deduced using the Montmorillonite content relation between both bentonites because of the Montmorillonite is the mineral in MX-80 responsible for sorption . Then, it is:

$$K_{d,FEBEX} = K_{d,MX80} \cdot \frac{92\ wt\%\ Montmorillonite\ FEBEX}{75\ wt\%\ Montmorillonite\ MX80} = 0.2 \frac{m^3}{kg} \cdot 1.23 = 0.245 \frac{m^3}{kg}$$

$\rho_b, \varepsilon\ and\ D$ are already provided during the setup section (5.6) for both bentonites.

The corresponding retardation factors (dimensionless) are:

$$R_{MX80} = 834.33$$

$$R_{FEBEX} = 1041.62$$

Breakthrough curves and concentration profiles for injections of 10^{-5} M and 10^{-7} M Nickel were calculated using the Kd approach. These concentrations of Nickel are concentrations levels that could be found in the repository nearfield where the sources of Nickel are the waste canisters.

Regarding the comparison between FEBEX and MX-80, an initial hypothesis would be that FEBEX has more retardation capacity, due to the higher content of Montmorillonite. This hypothesis is confirmed by the next plots, where there are lower concentrations of tracer (Ni) during the breakthrough time, i.e. the Nickel Breakthrough curve for FEBEX bentonite is stronger retarded compared to the one calculated for MX-80 bentonite.

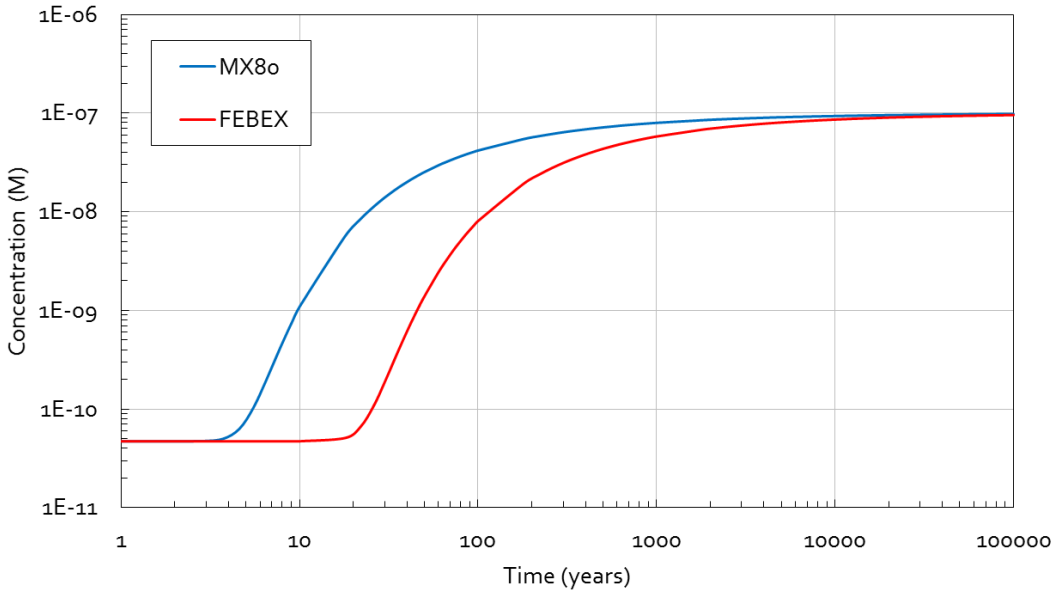

Fig. 44 Ni (II) breakthrough curves at x=0.0525 m into the bentonite calculated for the constant Kd approach. $(Ni(II)_{EQ}$ level is 10^{-7} M)

In **Fig. 44** the early increase of concentration in a position very near to the boundary (5 cm) for MX-80 and FEBEX are compared. As a first conclusion, this figure shows that according to the Kd model, the Nickel will need around 1000 years to reach its equilibrium concentration at points near the boundary.

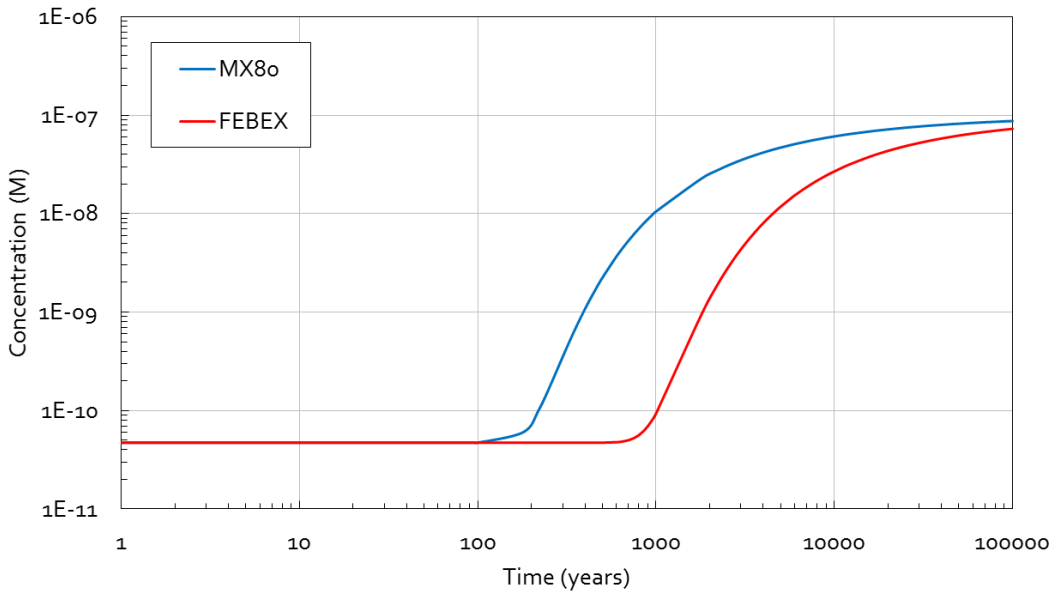

Fig. 45 Ni (II) breakthrough curves at x=0.3325 m into the bentonite calculated for the constant Kd approach. $(Ni(II)_{EQ}$ level is 10^{-7} M)

Furthermore, the initial hypothesis that FEBEX would be more retarding than MX-80 is confirmed. That means that the concentration of Ni increases later (17 years) within FEBEX than within MX-80, because the first one sorbs more Ni already in the first 5 cm.

For farther positions (**Fig. 46, Fig. 47**), the breakthroughs are obviously later, as the injected Ni needs longer times to diffuse until there.

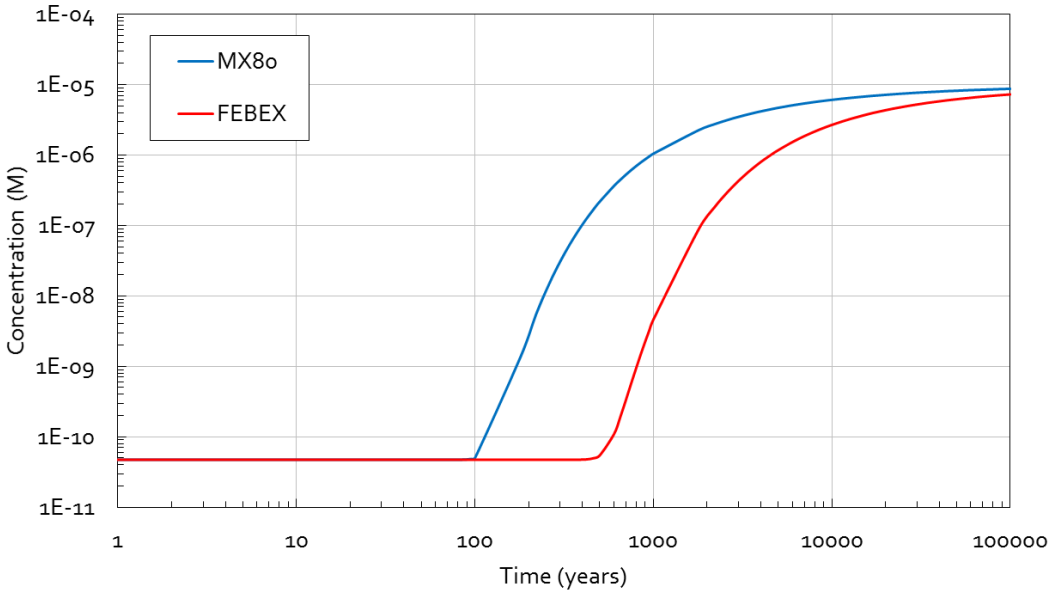

Fig. 46 Ni (II) breakthrough curves at x=0.3325 m into the bentonite calculated for the constant Kd approach. $(Ni(II)_{EQ}$ level is 10^{-5} M)

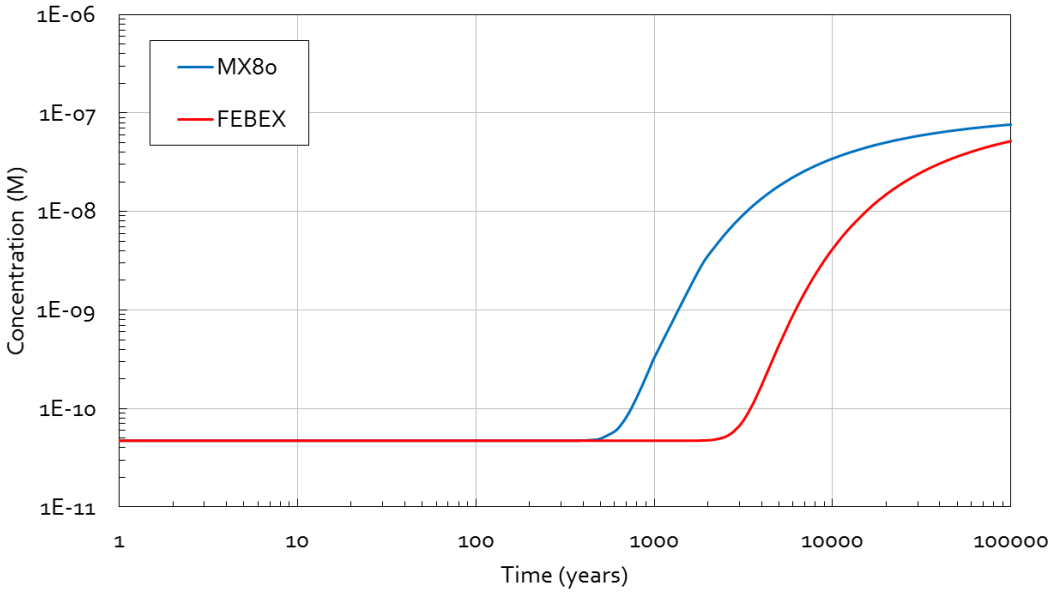

Fig. 47 Ni (II) breakthrough curves at x=0.6125 m into the bentonite calculated for the constant Kd approach. $(Ni(II)_{EQ}$ level is 10^{-7} M)

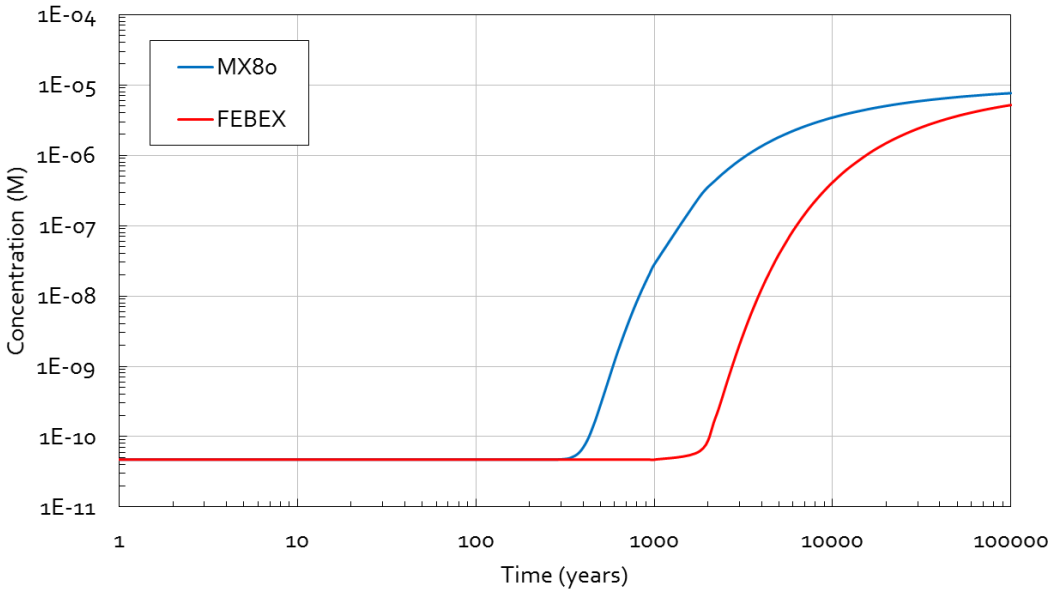

Fig. 48 Ni (II) breakthrough curves at x=0.6125 m into the bentonite calculated for the constant Kd approach. $(Ni(II)_{EQ}$ level is 10^{-5} M)

In **Fig. 48** the same Kd model at a position of 61 cm away from the Ni source is plotted, but with an important difference: the injection of Ni has now a higher concentration of 10^{-5}M. Logically, the equilibrium concentration after Ni diffuse until this distance is 10^{-5}M.

7.2 Reactive transport calculations: without Ni(II)-Fe(II) sorption competition

After calculating the diffusive transport using the Kd-model, in the following reactive transport calculations are performed using the mechanistic sorption model.

In this section, the implementation of MCOTAC to the MX-80 and FEBEX bentonite models will lead to a second comparison between both bentonite types. The competition of Ni(II) and Fe(II) for sorption sites is still not taken into account.

Firstly, as these are the first results of the reactive transport calculations, an appreciation about the curves that will be continuously shown and interpreted from now on is necessary. In **Fig. 49** the concentration of pure Ni tracer at x=0.61 meters is plotted. This position is located almost at the end of the bentonite thickness. As one can appreciate, the concentrations of pure Ni tracer both in the MX-80 and the FEBEX models do not reach the 10^{-5} M equilibrium concentration. What is missing? As chemical reactions are now taking part in the calculation, as this is reactive transport, Ni is not only diffusing individually but also involved in many complexation sorption reactions. That is why it is impossible that the pure Ni (tracer) final equilibrium concentration reaches the same value as the one injected at the boundary, as it is distributed to other species taking part in the bentonite medium. However, the total Ni(II) concentration in solution should reach this level.

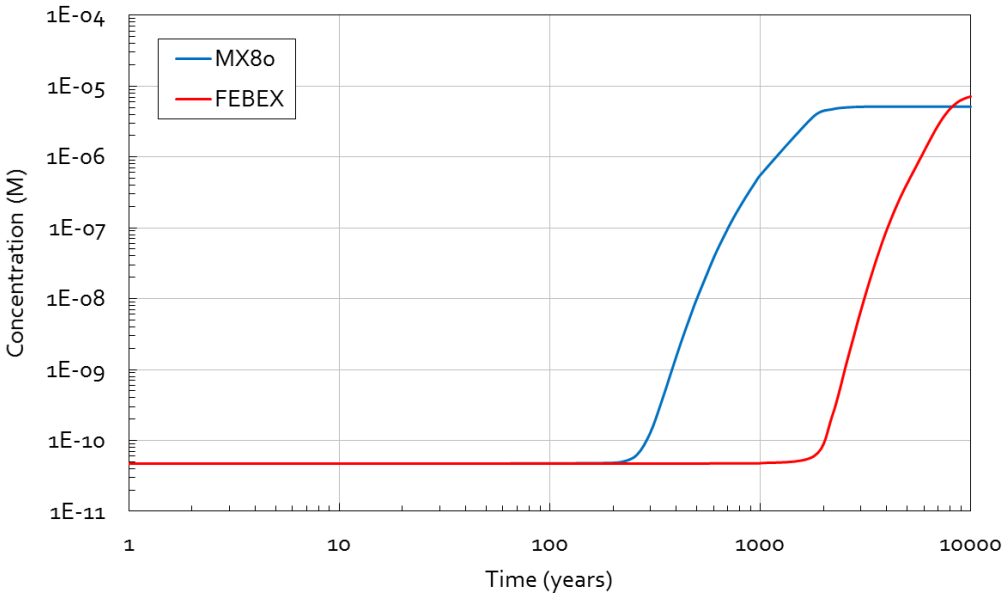

Fig. 49 (Pure tracer) Ni (II) breakthrough curves at x=0.6125 m into the bentonite calculated with MCOTAC. ($Ni(II)_{EQ}$ level is 10^{-5} M, no sorption competition with Fe(II))

The contribution of the complexes concentration is analyzed to get an idea about their importance on the interpretation of the results, i.e., to verify how different are the curves shown in **Fig. 49** if the complexes of Ni are taken into account (**Fig. 50**), TOTAL Ni Equilibrium concentrations).

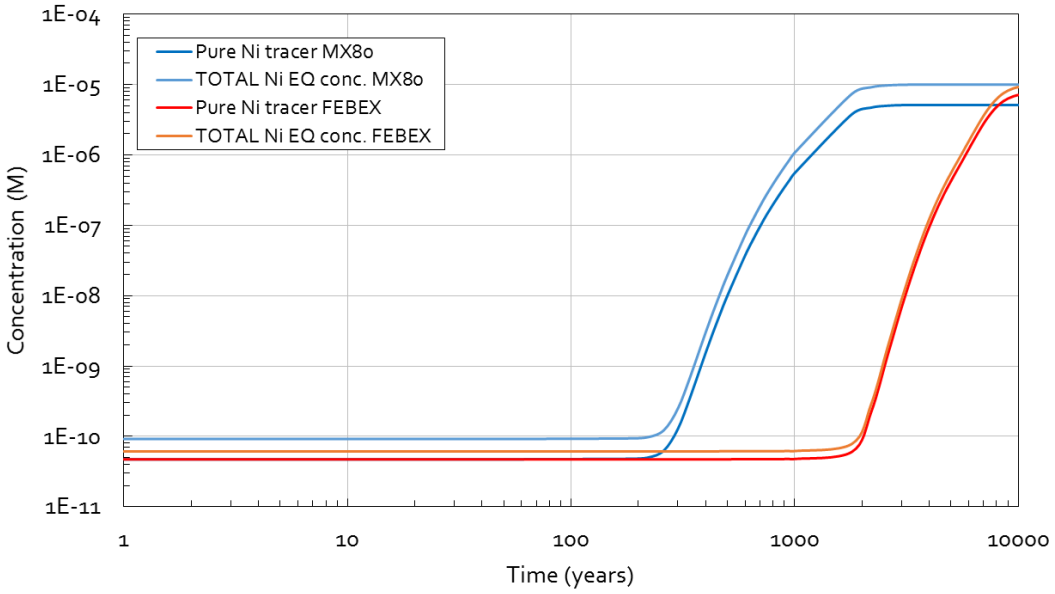

Fig. 50 Ni (II) breakthrough curves at x=0.6125 m into the bentonite calculated with MCOTAC. $(Ni(II)_{EQ}$ level is 10^{-5} M, no sorption competition with Fe(II))

In **Fig. 50** the contribution of the complexes is considered (visible differences between both cases). At the end, the total concentration of 10^{-5}M is reached, thanks to the contribution of the complexes, which is not low (logarithmic scale). However, they are not necessary for interpretation of the results, in terms of comparing diffusion transport of radionuclides in different bentonite conditions and in different configurations of the sorption model. However, one must keep in mind that complexation and sorption reactions are an essential point of the reactive transport calculations. Therefore, in further graphical results they will not be included, although they are taken into account in the models.

At this point transport predictions given by the Kd-model and the reactive transport results can be compared (MCOTAC, no sorption competition): **Fig. 51**.

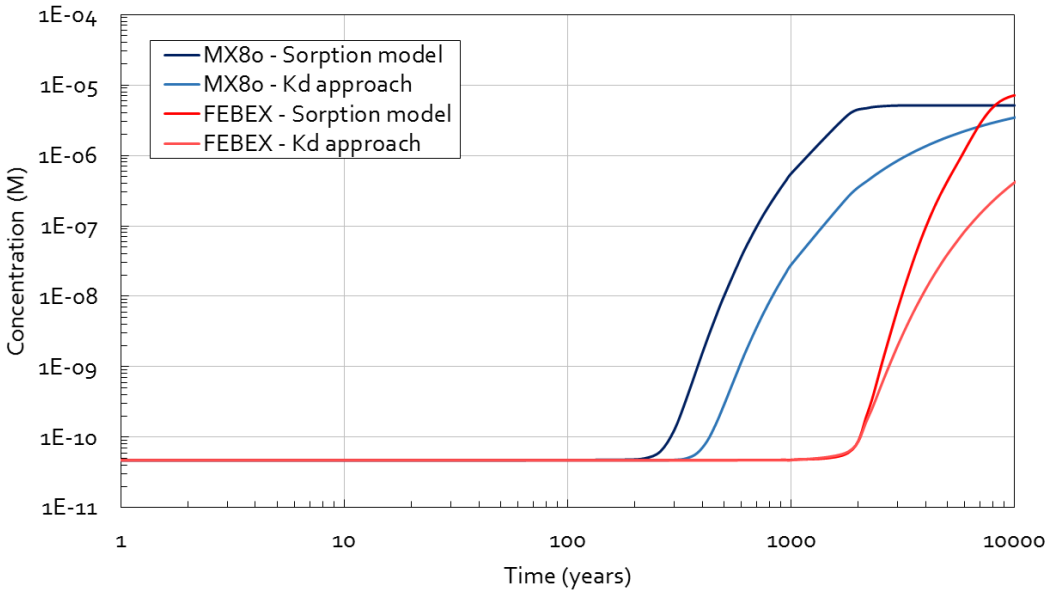

Fig. 51 Ni (II) breakthrough curves at x=0.6125 m into the bentonite calculated fot the constant Kd approach (Kd=0.2m^{3}kg^{-1}) and with MCOTAC ($Ni(II)_{EQ}$ level is 10^{-5} M, no sorption competition with Fe(II))

As the Kd approach for both bentonites is on the right of the MCOTAC calculation curves, i.e. later breakthrough times, one could easily conclude that the Kd approach is not (or less) conservative. Nonetheless, Nagra provides (**Fig. 52,** [19]) pessimistic and optimistic levels of Kd. In **Fig. 52** these pessimistic and optimistic levels are graphically compared. The experimental origin of this Kd values must be taken into account.

Elemer	K_d		
	Ref. case	**Lower limit (pessimistic)**	**Upper limit (optimistic)**
	[m^3 kg^{-1}]	**[m^3 kg^{-1}]**	**[m^3 kg^{-1}]**
H	**0**	0	0
Be	**0.2**	0.009	5
C_{inorg}	**6×10^{-5}**	2×10^{-5}	3×10^{-4}
C_{org}	**0**	0	0
Cl	**0**	0	0
Ca	**0.003**	5×10^{-4}	0.02
Ni	**0.2**	0.009	5
Se	**0**	0	0
Sr	**0.003**	5×10^{-4}	0.02

Fig. 52 Kd values by Nagra. Reference, optimistic and pessimistic cases.

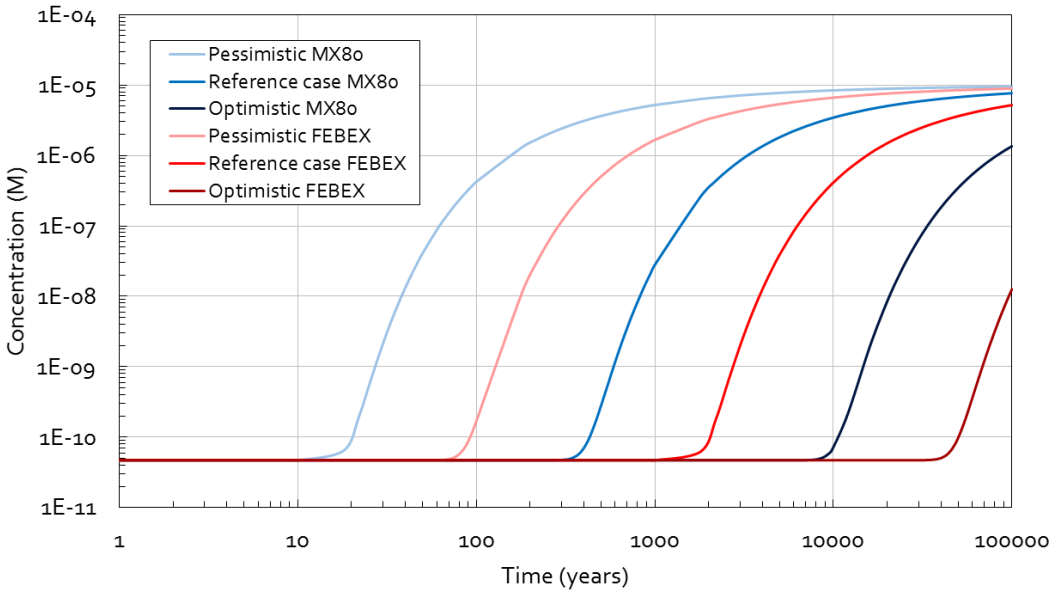

Fig. 53 Ni (II) breakthrough curves at x=0.6125 m into the bentonite calculated for the constant Kd approach $(Ni(II)_{EQ}$ level is 10^{-5} M, no sorption competition with Fe(II))

Fig. 53 shows the large differences between the optimistic, reference and pessimistic cases. From now on only the reference case will be considered and represented, but this wide range must be kept in mind when comparing the Kd model to reactive transport calculations.

At this point, the comparison between MX-80 and FEBEX is ready. Up to now, for the case without considering Ni(II) and Fe(II) competing for sorption sites, it seems that the breakthroughs for MX-80 happen earlier than for FEBEX. That means that the concentration increase before in MX-80, which makes this kind of bentonite less retarding and therefore worse for the deep geological repository if only its retardation capacity is considered. To complete this comparison it is necessary to compare the evolution of the concentration in time and space. The next **Fig. 54** provides another of view of the results, which is that of the concentration profile along the column at different times.

These concentration profiles confirm that FEBEX is performing a higher retardation to the Ni tracer (not only in the Kd model but also in the MCOTAC sorption model). Without any references about the case that considers sorption competition between Ni(II) and Fe(II), it seems that there are modelling evidences that the FEBEX bentonite has more retardation capacity than MX-80.

*(**MX-80 vs FEBEX:** No Ni(II)-Fe(II) sorption competition)*

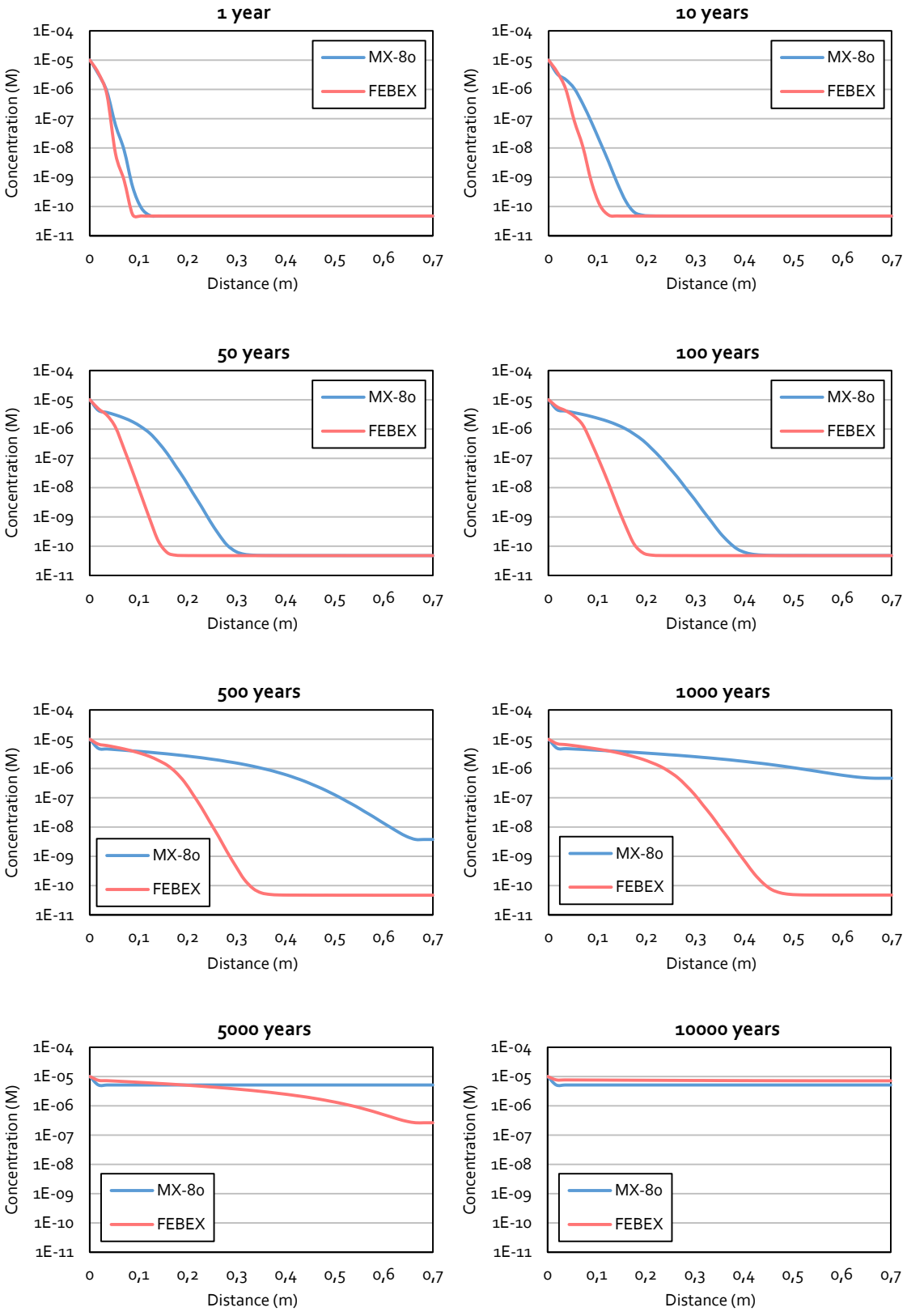

Fig. 54 Concentration profiles of tracer of Ni (II) into the 0.7 meters column of bentonite for different times ($(Ni(II)_{EQ}$ level is 10^{-5} M, no sorption competition with Fe(II)).

7.3 Reactive transport calculations: with Ni(II)-Fe(II) sorption competition

In this section the same MCOTAC calculations are carried out, but incorporating the surface complexation reactions for Fe(II). Therefore, bentonites are expected to have less retardation capacity of Ni, due to that sorption sites are occupied not only by Ni but also by Fe.

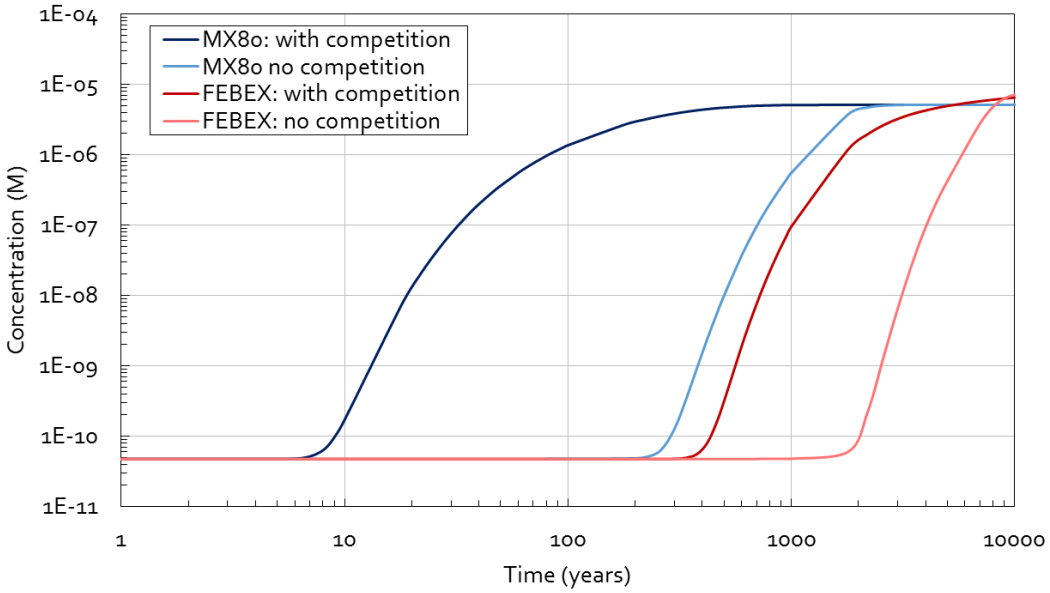

Fig. 55 Ni (II) breakthrough curves at x=0.6125 m into the bentonite calculated with MCOTAC. $(Ni(II)_{EQ}$ level is 10^{-5} M)

The differences between curves in each bentonite are only caused by the presence of Fe sorbing on sorption sites. Therefore, one can determine the consequences of this phenomena comparing these curves in each bentonite.

As it can be appreciated in **Fig. 55**, the presence of Fe sorbing on sorption sites has a big influence on the sorption and migration of Ni(II) both in FEBEX and MX-80, anticipating the breakthrough curve.

Regarding the comparison between FEBEX and MX-80, FEBEX has still more retardation capacity than MX-80 regardless of the sorption competition. Its content of Montmorillonite is higher, which makes the concentration of sorption sites also higher, available now for sorbing Ni(II) and Fe(II). The concentrations of Na and Cl are higher in MX-80, so (according to section **5.7**) the surface complexation constants are lower in MX-80 than in FEBEX both for Ni(II) and Fe(II) (**Table 7**, section **5.7**), which induces also a lower sorption than FEBEX.

Furthermore, the specific influence of the sorption competition within each bentonite type must be also analyzed. In a first observation it seems that the transport within FEBEX is more

affected by the sorption competition (logarithmic scale). Comparing initial breakthroughs, the absolute time differences for FEBEX are about 1600 years, while in MX-80 these are around 250 years. However, comparing relative differences, FEBEX has only delays of 5 times and MX-80 about 35 times. Related to the duration of the breakthrough and the necessary time to reach the final equilibrium concentration, relative differences between the two curves are always higher for MX-80 (duration up to 4 times longer, only 2 for FEBEX), but the absolute time differences are always higher for FEBEX.

Reasoning which bentonite is more affected by competition, it is necessary to take into account the final application of this analysis. From the scientific point of view, one could compare the relative differences of each individual bentonite. In this case MX-80 would be considered the bentonite most affected by competition. However, as the final interest of this project is the application of these calculations to safety assessments of the geological repository, absolute differences will be used to conclude which bentonite is more affected by competition. Therefore, taking into account the differences mentioned before, FEBEX is more affected by bentonite than MX-80.

The next figures show breakthrough curves for other positions and for lower Ni(II) $_{EQ}$ concentrations (10^{-7}).

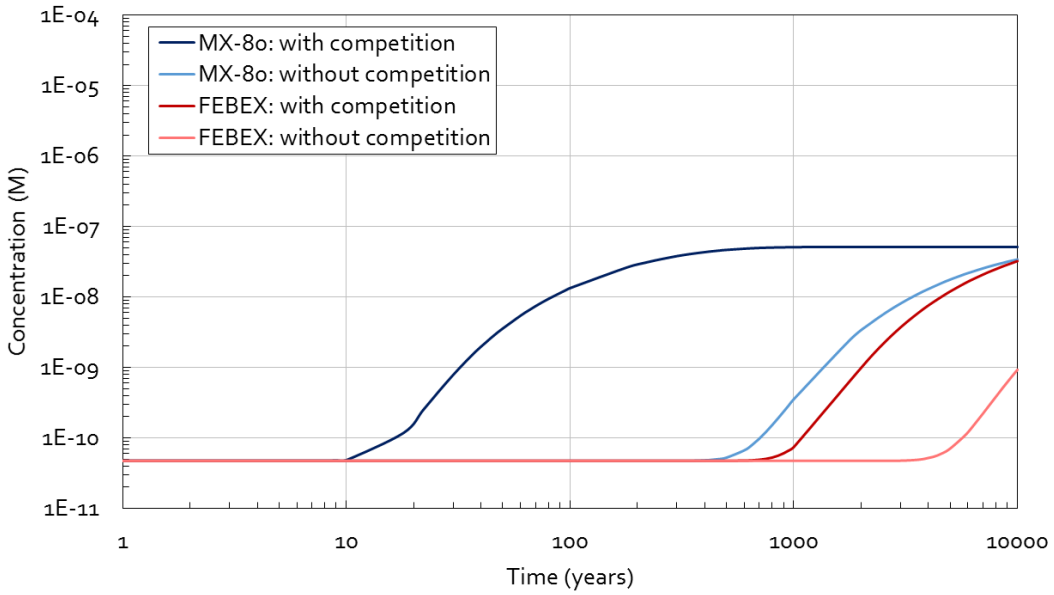

Fig. 56 Ni (II) breakthrough curves at x=0.6125 m into the bentonite calculated with MCOTAC. ($Ni(II)_{EQ}$ level is 10^{-7} M)

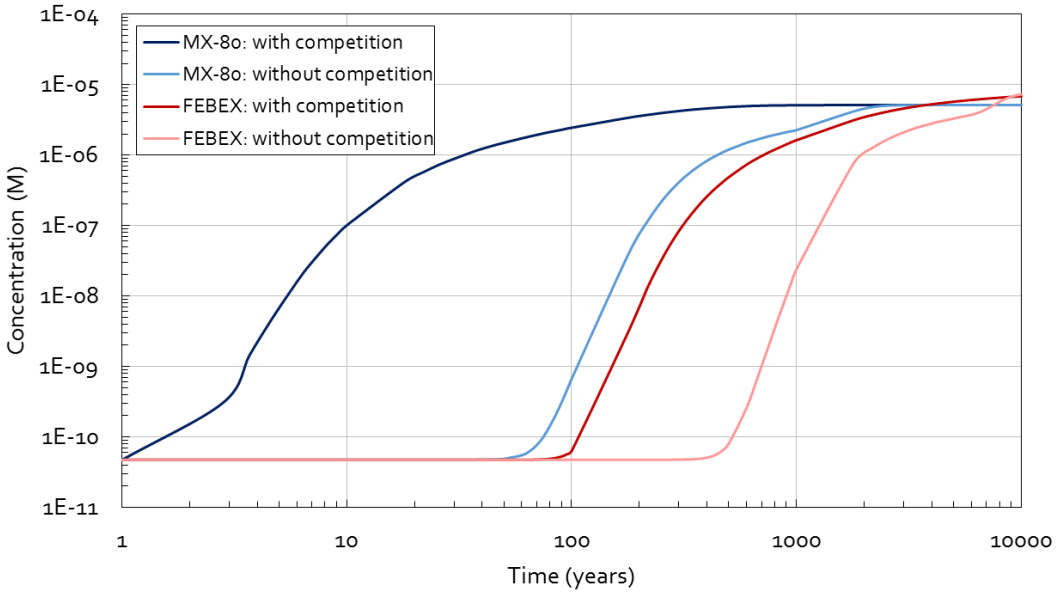

Fig. 57 Ni (II) breakthrough curves at x=0.3325 m into the bentonite calculated with MCOTAC. $(Ni(II)_{EQ}$ level is 10^{-5} M)

The next figures **Fig. 58, Fig. 59** and **Fig. 60** provide the concentration profiles along the column at different times. At the latest times, the concentration of Ni along the column obviously reaches the injected concentration (equilibrium). They are a good reference for observing how the concentration evolves with time.

Considering the first two figures, significant differences are found when sorption competition is incorporated to the model. For the first decades of diffusion, competition reduces much more the retardation transport of Ni(II) in the MX-80 bentonite than within the FEBEX bentonite. With this, one can conclude that the competition affects the MX-80 bentonite at earlier times than the FEBEX.

Besides, according to the most conservative (but realistic) calculation, that is the one considering competition for sorption sites, Ni only needs only one hundred years to reach (almost) the equilibrium concentration at the outer boundary of MX-80 bentonite buffer. This is even earlier than the prediction made using the pessimistic case of the Kd model (**Fig. 53**), which is such a significant result for the safety assessment of the HLW and SF repository in deep geological formations (where the Kd model is still used).

On the other hand, for the FEBEX bentonite the results are similar but not worse that the pessimistic prediction of the Kd model.

*(**FEBEX** Ni(II)-Fe(II) sorption competition analysis)*

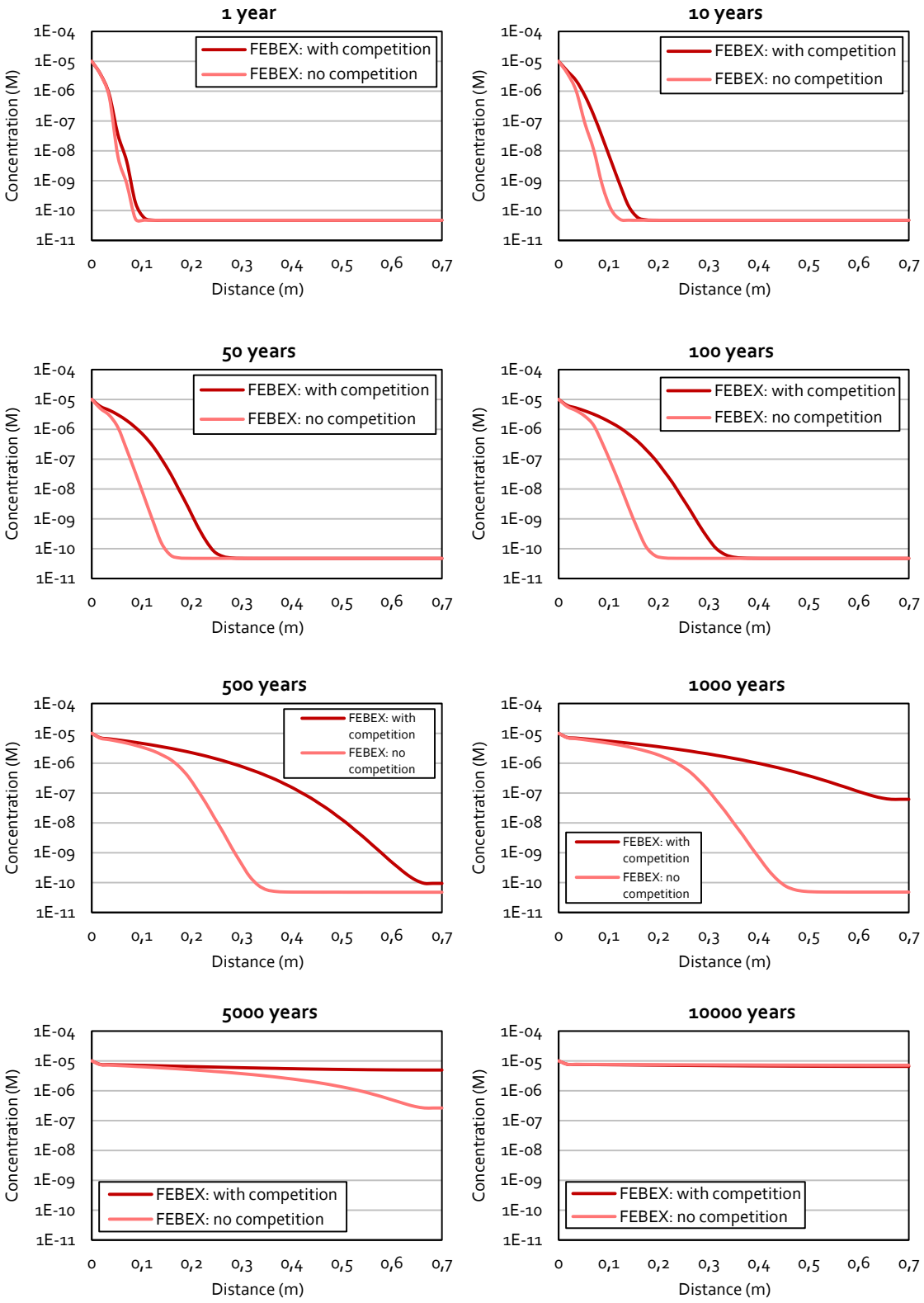

Fig. 58 Concentration profiles of tracer of Ni (II) into the 0.7 meters column of FEBEX bentonite for different times ($Ni(II)_{EQ}$ level is 10^{-5} M).

*(**MX-80** Ni(II)-Fe(II) sorption competition analysis)*

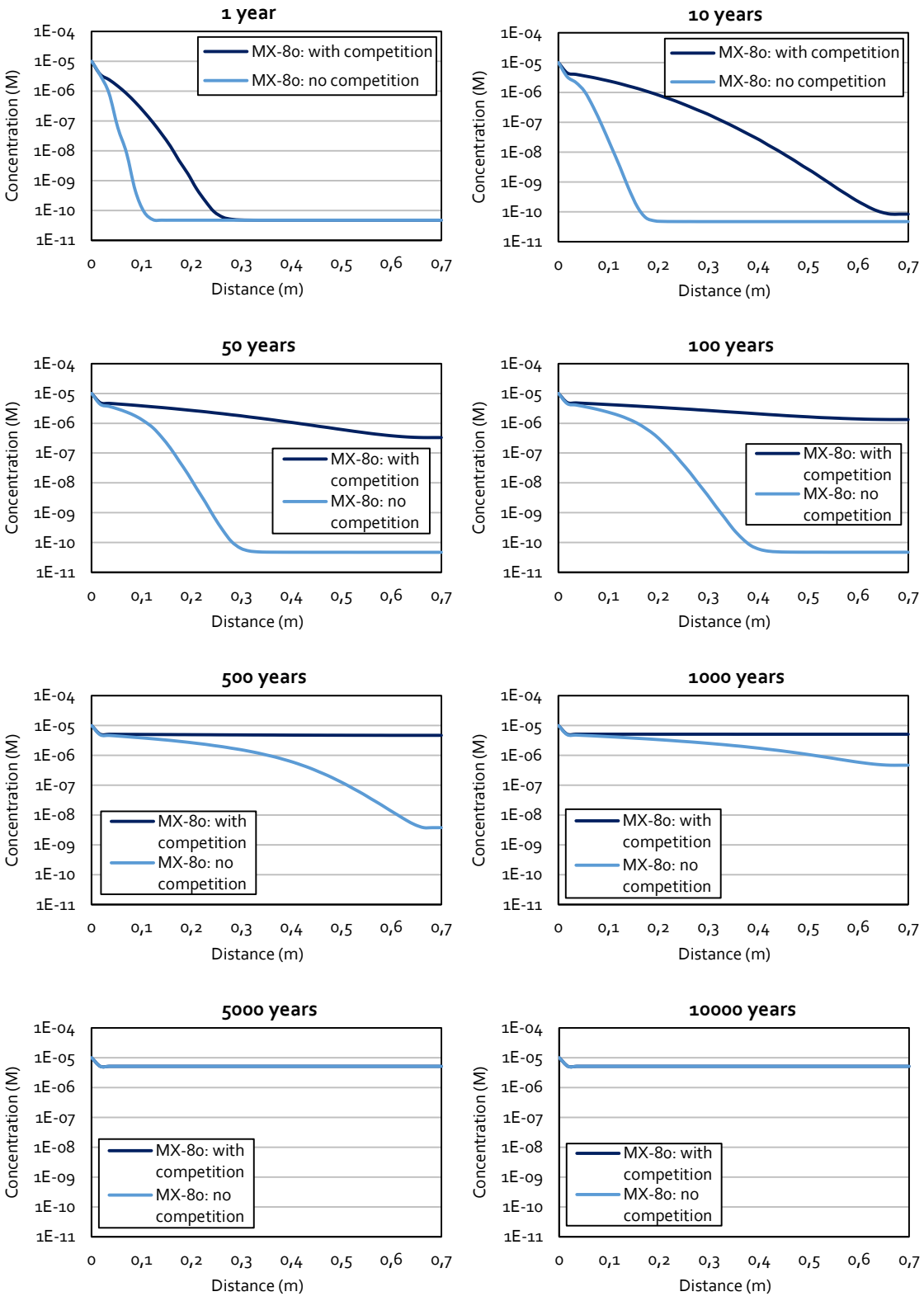

Fig. 59 Concentration profiles of tracer of Ni (II) into the 0.7 meters column of MX-80 bentonite for different times ($Ni(II)_{EQ}$ level is 10^{-5} M).

*(**MX-80 vs FEBEX:** with Ni(II)-Fe(II) sorption competition)*

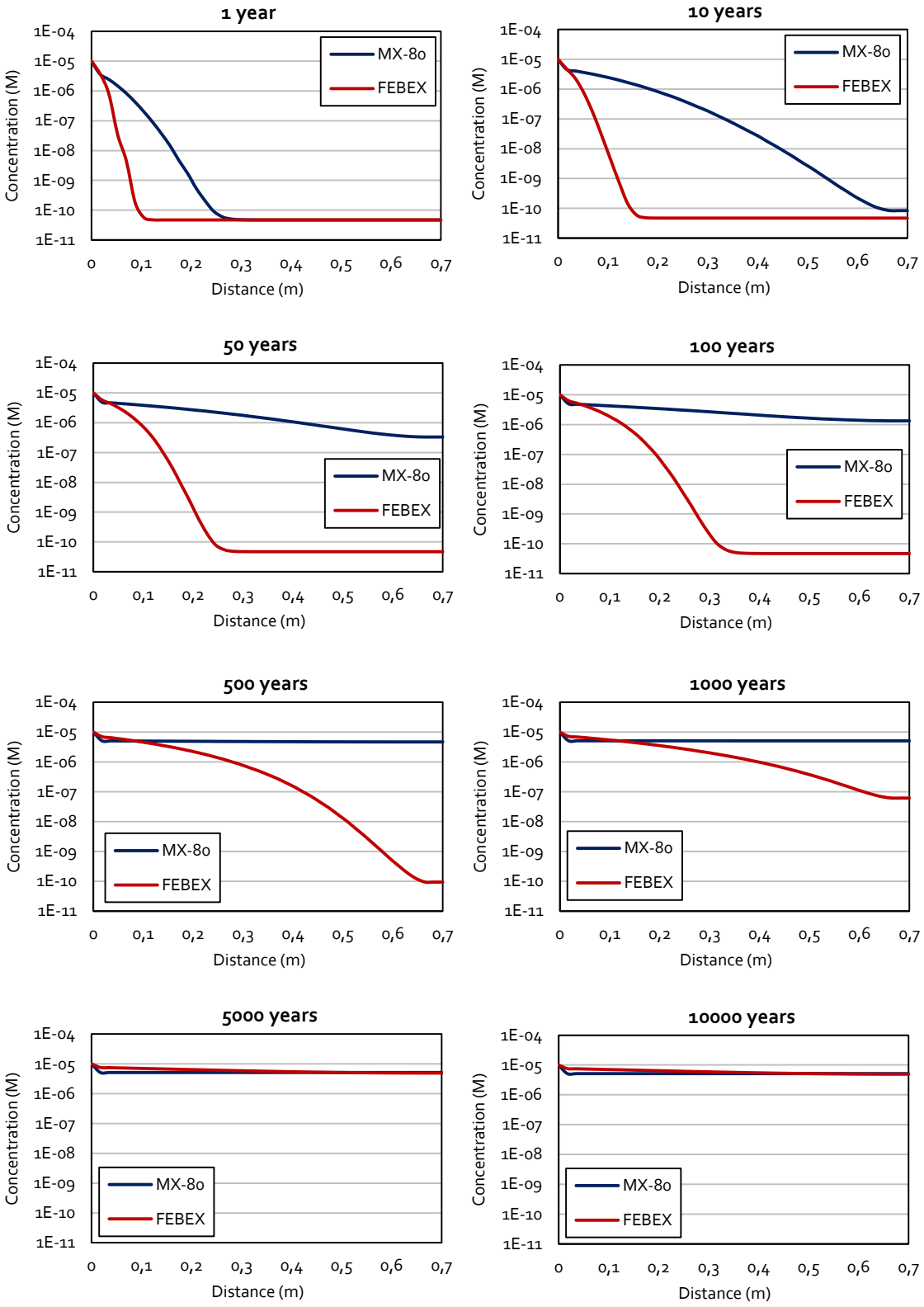

Fig. 60 Concentration profiles of tracer of Ni (II) into the 0.7 meters column of bentonite for different times ($Ni(II)_{EQ}$ level is 10^{-5} M, with sorption competition with Fe(II))..

Finally, regarding the comparison of FEBEX against MX-80, the first one has more retardation capacity. This higher capacity can be quantified for the case with Ni(II)-Fe(II) competition taking as reference the 50% of the final concentration level of pure Ni(II) cation.

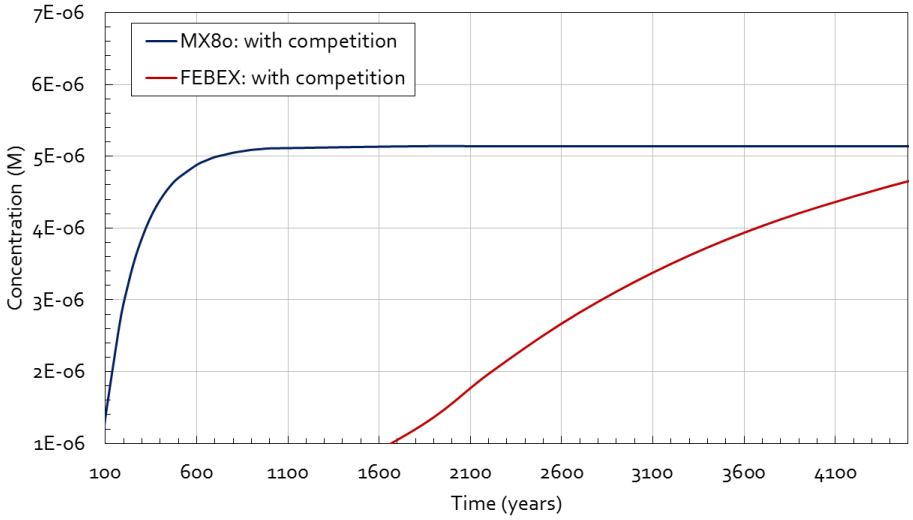

Fig. 61 Zoom to **Fig. 55,** for a better inspection of the 50% of the final concentration levels. Linar scale and restricted limits of the axis.

The Ni(II) final concentration level for FEBEX is approximately $7.5 \cdot 10^{-6}$M, and $5.1 \cdot 10^{-6}$M for MX-80. Then, the 50 % levels are

$$\text{FEBEX: } \frac{7.50 \cdot 10^{-6}\text{M}}{2} = 3.75 \cdot 10^{-6} M; \qquad \text{MX-80: } \frac{5.14 \cdot 10^{-6}\text{M}}{2} = 2.57 \cdot 10^{-6} M$$

In **Fig. 61** this levels are reached after 3400 years for FEBEX and after 180 years for MX-80. Therefore, the ratio between this values gives a quantification of the retardation capacity difference between both bentonites:

$$\frac{3400}{180} = 18.9 \approx 19 \; times$$

That means that FEBEX has 19 times more retardation capacity than MX-80.

8 Linear vs non-linear sorption

So far, two contaminant transport methods have been distinguished: Kd model and reactive transport model. They have been conceived as independent methods with different characteristics, able to provide more or less precise results. What is clear is that Kd model is simpler and that reactive transport models is more accurate describing the whole geochemical system.

Nevertheless, the possibility to match both methods or to make them complementing each other was not considered, up to now. This section contemplates and propose a possible direction of making the methods complement each other, to get good results easier. In fact, none additional calculation is necessary, because one can take advantage of previous calculations made with both methods.

The main idea comes from the definition of Kd, which allows that by means of the consideration of the surface complexes and complexes in solution included in the reactive transport model, a Kd value is calculated.

First, the definition of Kd is again necessary:

$$K_d = \frac{Mass\ of\ adsorbate\ sorbed}{Mass\ of\ adsorbate\ in\ solution} = \frac{\frac{mols\ of\ adsorbate}{kg\ of\ soil}}{\frac{mols\ of\ adsorbate}{l\ of\ liquid}} = [l/kg]$$

This means that if one has the total concentration in solution of an element and also the surface concentration (adsorbate sorbed), it is possible to determine the Kd value. The results of reactive transport calculations provide a number of complexes concentrations both in solution and in the mineral surface. Therefore one can determine the total concentration in solution and in the surfaces adding up all the complexes taken into account.

Fig. 62 provides a representation that has not been used up to now. It is the called sorption isotherm, which gives more information about the dependency between the sorbed Ni and the total Ni equilibrium concentration in solution, obtained with the MCOTAC outputs. It is clear that this dependency, for the specific case of MX-80, with a Ni(II) source concentration of 10^{-5} M and Fe

concentration saturated with siderite competing for sorption sites, is linear. **Fig. 63** express the same but shows explicitly the constant value of Kd in this system.

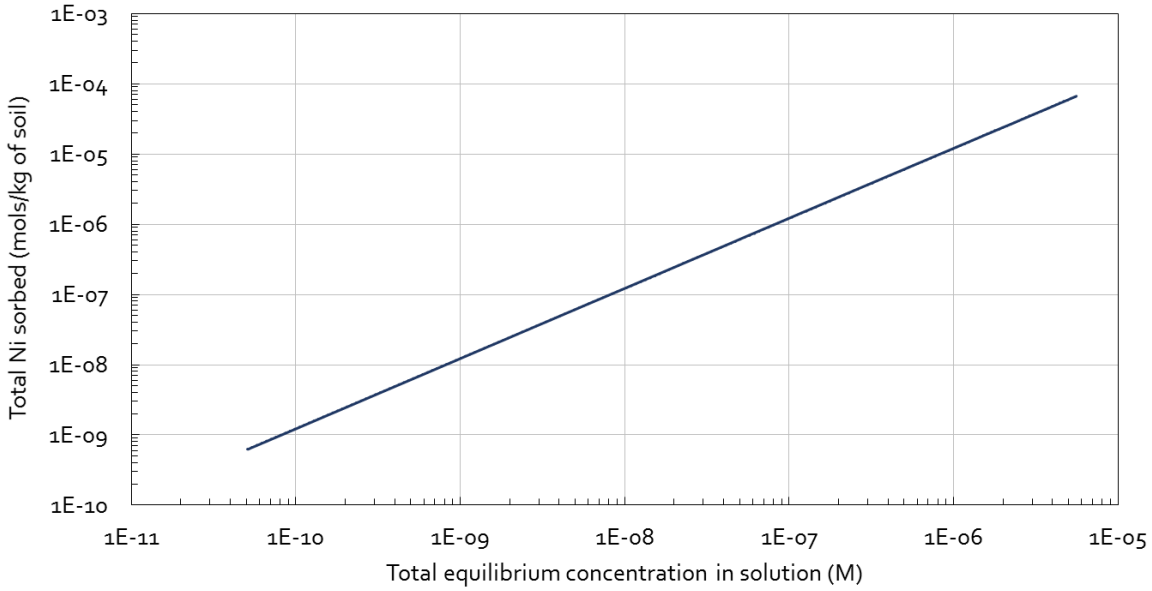

Fig. 62 Sorption isotherms of Ni(II). $(Ni(II)_{EQ}$ level is 10-5 M, sorption competition assumed).

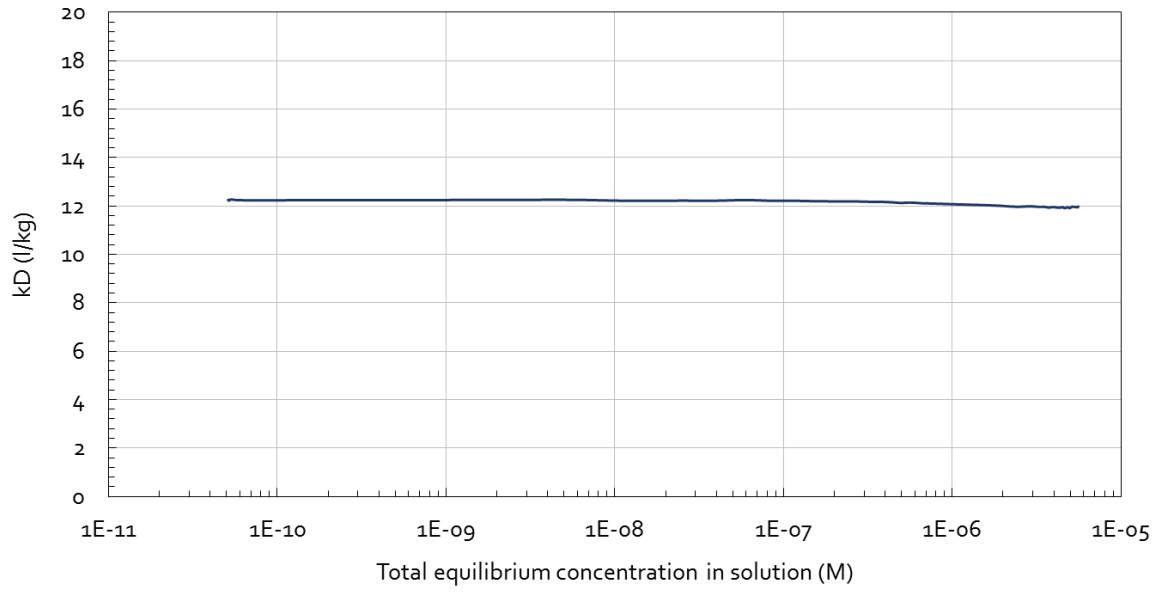

Fig. 63 Same results expressed as the Ni(II) distribution ratio (Kd) as a function of Ni(II) equilibrium concentration in solution.

The Kd results approximately in 12 l/kg. This value is found between the pessimistic and the optimistic cases for Kd, provided by Nagra (**Fig. 52**), which is a signal of consistency.

To demonstrate that sorption is not always linear it is useful to explicitly show an example of non-linear sorption. In **Fig. 64** the non-linear sorption case of the already analyzed case without Ni(II)-Fe(II) competition is clearly observed.

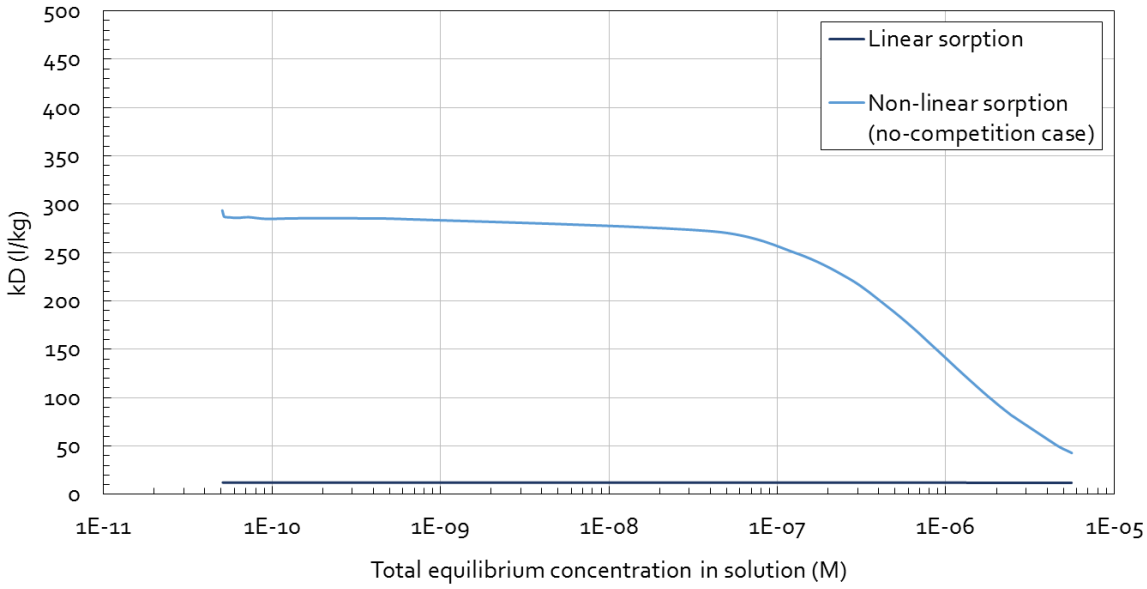

Fig. 64 Ni(II) distribution ratio (Kd) as a function of Ni(II) equilibrium concentration in solution for two different cases: linear sorption and non-linear sorption, depending on the system conditions.

Then, reactive transport could support the Kd models in cases of linear sorption systems. When it is the case that after a reactive transport calculation, the transport of a contaminant meets with a linear description, the Kd coefficient can be provided also by this reactive transport calculation. So reactive transport, demonstrating the linearity and providing the Kd value, allows to use the easier Kd model for further calculations with exactly the same system.

However, for non-linear cases, the Kd model cannot be used anymore and a more sophisticated description of the model is necessary, which corresponds to reactive transport calculations.

In addition, it is important to remark that reactive transport calculations allow an individual adjustment of every single parameter of the model. Therefore, as each Kd constant is only valid for each different system and it difficult to measure, for linear and common systems Kd values can be calculated using reactive transport calculations.

Since, for the case considered in this thesis, the Fe(II) concentration in the near field of a HLW repository may change with time and space, the transport of bivalent transition metal radionuclides can only be adequately modelled using a multi-species reactive transport method which including a sorption model.

9 Environmental impact

Radioactive material management is always related to its environmental impact and the consequent safety assessments. In the case of this thesis, the environmental impact will be studied in 3 directions:

1- General remarks on the vectors of environmental impact assessment of the whole repository will be pointed.

2. The bentonite lifecycle.

3- Advantages and shortcomings of MX-80 and FEBEX bentonites.

9.1 The whole repository impact

The environmental impact that would suppose the whole HLW/SF repository in a deep geological formation is absolutely out of this project, since it is focused only on the transport of radionuclides through the bentonite buffer. However, like it is carried out in the first sections of the thesis, a general scheme pointing the main environmental impact vectors of concern is provided.

The environmental impact vectors are: water, air, flora, fauna, landscape, humans and land. The 10000 years placement of the waste inside the canister must be taken into account, as well as the posterior retardation (around other 10000 years) of its content migration through the multiple engineered and natural barriers of the facility.

Moreover, as the chosen zones of emplacements are seismically low active areas, the seismic movements are considered of very low probability. In any case the should be considered in an extended version of this environmental impact assessment.

1. Water: the underground water (repositories will be located about 500 to 800 meters of depth) is the main water affected. If the repository is located in clay host rocks, where the content of water is high but where there are not aquifers or water circulation of any kind. That is why in the short-term the affection is almost negligible. In the long-term (after radioactive nuclides escape

from the canister), the bentonite porewater will be contaminated, and afterwards the host rock. The radioactivity evolution of the radionuclides has to be compared with the containment and migration times for further analysis of the contamination of surface water.

2. Air, flora and fauna: no affection until the radionuclides reach the surface, and the concentration will be so low that no contamination is expected. During the waste transport CO_2 may be emitted, and despite the accident risk during transport is low, it should be also evaluated.

3. Landscape: visual impact of the facility, probably in isolated areas.

4. Humans: apart from a low likely accident during waste transport, humans would not receive any dose. When radionuclides reach the surface after many thousands of years, they will have very low concentrations, so the expected contamination may be irrelevant.

5. Land: the most affected vector, because of the digging in the repository area and the alteration of its natural state. Composition in the near field of the host-rock from the canister may be altered due to its interaction with the bentonite buffer.

9.2 Bentonite lifecycle

The bentonite is obtained via the processing of the mineral to obtain the granulated form used in the repository. Its extraction generate an alteration of its original media and requires energy. The kind of bentonite used for the repository are extracted from very particular areas where the mineral has the appropriate features for this application. Its processing may generate also CO_2 emissions and needs energy, mainly electricity. Afterwards, depending on the transport methods there will energy needs and Co_2 emissions.

9.3 MX-80 vs FEBEX

The main point of this comparison is the retardation capacity of each bentonite on the migration of radionuclides. This thesis studies the retardation capacity of Ni(II) as an example of bivalent transition metal leaching from the canister. The more the corresponding radioisotopes are retarded, the less environmental impact. Therefore, as FEBEX has a retardation capacity quantified as 19 times better than MX-80 (section 7.3), its use would come together with a lower environmental impact to the host rock, concerning its porewater composition and surface complexes.

10 Budget

Scientific publications are the main tools used for the performing of this project, because all the computational resources did not carry any cost. The Paul Scherrer Institut is subscribed to the main internet sites purchasing scientific publications, and that's why each individual publication cost is underestimated, and the number of papers as well. Together with the intern and master student salary of the author during the 5 months, the budget of the project becomes 8100 CHF (6640 €). In **Table 10** the budget is detailed. The values are given in Swiss Francs, but the equivalent quantity in Euros is finally given.

Reason	Unit cost	Units	Cost (CHF)
Science papers and books	~40CHF/paper	15 papers	600 CHF
Intern salary	2100 CHF/month	3 months	6300 CHF
Master student scholarship	600 CHF/month	2 months	1200 CHF
MCOTAC license	-	-	-
Total		**8100 CHF (6640 €)**	

Table 10 Project costs

In addition, the author received an *Erasmus internships* scholarship and a grant from the European Union for the presentation of part of the project in a workshop organized by the Karlsruhe Institut of Technology about reactive transport modelling.

Reason	Unit cost	Units	Cost (CHF)
Erasmus interships scolarship	369 CHF/month	5 months	1845 CHF
EU Talisman grant	1200 CHF/event	1 workshop	1200 CHF
Total additional costs		**3045 CHF (2496 €)**	

Table 11 Scholarships

Conclusions

The first part of the thesis consists of an approximation to radioactive waste management and reactive transport modelling, followed by the setup of the models (data gathering from several references) and a series of calculations and analysis. Main conclusions are extracted from these last analysis, and are discussed in the corresponding sections of this thesis. However, from the first pages one can understand why the geological repository is necessary, how important are the barriers of this geological repository and why transport of radionuclides has to be predicted for safety assessments. Besides, the bentonite models prepared are robust, which was a prior aim.

Already from the radionuclide transport calculations, first of all the uncertainty propagation of the LFER sorption parameters to reactive transport calculations was demonstrated in section 6. Particularly, it was found that when competition is included in the model, the differences between the possible results decrease due to the earlier breakthroughs; when weak sites are incorporated, these differences increase. The bandwidths depend also on the system: FEBEX has always wider bandwidths, due to its higher retardation capacity. The order of magnitude of these bandwidths is found between 10^1 and 10^3 years, which apparently is not of high significance compared to the lifetime of a high level nuclear waste repository.

Further aims were to compare FEBEX and MX-80, assess the effect of Ni(II)-Fe(II) competition for sorption sites and discuss the convenience of the Kd model. That is why calculations with three different methods and setups were carried out: Kd model, reactive transport without and with Ni(II)-Fe(II) competition. All calculations demonstrated that FEBEX bentonite has more retardation capacity than MX-80, mainly due to its higher content of Montmorillonite in its mineralogy. This capacity was quantified to be 19 times higher for FEBEX than for MX-80.

It is also demonstrated that the incorporation of Fe(II) sorbing to the clay surfaces induces a lower sorption to Ni(II), which means a faster migration of Ni(II) radionuclides. FEBEX is 6 times more affected by competition than MX-80 if absolute time differences are considered.

It is also important to remark that for MX-80 only one hundred years are necessary for Ni(II) to reach the an important concentration level at the outer boundary of the MX-80 bentonite buffer, which is even earlier than what is predicted by the pessimistic prediction made by the Kd model. This should be taken into account for next safety assessments of the Swiss geological repository.

Section 8 settles a possible situation where the two contaminant transport models could support each other, which is that of the linear sorption for a particular system.

Future work

The final aim of the research line in which this thesis was involved is to produce reactive transport models capable of predicting migration of contaminants with such a reliability that they can be included in safety assessments of geological repositories. To this end, it is necessary to go step by step, and the direct next step that could follow this thesis is a modification introduced to the code to generate calculations with a more complex geometry: a radial geometry.

MCOTAC code change: radial geometry

A modification in the MCOTAC code should be introduced. The intention of this change is to approximate even more the results to the real system – radial symmetric geometry of a high level nuclear waste container surrounded by bentonite- using the same 1D description.

Up to now, the main variable changing in the chemical equilibrations and transport calculations was the concentration of the basis and complex species. That means that both the chemical reactions and the transport of the particles had as main output the recalculation of the concentrations of these species. In a 1D column where the volume of all cells is the same, as it is the model used so far, this is valid. But this hypothesis would not be valid if the volume of the cells change along the column, as it happens with the radial model proposed.

The 1D column change from equal cubic cells along to circumferential cells in the radial direction. That results in a changing-volume cells distribution, and a new procedure to calculate the concentration in the cells has to be performed, i.e. species masses have to be calculated in the different cell volumes to calculate the species concentrations in the cells and no longer could species concentration vectors in the random walk description be used.

As the chemical equilibrium calculations require the concentration of the species, the main conceptual change is that the transport calculation will be now carried out with the total mass of the species in each cell, not with concentration as it was done until now. The code changes are summed up schematically.

The incorporated code changes the matrixes of basis and complexes species concentrations in each cell. These concentration matrixes become mass matrixes before the transport calculation taking into account the corresponding volume of the cell, which changes from cell to cell due to the radial geometry, according to:

$$bn_{mass}[i][j] = bn_{concentration}[i][j] \cdot \pi(R^2 - r^2)$$

where

bn_{mass}: mass of basis species j in cell i

$bn_{concentration}$: concentration of basis species j in cell i

R: external radius of the cell i

r: internal radius of the cell i

And the same with the complexes matrix cn[i][j].

After the transport calculation, the matrixes are changed back to concentration values to carry out the chemical equilibrium calculations:

$$bn_{mass}[i][j] = bn_{concentration}[i][j]/(\pi(R^2 - r^2))$$

At time t:

- Transfer concentration in the cells to particle-mass vectors depending on the number of particles in the cell and the cell volume.
- Move particles by random walk during time Δt.
- Sum up particles for each cell.
- Sum up the particle-mass-vectors in each cell and calculated new concentration in the cells depending on the cell volumes.
- Go on with chemical equilibrium calculation for time Δt.

Some extra programming would be necessary to take into account the increasing number of sorption sites with distance for radial symmetry compared to 1D linear geometry. The same for solid species.

Conferences, workshops and research dissemination

During the developing of this thesis and the previous semester of lectures at the ETH Zurich, the author had the opportunity to visit related facilities and to participate in workshops about reactive transport modelling focused in safety assessments of radioactive waste geological repositories.

First, in May 2013, he visited the Mont Terri Project, St-Ursanne, Switzerland, which is a rock laboratory where various experiments in Opalinus Clay (foreseen host rock for the disposal of radioactive waste) are carried out since the mid-1990s. The subsurface visit was guided, and security equipment necessary.

Also in May 2013, a guided visit to the Gösgen NPP was organized for the students of the Nuclear Energy Systems course.

From 10th to 11th October 2013, he took part in the 3rd workshop of the PhD network on Reactive Transport Modelling and Experiments organized at the PSI. It was a very good occasion to get in touch with different research projects carried out worldwide.

Later, the PSI organized a visit to Zwilag, the facility responsible for storing radioactive waste while it is still not disposed in the long-term geological disposal. There, a number of detailed explanations about the facility and the Swiss policy with radioactive waste was offered to the participants, together with multimedia resources and talks with the workers. Moreover, the guide showed the participants: HLW and SF canisters through safe windows, live waste treatment and transport and the plasma oven in operation.

Finally, apart from the presentation at the UPC, part of the project will be presented at the III TrePro workshop about Reactive Transport Modeling organized by the Karlsruhe Institut of Technology from 5th to 7th March 2014 in Karlsruhe, Germany.

Acknowledgments

I would like to thank many people for their help and support during this stay at the PSI. I feel very grateful to the PSI institution for granting me this amazing opportunity of working there during the last 5 months.

More particularly, I want to acknowledge Dr. Wilfried Pfingsten, my supervisor at the PSI, for guiding me all along the project, from the very beginning, when I had only a minor idea about radioactive waste management, to the end of the thesis. He was really patient solving all my questions and proposing ideas. I also thank Wolfgang Hummel, teacher at ETH Zurich, for encouraging me to join the Laboratory for Waste Management. At the same time I am very thankful to Dr. Javier Dies, from the UPC, for accepting the supervision of the thesis and for always being available to solve my doubts, regardless of the distance.

I want to thank the LES team for their hosting, both in the working environment and in informal contexts such as coffee breaks and team meetings. Besides, from the PSI I also kindly thank PhD student Jenna Ponoosamy, PhD student Amir Shafizadeh, Dr. Luis Pegado, master student Marc Raventós and Dr. Henar Rojo, not only for their advice but also for the off-topic conversation at the office and shared coffees, meals and matches.

I would like to take the time to deeply thank the members of the Futsal Brugg for their incredible welcome, in spite of the language barrier, and for being such incredible team mates. I am also very grateful to the Catalan group for the shared experiences, especially during the weekends, and all my friends both in Catalonia and Switzerland for making my stay away from home much easier with their support.

Finally, I thank my parents, Jordi and Berta; my brother, Uri; and my sister, Marta, for their constant support.

Bibliography

Bibliographic references

[1] NAGRA. *Project Opalinus Clay: Safety Report. Demonstration of Disposal Feasability for Spent Fuel, Vitrified High-level Waste and Long-lived Intermediate-level Waste.* Nagra Technical Report NTB 02-05. Wettingen, Switzerland, 2002.

[2] ENRESA. *Full-scale engineered barriers experiment for a deep geological repository for high level radioactive waste in crystalline host rock. FINAL REPORT*. Madrid, Spain, 2000.

[3] BRADBURY, M.H., BAEYENS, B. *A mechanistic description of Ni and Zn sorption on Na-montmorillonite. Part I: Titration and sorption measurements.* Journal of Contaminant Hydrology. vol. 27, p. 199–222, 1997.

[4] BRADBURY, M.H., BAEYENS, B. *A mechanistic description of Ni and Zn sorption on Na-montmorillonite Part II: modelling.* Journal of Contaminant Hydrology, vol. 27, p. 223-248, 1997.

[5] IAEA. *Classification of radioactive waste*. *General Safety Guide*. IAEA Safety Standards for protecting people and the environment, No. GSG-1, Vienna, Austria, 2009.

[6] IAEA. *Application of the concepts of exclusion, exemption and clearance.* IAEA Safety Standards Series No. RS-G-1.7. Vienna, Austria, 2004.

[7] HUMMEL, W. *Slides corresponding to Nuclear Energy Systems lectures,* Master of Science in Nuclear Engineering, ETH Zurich, Switzerland.

[8] GRIMSEL TEST SITE, [www.grimsel.com, November 2013]

[9] ENCYCLOPEDIA BRITANNICA, [www.britannica.com, December 2013]

[10] PFINGSTEN, W. *Efficient modelling of reactive transport phenomena by a multispecies random walk coupled to chemical equilibrim.* Nuclear Technology, vol. 116, p. 208 - 221, 1996.

[11] PFINGSTEN, W. *MCOTAC. Code Description and Manual, 2010.*

[12] PFINGSTEN, W. *Modular Coupling of Transport and Chemistry: Theory and Model Applications,* 1994.

[13] UNIVERSIDAD AUTÓNOMA DE MADRID [http://www.uam.es/personal_pdi/ciencias/jaimefa/jaimecuevas/clase%2012-2.pdf, November 2013]

[14] PFINGSTEN, W., BRADBURY, M.H., BAEYENS, B. *The influence of Fe(II) competition on the sorption and migration of Ni(II) in MX-80 bentonite.* Applied Geochemistry, vol. 26, 2011.

[15] M. GARCÍA-GUTIÉRREZ, J. et al. *Overview of laboratory methods employed for obtaining diffusion coefficients in FEBEX compacted bentonite. Journal Iberian Geology,* vol. 32, p. 37-53, 2006.

[16] E. CURTI, P. WERSIN, *Assessment of porewater chemistry in the bentonite backfill for the Swiss SF/HLW Repository.* NAGRA, Wettingen, Switzerland, 2002.

[17] HUMMEL, W. *Nagra/PSI Thermochemical database 01/01. Nagra Technical Report NTB 02-16.* Switzerland, 2002.

[18] BRADBURY, M.H., BAEYENS, B. *Modelling the sorption of Mn(II), Co(II), Ni(II), Zn(II), Cd(II), Eu(III), Am(III), Sn(IV), Th(IV), Np(V), and U(VI) on montmorillonite: linear free energy relationships and estimates of surface binding constants for some selected heavy metals and actinid. Geochimica et Cosmochimica Acta,* vol. 69, p. 875-892, 2005.

[19] BRADBURY, M.H., BAEYENS, B., *Near field sorption data bases for compacted MX-80 bentonite for performance assessment of a high-level radioactive waste repository in Opalinus clay host rock.* PSI Bericht Nr. 03-07, Nagra NTB 02-18, 2003.

[20] WORLD NUCLEAR ASSOCIATION [http://www.world-nuclear.org/ , December 2013].

[21] ENRESA, *Sexto Plan General de Residuos Radiactivos*, 2006.

Complementary references

OELKERS, E.H., SCHOTT, J., *Thermodynamics and Kinetics of Water-Rock Interaction. Reviews in Mineralogy & Geochemistry, vol. 70*

BRADBURY, M.H., BAEYENS, B., *Porewater chemistry in compacted re-saturated MX-80 bentonite,* Journal of Contaminant Hydrology, vol 61, p. 329– 338, 2003

BRADBURY, M.H., BAEYENS, B., *A physicochemical characterisation and geochemical modelling approach for determining porewater chemistries in argillaceous rocks*, Geochimica et Cosmochimica Acta, vol. 62, p. 783–795, 1998

FERNÁNDEZ, A.M., CUEVAS, J., RIVAS, P. *Pore Water Chemistry of the Febex Bentonite, MRS Proceedings, vol. 663,* 2000.

FERNÁNDEZ, A.M., *Analysis of the porewater chemical composition of a Spanish compacted bentonite used in an engineered barrier,* Physics and Chemistry of the Earth, vol. 29, p. 105–118, 2004

GLYNN, P., Slides about *Sorption Reactions,* USGS, 2003

NÜTZMANN, G., VIOTTI, P., AAGAARD, P., *Reactive Transport in Soil and Groundwater,* Springer-Verlag Berlin Heidelberg, 2005

ABBASPOUR, K.C. Slides *All about Soil Physics!* (for Modelling Flow and Transport), EAWAG, 2004

EPPING, P.A., GIMMI, T., Slides corresponding to *Geochemical Modeling II: Reactive transport* lectures at University of Bern, 2013

APPENDICES

Appendix A: MCOTAC files

Below, the input and output files created and obtained before and after the calculations are shown. All the files shown here correspond to the same calculation, which is the one corresponding to the Strong&Weak sorption sites, with Ni(II)-Fe(II) competition, reference surface complexation constants, FEBEX bentonite case. Only the most important files are shown.

A.1 Input files

This is an example of how a model is created to let MCOTAC read the model and carry out the corresponding calculation. All of the files are notepads, which need to be edited according to the appropriate spacing and lining up. Each data represents a characteristic of the model and is explained in section 5 of the thesis, models setup.

A.1.1 Test11

```
itest    : 1
ncyc     : 1
ntim     : 51
de       : 1.0
tmult    : 31557600.
nx       : 41
ny       : 1
dxx      : 0.0175
dyy      : 0.01
itest    : 1
inma     : 0
ipfile   : 0
npin     : 4000
npkt     : 0
backg    : 0.0
rd       : 1.0
lambda   : 0.e-00
lambt0   : 0.0
along    : .00000
vxx      : 1.e-17
dm       : 1.49e-10
dtmax    : 1.028e6
ismooth  : 1
i_sorb   : 39
j_sorb   : 15
j_decay  : 0
i_bou_c  : 13
c_i_bou  : 1.e-05
```

A.1.2 TEST.INI

This file contains all the concentration data of all the species involved in the model: basis, complexes, immobile species and solids.

```
 2 MODE          0         1         0
 3 ITER      10000       500
 4 CONV     1.E-08       1.5       1.2    90     5    90    90
 5 GRID         49        2.      10.7
 6 TIME          8    2.e+07    1.E+06
 7 PRINT 3.15576+073.15576+081.57788+093.15576+091.57788+103.15576+101.57788+11
 7 PRINT 3.15576+11
 8 TRANS        0.        0.        0.
 9 BOUND         0         0
10 T MODE        0
10A TEMP       25.
11 NUMS         19        63         0         0        12         0         0
Na+          1    1 9.1345-02 9.1345-02    1 9.1345-02 9.1345-02    2 0.0000-00 0.0000-00    2 4.0000-02 4.0000-02
K+           1    1 3.8365-04 3.8365-04    1 3.8365-04 3.8365-04    2 0.0000-00 0.0000-00    2 4.0000-02 4.0000-02
Ca+2         2    1 1.2725-02 1.2725-02    1 1.2725-02 1.2725-02    2 0.0000-00 0.0000-00    2 4.0000-02 4.0000-02
Mg+2         2    1 1.6046-02 1.6046-02    1 1.6046-02 1.6046-02    2 0.0000-00 0.0000-00    2 4.0000-02 4.0000-02
Sr+2         2    1 8.5597-05 8.5597-05    1 8.5597-05 8.5597-05    2 0.0000-00 0.0000-00    2 4.0000-02 4.0000-02
Fe+2         2    1 1.6115-06 1.6115-06    1 1.6115-06 1.6115-06    2 0.0000-00 0.0000-00    2 4.0000-02 4.0000-02
CO3-2       -2    2 2.1799-03 1.8437-06    2 2.1799-03 1.8437-06    2 0.0000-00 0.0000-00    2 4.0000-02 4.0000-02
SO4-2       -2    2 1.3116-02 1.3116-02    2 1.3116-02 1.3116-02    2 0.0000-00 0.0000-00    2 4.0000-02 4.0000-02
Cl-         -1    2 1.1283-01 1.1283-01    2 1.1283-01 1.1283-01    2 0.0000-00 0.0000-00    2 4.0000-02 4.0000-02
Dummy_F-    -1    1 1.0000-10 1.0000-10    1 1.0000-10 1.0000-10    2 0.0000-00 0.0000-00    2 4.0000-02 4.0000-02
DummyH2Si   -2    1 1.0000-10 1.0000-10    1 1.0000-10 1.0000-10    2 0.0000-00 0.0000-00    2 4.0000-02 4.0000-02
H+           1    1 5.5302-08 5.5302-08    1 5.5302-08 5.5302-08    2 0.0000-00 0.0000-00    2 4.0000-02 4.0000-02
trac_Ni      2    1 4.7175-11 4.7175-11    1 4.7175-11 4.7175-11    2 0.0000-00 0.0000-00    2 4.0000-02 4.0000-02
trac_X      -2    1 1.6890-07 1.6890-07    1 1.6890-07 1.6890-07    2 0.0000-00 0.0000-00    2 4.0000-02 4.0000-02
Ni_s_kd      0    1 1.0000-10 1.0000-10    1 1.0000-10 1.0000-10    2 0.0000-00 0.0000-00    2 4.0000-02 4.0000-02
Ss1_OH       0    2 1.8400-03 0.9200-03    2 1.8400-03 0.9200-03    2 0.0000-00 0.0000-00    2 4.0000-02 4.0000-02
Sw1_OH       0    2 3.6800-02 1.8400-02    2 3.6800-02 1.8400-02    2 0.0000-00 0.0000-00    2 4.0000-02 4.0000-02
Sw2_OH       0    1 3.6800-02 1.8400-02    1 3.6800-02 1.8400-02    2 0.0000-00 0.0000-00    2 4.0000-02 4.0000-02
Na-Mont      0    2 0.96539-0 0.79917-0    2 0.96539-0 0.79917-0    2 0.0000-00 0.0000-00    2 4.0000-02 4.0000-02
OH-          1       -14.000        0.          0.          0.
             0    0    0    0    0    0    0    0    0    0    0   -1    0    0    0    0    0    0    0    0    0    0    0    0    0    0    0    0    0
           7.3e-8    7.3e-8    7.3e-7    1.000-7
NiOH+        1   -9.86              0.          0.          0.
             0    0    0    0    0    0    0    0    0    0    0   -1    1    0    0    0    0    0    0    0    0    0    0    0    0    0    0    0    0
           2.8e-15   2.8e-15    7.3e-7    1.000-7
NiOH         1   -19.00             0.          0.          0.
             0    0    0    0    0    0    0    0    0    0    0   -2    1    0    0    0    0    0    0    0    0    0    0    0    0    0    0    0    0
           2.8e-19   2.8e-19    7.3e-7    1.000-7
NiOH-        1   -30.0              0.          0.          0.
             0    0    0    0    0    0    0    0    0    0    0   -3    1    0    0    0    0    0    0    0    0    0    0    0    0    0    0    0    0
           2.8e-25   2.8e-25    7.3e-7    1.000-7
CaHCO3       1    11.435            0.          0.          0.
             0    0    1    0    0    0    1    0    0    0    0    1    0    0    0    0    0    0    0    0    0    0    0    0    0    0    0    0    0
           7.3e-10   7.30-10    7.3e-7    1.000-7
CaSO4aq      1    2.3               0.          0.          0.
             0    0    1    0    0    0    0    1    0    0    0    0    0    0    0    0    0    0    0    0    0    0    0    0    0    0    0    0    0
```

```
CaCO3          0      3.224             0.            0.            0.
               0     0     1     0     0     0     1     0     0     0     0     0     0     0     0     0     0     0     0     0     0     0     0     0     0     0     0     0     0     0
          1.0e-7    1.000-7    7.3e-7    1.000-7
CaOH           1    -12.780             0.            0.            0.
               0     0     1     0     0     0     0     0     0     0     0    -1     0     0     0     0     0     0     0     0     0     0     0     0     0     0     0     0     0
          3.0e-08    3.000-8    7.3e-7    1.000-7
MgCO3aq        1      2.980             0.            0.            0.
               0     0     0     1     0     0     1     0     0     0     0     0     0     0     0     0     0     0     0     0     0     0     0     0     0     0     0     0     0
          7.3e-7    1.000-7    7.3e-7    1.000-7
MgSO4aq        1     2.37              0.            0.            0.
               0     0     0     1     0     0     0     1     0     0     0     0     0     0     0     0     0     0     0     0     0     0     0     0     0     0     0     0     0
          1.8e-3    1.800-3    7.3e-7    1.000-7
MgHCO3         1    11.397             0.            0.            0.
               0     0     0     1     0     0     1     0     0     0     0     1     0     0     0     0     0     0     0     0     0     0     0     0     0     0     0     0     0
          1.2e-5    1.200-5    7.3e-7    1.000-7
MgOH-          1   -11.440             0.            0.            0.
               0     0     0     1     0     0     0     0     0     0     0    -1     0     0     0     0     0     0     0     0     0     0     0     0     0     0     0     0     0
          7.3e-7    1.000-7    7.3e-7    1.000-7
SrHCO3         1    11.514             0.            0.            0.
               0     0     0     0     1     0     1     0     0     0     0     1     0     0     0     0     0     0     0     0     0     0     0     0     0     0     0     0     0
          7.3e-7    7.300-7    7.3e-7    1.000-7
SrSO4aq        1     2.29              0.            0.            0.
               0     0     0     0     1     0     0     1     0     0     0     0     0     0     0     0     0     0     0     0     0     0     0     0     0     0     0     0     0
          7.3e-7    7.300-7    7.3e-7    1.000-7
SrOH+          1    -13.290             0.            0.            0.
               0     0     0     0     1     0     0     0     0     0     0    -1     0     0     0     0     0     0     0     0     0     0     0     0     0     0     0     0     0
          7.3e-7    1.000-7    7.3e-7    1.000-7
SrCO3          1     2.805              0.            0.            0.
               0     0     0     0     1     0     1     0     0     0     0     0     0     0     0     0     0     0     0     0     0     0     0     0     0     0     0     0     0
          1.0e-7    1.000-7    7.3e-7    1.000-7
KOH            1    -14.460             0.            0.            0.
               0     1     0     0     0     0     0     0     0     0     0    -1     0     0     0     0     0     0     0     0     0     0     0     0     0     0     0     0     0
          7.3e-7    1.000-7    7.3e-7    1.000-7
KSO4-          1     0.85               0.            0.            0.
               0     1     0     0     0     0     0     1     0     0     0     0     0     0     0     0     0     0     0     0     0     0     0     0     0     0     0     0     0
          7.3e-7    7.300-7    7.3e-7    1.000-7
NaSO4-         1     0.70               0.            0.            0.
               1     0     0     0     0     0     0     1     0     0     0     0     0     0     0     0     0     0     0     0     0     0     0     0     0     0     0     0     0
          7.3e-7    7.300-7    7.3e-7    1.000-7
NaCO3-         1     1.270              0.            0.            0.
               1     0     0     0     0     0     1     0     0     0     0     0     0     0     0     0     0     0     0     0     0     0     0     0     0     0     0     0     0
          7.3e-7    1.000-7    7.3e-7    1.000-7
NaHCO3         1    10.079             0.            0.            0.
               1     0     0     0     0     0     1     0     0     0     0     1     0     0     0     0     0     0     0     0     0     0     0     0     0     0     0     0     0
          3.3e-5     3.3e-5    7.3e-7    1.000-7
NaOHaq         1    -14.180             0.            0.            0.
               1     0     0     0     0     0     0     0     0     0     0    -1     0     0     0     0     0     0     0     0     0     0     0     0     0     0     0     0     0
          5.3e-8    5.000-8    7.3e-7    1.000-7
```

```
HCO3-       1   10.329        0.          0.          0.
  0   0   0   0   0   0   1   0   0   0   0   1   0   0   0   0   0   0   0   0   0   0   0   0   0   0   0   0   0
6.3e-4  6.300-4  7.3e-7  1.000-7
H2CO3aq     1   16.681        0.          0.          0.
  0   0   0   0   0   0   1   0   0   0   0   2   0   0   0   0   0   0   0   0   0   0   0   0   0   0   0   0   0
1.3e-5  7.300-7  1.3e-5  1.000-7
HSO4-       1    1.988         0.          0.          0.
  0   0   0   0   0   0   0   1   0   0   0   1   0   0   0   0   0   0   0   0   0   0   0   0   0   0   0   0   0
1.3e-9  1.000-9  7.3e-7  1.000-7
FeSO4aq     1    2.250         0.          0.          0.
  0   0   0   0   0   1   0   1   0   0   0   0   0   0   0   0   0   0   0   0   0   0   0   0   0   0   0   0   0
8.3e-6  8.000-6  7.3e-7  1.000-7
FeHCO3      1   12.329         0.          0.          0.
  0   0   0   0   0   1   1   0   0   0   0   1   0   0   0   0   0   0   0   0   0   0   0   0   0   0   0   0   0
5.0e-7  5.000-7  7.3e-7  1.000-7
FeCO3       1    4.380         0.          0.          0.
  0   0   0   0   0   1   1   0   0   0   0   0   0   0   0   0   0   0   0   0   0   0   0   0   0   0   0   0   0
3.0e-7  3.000-7  7.3e-7  1.000-7
FeHSO4+     1    3.068         0.          0.          0.
  0   0   0   0   0   1   0   1   0   0   0   1   0   0   0   0   0   0   0   0   0   0   0   0   0   0   0   0   0
8.0e-6  8.000-6  7.3e-7  1.000-7
FeCl        1    0.14          0.          0.          0.
  0   0   0   0   0   1   0   0   1   0   0   0   0   0   0   0   0   0   0   0   0   0   0   0   0   0   0   0   0
2.0e-6  2.000-6  7.3e-7  1.000-7
FeOH        1   -9.500         0.          0.          0.
  0   0   0   0   0   1   0   0   0   0   0  -1   0   0   0   0   0   0   0   0   0   0   0   0   0   0   0   0   0
2.0e-7  2.000-7  7.3e-7  1.000-7
NiCl+       1    0.40          0.          0.          0.
  0   0   0   0   0   0   0   0   1   0   0   0   1   0   0   0   0   0   0   0   0   0   0   0   0   0   0   0   0
6.0e-9  2.00-16  7.3e-7  1.000-7
NiCl2       1    0.96          0.          0.          0.
  0   0   0   0   0   0   0   0   2   0   0   0   1   0   0   0   0   0   0   0   0   0   0   0   0   0   0   0   0
2.0e-9  2.00-19  7.3e-7  1.000-7
NiSO4aq     1    2.310         0.          0.          0.
  0   0   0   0   0   0   0   1   0   0   0   0   1   0   0   0   0   0   0   0   0   0   0   0   0   0   0   0   0
3.3e-9  8.00-17 7.3e-7  1.000-7
NiSO42      1    3.200         0.          0.          0.
  0   0   0   0   0   0   0   2   0   0   0   0   1   0   0   0   0   0   0   0   0   0   0   0   0   0   0   0   0
3.3e-9  8.00-17 7.3e-7  1.000-7
NiCO3       1    4.200         0.          0.          0.
  0   0   0   0   0   0   1   0   0   0   0   0   1   0   0   0   0   0   0   0   0   0   0   0   0   0   0   0   0
3.0e-6  3.000-7  7.3e-7  1.000-7
NiCO32      1    6.200         0.          0.          0.
  0   0   0   0   0   0   2   0   0   0   0   0   1   0   0   0   0   0   0   0   0   0   0   0   0   0   0   0   0
3.0e-6  3.000-7  7.3e-7  1.000-7
NiHCO3      1   11.720         0.          0.          0.
  0   0   0   0   0   0   1   0   0   0   0   1   1   0   0   0   0   0   0   0   0   0   0   0   0   0   0   0   0
3.0e-6  3.000-7  7.3e-7  1.000-7
```

```
Ni_sKd      1    2.909            0.          0.          0.
            0    0    0    0    0    0    0    0    0    0    0    0    0    0    1    0    0    0    0    0    0    0    0    0    0    0    0    0    0    0
          6.0e-9    2.00-16   7.3e-7    1.000-7
XSOH        1         5.57           0.          0.          0.
            0    0    0    0    0    0    0    0    1    0    0    1    0    0    0    1    0    0    0    0    0    0    0    0    0    0    0    0    0    0
          1.00-10  1.000-10  1.0E-10  1.000-10
XSO         1        -6.74           0.          0.          0.
            1    0    0    0    0    0    0    0    0    0    0   -1    0    0    0    1    0    0    0    0    0    0    0    0    0    0    0    0    0    0
          5.00-10 1.000-10   1.0E-10  1.000-10
XSONi       1       0.2963           0.          0.          0.
            0    0    0    0    0    0    0    0    1    0    0   -1    1    0    0    1    0    0    0    0    0    0    0    0    0    0    0    0    0    0
          2.00-16  1.000-16  1.0E-10  1.000-10
XSNiOH      1        -9.00           0.          0.          0.
            0    0    0    0    0    0    0    0    0    0    0   -2    1    0    0    1    0    0    0    0    0    0    0    0    0    0    0    0    0    0
          1.00-18 1.000-18  1.00-18 1.000-18
XSONi-Na    1       -17.738          0.          0.          0.
            1    0    0    0    0    0    0    0    0    0    0   -3    1    0    0    1    0    0    0    0    0    0    0    0    0    0    0    0    0    0
          6.00-21 1.000-21  1.0E-10  1.000-10
Xw1OH       1         5.8            0.          0.          0.
            0    0    0    0    0    0    0    0    1    0    0    1    0    0    0    0    1    0    0    0    0    0    0    0    0    0    0    0    0    0
          1.00-10  1.000-10  1.0E-10  1.000-10
Xw1O        1        -6.3            0.          0.          0.
            1    0    0    0    0    0    0    0    0    0    0   -1    0    0    0    0    1    0    0    0    0    0    0    0    0    0    0    0    0    0
          1.00-10 1.000-10   1.0E-10  1.000-10
K-CE-mon    1        1.11            0.          0.          0.
           -1    1    0    0    0    0    0    0    0    0    0    0    0    0    0    0    0    1    0    0    0    0    0    0    0    0    0    0    0    0
          1.00-02 1.000-02   1.0E-10  1.000-10
Ca-CE-mon   1         5.03           0.          0.          0.
           -2    0    1    0    0    0    0    0    0    0    0    0    0    0    0    0    0    2    0    0    0    0    0    0    0    0    0    0    0    0
          1.00-03 1.000-03   1.0E-10  1.000-10
Mg-CE-mon   1         5.03           0.          0.          0.
           -2    0    0    1    0    0    0    0    0    0    0    0    0    0    0    0    0    2    0    0    0    0    0    0    0    0    0    0    0    0
          1.00-10 1.000-04    1.0E-10  1.000-10
Sr-CE-mon   1         5.03           0.          0.          0.
           -2    0    0    0    1    0    0    0    0    0    0    0    0    0    0    0    0    2    0    0    0    0    0    0    0    0    0    0    0    0
          1.00-10 1.000-10   1.0E-10  1.000-10
Ni-CE-mon   1         5.08           0.          0.          0.
           -2    0    0    0    0    0    0    0    0    0    0    0    1    0    0    0    0    0    2    0    0    0    0    0    0    0    0    0    0    0
          1.00-10 1.000-10   1.0E-10  1.000-10
Fe-CE-mon   1         5.08           0.          0.          0.
           -2    0    0    0    0    1    0    0    0    0    0    0    0    0    0    0    0    0    2    0    0    0    0    0    0    0    0    0    0    0
          1.00-10 1.000-10   1.0E-10  1.000-10
XSOFe       1       0.6203           0.          0.          0.
            0    0    0    0    0    1    0    0    1    0    0   -1    0    0    0    1    0    0    0    0    0    0    0    0    0    0    0    0    0    0
          2.00-16  1.000-16  1.0E-10  1.000-10
XSFeOH      1       -10.44           0.          0.          0.
            0    0    0    0    0    1    0    0    0    0    0   -2    0    0    0    1    0    0    0    0    0    0    0    0    0    0    0    0    0    0
          1.00-18 1.000-18  1.00-18 1.000-18
```

```
Ca-CE-mon   1       5.03      0.        0.        0.
           -2   0   1   0   0   0   0   0   0   0   0   0   0   0   0   0   0   0   2   0   0   0   0   0   0   0   0   0   0
           1.00-03 1.000-03  1.0E-10  1.000-10
Mg-CE-mon   1       5.03      0.        0.        0.
           -2   0   0   1   0   0   0   0   0   0   0   0   0   0   0   0   0   0   2   0   0   0   0   0   0   0   0   0   0
           1.00-10 1.000-04  1.0E-10  1.000-10
Sr-CE-mon   1       5.03      0.        0.        0.
           -2   0   0   0   1   0   0   0   0   0   0   0   0   0   0   0   0   0   2   0   0   0   0   0   0   0   0   0   0
           1.00-10 1.000-10  1.0E-10  1.000-10
Ni-CE-mon   1       5.08      0.        0.        0.
           -2   0   0   0   0   0   0   0   0   0   0   0   1   0   0   0   0   0   2   0   0   0   0   0   0   0   0   0   0
           1.00-10 1.000-10  1.0E-10  1.000-10
Fe-CE-mon   1       5.08      0.        0.        0.
           -2   0   0   0   0   1   0   0   0   0   0   0   0   0   0   0   0   0   2   0   0   0   0   0   0   0   0   0   0
           1.00-10 1.000-10  1.0E-10  1.000-10
XSOFe       1       0.6203     0.        0.        0.
            0   0   0   0   0   1   0   0   1   0   0  -1   0   0   0   1   0   0   0   0   0   0   0   0   0   0   0   0   0
           2.00-16  1.000-16  1.0E-10  1.000-10
XSFeOH     1       -10.44      0.        0.        0.
            0   0   0   0   0   1   0   0   0   0   0  -2   0   0   0   1   0   0   0   0   0   0   0   0   0   0   0   0   0
           1.00-18 1.000-18 1.00-18 1.000-18
XSOFe-Na   1       -18.637      0.        0.        0.
            1   0   0   0   0   1   0   0   0   0   0  -3   0   0   0   1   0   0   0   0   0   0   0   0   0   0   0   0   0
           6.00-21 1.000-21 1.0E-10  1.000-10
Xw1ONi+Cl  1       -2.148      0.        0.        0.
            0   0   0   0   0   0   0   0   1   0   0  -1   1   0   0   0   1   0   0   0   0   0   0   0   0   0   0   0   0
           1.00-18 1.000-18 1.00-18 1.000-18
Xw1NiOH    1        -12.42      0.        0.        0.
            0   0   0   0   0   0   0   0   0   0   0  -2   1   0   0   0   1   0   0   0   0   0   0   0   0   0   0   0   0
           1.00-18 1.000-18 1.00-18 1.000-18
Xw1ONi-Na  1        -21.634     0.        0.        0.
            1   0   0   0   0   0   0   0   0   0   0  -3   1   0   0   0   1   0   0   0   0   0   0   0   0   0   0   0   0
           6.00-21 1.000-21 1.0E-10  1.000-10
Xw1OFe+Cl  1        -1.795      0.        0.        0.
            0   0   0   0   0   1   0   0   1   0   0  -1   0   0   0   0   1   0   0   0   0   0   0   0   0   0   0   0   0
           1.00-18 1.000-18 1.00-18 1.000-18
Xw1FeOH    1        -13.99      0.        0.        0.
            0   0   0   0   0   1   0   0   0   0   0  -2   0   0   0   0   1   0   0   0   0   0   0   0   0   0   0   0   0
           1.00-18 1.000-18 1.00-18 1.000-18
Xw1OFe-Na  1        -22.61      0.        0.        0.
            1   0   0   0   0   1   0   0   0   0   0  -3   0   0   0   0   1   0   0   0   0   0   0   0   0   0   0   0   0
           6.00-21 1.000-21 1.0E-10  1.000-10
Xw2OH      1         7.07       0.        0.        0.
            0   0   0   0   0   0   0   0   1   0   0   1   0   0   0   0   0   1   0   0   0   0   0   0   0   0   0   0   0
           1.00-10 1.000-10  1.0E-10  1.000-10
Xw2O       1        -9.338      0.        0.        0.
            1   0   0   0   0   0   0   0   0   0   0  -1   0   0   0   0   0   1   0   0   0   0   0   0   0   0   0   0   0
           1.00-10 1.000-10  1.0E-10  1.000-10
```

A.1.3 Poro01

Porosity defined for each node.

```
          51        1.0e-02

   39  39  39  39  39  39  39  39  39  39  39  39  39  39  39  39
39  39  39  39  39  39  39  39  39  39  39  39  39  39  39
39  39  39  39  39  39  39  39  39  39  39  39  39  39  39
39  39  39  39  39  39
```

A.1.4 Input_1

Nodes for which there will be an output file recording the evolution of concentrations with time: to later get the breakthrough curves.

```
A405 locations i for breakthrough curves:   4,10,20,30,36
```

A.1.5 Hoo001

Hydraulic loads for each node.

```
          51        1.0e-0
0000  10  10  10  10  10  10  10  10  10  10  10  10  10  10
10  10  10  10  10  10  10  10  10  10  10  10  10  10  10  10
10  10  10  10  10  10  10  10  10  10  10  10  10  10  10  10
10  10  10  10  10  10  10  10  10  10
```

A.1.6 Icheo1

Defines which system defined in TEST.INI file is used in each node.

```
          51        1.0e-00
   2   1   1   1   1   1   1   1   1   1   1   1   1   1   1
1   1   1   1   1   1   1    1   1   1   1   1   1   1   1   1
1   1   1   1   1   1   1   1   1   1   1   1   1   1   1   1
1   1   1   1   1
```

A.2 Output files

A.2.1 Initial.out

Description of the model before the calculation begins.

```
unit of mass is kilogram          unit of length is meter
unit of time is second            unit of electrical potential is volt
unit of temperature is celsius    unit of heat is joule
exception: units for standard enthaply of reaction (input by user) are kJ/mol
itype,idynam,idismdl            0            1            0
in1,in2        10000           500
nxmax,xmax,gc,rw            49    2.000000000000000
   10.70000000000000          0.000000000000000
           8    31557600.00000000           315576000.0000000
   1577880000.000000          3155760000.000000          15778800000.00000
   31557600000.00000          157788000000.0000          315576000000.0000
                  19          63          0          0          12          0          0
this simulation is isothermal, temperature =  25.

number of pr87int outs =   8    given at the followi times:
    3.16E+07 3.16E+08 1.58E+09 3.16E+09 1.58E+10 3.16E+10 1.58E+11 3.16E+11


err=  1.00E-08      dtmult= 1.50      dtdiv= 1.20
iterm=  90     iterj=    5     iterd=  90      ndiv=   90

  19 basis species          initial  conditions        boundary  conditions
             charge         type        value          type        value
     Na+         1.           1        9.1345E-02        1        9.1345E-02          2       0.0000E+00          2       4.0000E-02
     K+          1.           1        3.8365E-04        1        3.8365E-04          2       0.0000E+00          2       4.0000E-02
     Ca+2        2.           1        1.2725E-02        1        1.2725E-02          2       0.0000E+00          2       4.0000E-02
     Mg+2        2.           1        1.6046E-02        1        1.6046E-02          2       0.0000E+00          2       4.0000E-02
     Sr+2        2.           1        8.5597E-05        1        8.5597E-05          2       0.0000E+00          2       4.0000E-02
     Fe+2        2.           1        1.6115E-06        1        1.6115E-06          2       0.0000E+00          2       4.0000E-02
     CO3-2      -2.           2        2.1799E-03        2        2.1799E-03          2       0.0000E+00          2       4.0000E-02
     SO4-2      -2.           2        1.3116E-02        2        1.3116E-02          2       0.0000E+00          2       4.0000E-02
     Cl-        -1.           2        1.1283E-01        2        1.1283E-01          2       0.0000E+00          2       4.0000E-02
     Dummy_F-   -1.           1        1.0000E-10        1        1.0000E-10          2       0.0000E+00          2       4.0000E-02
     DummyH2Si  -2.           1        1.0000E-10        1        1.0000E-10          2       0.0000E+00          2       4.0000E-02
     H+          1.           1        5.5302E-08        1        5.5302E-08          2       0.0000E+00          2       4.0000E-02
     trac_Ni     2.           1        4.7175E-11        1        4.7175E-11          2       0.0000E+00          2       4.0000E-02
     trac_X     -2.           1        1.6890E-07        1        1.6890E-07          2       0.0000E+00          2       4.0000E-02
     Ni_s_kd     0.           1        1.0000E-10        1        1.0000E-10          2       0.0000E+00          2       4.0000E-02
     Ss1_OH      0.           2        1.8400E-03        2        1.8400E-03          2       0.0000E+00          2       4.0000E-02
     Sw1_OH      0.           2        3.6800E-02        2        3.6800E-02          2       0.0000E+00          2       4.0000E-02
     Sw2_OH      0.           1        3.6800E-02        1        3.6800E-02          2       0.0000E+00          2       4.0000E-02
     Na-Mont     0.           2        9.6539E-01        2        9.6539E-01          2       0.0000E+00          2       4.0000E-02
OH-            1-0.14000E+02  0.00000E+00  0.00000E+00  0.00000E+00
               0    0    0    0    0    0    0    0    0    0    -1    0    0    0    0    0    0    0
            0.730E-07 0.730E-07 0.730E-06 0.100E-06
NiOH+          1-0.98600E+01  0.00000E+00  0.00000E+00  0.00000E+00
               0    0    0    0    0    0    0    0    0    0    -1    1    0    0    0    0    0    0
```

```
NiOH+          1-0.98600E+01 0.00000E+00 0.00000E+00 0.00000E+00
                 0    0    0    0    0    0    0    0    0    0    0   -1    1    0    0    0    0    0    0
               0.280E-14 0.280E-14 0.730E-06 0.100E-06
NiOH           1-0.19000E+02 0.00000E+00 0.00000E+00 0.00000E+00
                 0    0    0    0    0    0    0    0    0    0    0   -2    1    0    0    0    0    0    0
               0.280E-18 0.280E-18 0.730E-06 0.100E-06
NiOH-          1-0.30000E+02 0.00000E+00 0.00000E+00 0.00000E+00
                 0    0    0    0    0    0    0    0    0    0    0   -3    1    0    0    0    0    0    0
               0.280E-24 0.280E-24 0.730E-06 0.100E-06
CaHCO3         1 0.11435E+02 0.00000E+00 0.00000E+00 0.00000E+00
                 0    0    1    0    0    0    1    0    0    0    0    1    0    0    0    0    0    0    0
               0.730E-09 0.730E-09 0.730E-06 0.100E-06
CaSO4aq        1 0.23000E+01 0.00000E+00 0.00000E+00 0.00000E+00
                 0    0    1    0    0    0    0    1    0    0    0    0    0    0    0    0    0    0    0
               0.730E-08 0.730E-08 0.730E-06 0.100E-06
CaCO3          0 0.32240E+01 0.00000E+00 0.00000E+00 0.00000E+00
                 0    0    1    0    0    0    1    0    0    0    0    0    0    0    0    0    0    0    0
               0.100E-06 0.100E-06 0.730E-06 0.100E-06
CaOH           1-0.12780E+02 0.00000E+00 0.00000E+00 0.00000E+00
                 0    0    1    0    0    0    0    0    0    0    0   -1    0    0    0    0    0    0    0
               0.300E-07 0.300E-07 0.730E-06 0.100E-06
MgCO3aq        1 0.29800E+01 0.00000E+00 0.00000E+00 0.00000E+00
                 0    0    0    1    0    0    1    0    0    0    0    0    0    0    0    0    0    0    0
               0.730E-06 0.100E-06 0.730E-06 0.100E-06
MgSO4aq        1 0.23700E+01 0.00000E+00 0.00000E+00 0.00000E+00
                 0    0    0    1    0    0    0    1    0    0    0    0    0    0    0    0    0    0    0
               0.180E-02 0.180E-02 0.730E-06 0.100E-06
MgHCO3         1 0.11397E+02 0.00000E+00 0.00000E+00 0.00000E+00
                 0    0    0    1    0    0    1    0    0    0    0    1    0    0    0    0    0    0    0
               0.120E-04 0.120E-04 0.730E-06 0.100E-06
MgOH-          1-0.11440E+02 0.00000E+00 0.00000E+00 0.00000E+00
                 0    0    0    1    0    0    0    0    0    0    0   -1    0    0    0    0    0    0    0
               0.730E-06 0.100E-06 0.730E-06 0.100E-06
SrHCO3         1 0.11514E+02 0.00000E+00 0.00000E+00 0.00000E+00
                 0    0    0    0    1    0    1    0    0    0    0    1    0    0    0    0    0    0    0
               0.730E-06 0.730E-06 0.730E-06 0.100E-06
SrSO4aq        1 0.22900E+01 0.00000E+00 0.00000E+00 0.00000E+00
                 0    0    0    0    1    0    0    1    0    0    0    0    0    0    0    0    0    0    0
               0.730E-06 0.730E-06 0.730E-06 0.100E-06
SrOH+          1-0.13290E+02 0.00000E+00 0.00000E+00 0.00000E+00
                 0    0    0    0    1    0    0    0    0    0    0   -1    0    0    0    0    0    0    0
               0.730E-06 0.100E-06 0.730E-06 0.100E-06
SrCO3          1 0.28050E+01 0.00000E+00 0.00000E+00 0.00000E+00
                 0    0    0    0    1    0    1    0    0    0    0    0    0    0    0    0    0    0    0
               0.100E-06 0.100E-06 0.730E-06 0.100E-06
KOH            1-0.14460E+02 0.00000E+00 0.00000E+00 0.00000E+00
                 0    1    0    0    0    0    0    0    0    0    0   -1    0    0    0    0    0    0    0
               0.730E-06 0.100E-06 0.730E-06 0.100E-06
```

```
KSO4-      1 0.85000E+00 0.00000E+00 0.00000E+00 0.00000E+00 0.00000E+00
             0     1     0     0     0     0     0     0     0     0     0
           0.730E-06 0.730E-06 0.730E-06 0.100E-06
NaSO4-       1 0.70000E+00 0.00000E+00 0.00000E+00 0.00000E+00 0.00000E+00
             1     0     0     0     1     0     0     0     0     0     0
           0.730E-06 0.730E-06 0.730E-06 0.100E-06
NaCO3-       1 0.12700E+01 0.00000E+00 0.00000E+00 0.00000E+00 0.00000E+00
             1     0     0     0     1     0     0     0     0     0     0
           0.730E-06 0.100E-06 0.730E-06 0.100E-06
NaHCO3       1 0.10079E+02 0.00000E+00 0.00000E+00 0.00000E+00 0.00000E+00
             1     0     0     0     1     0     0     0     0     0     0
           0.330E-04 0.330E-04 0.730E-06 0.100E+01
NaOHaq      1-0.14180E+02 0.00000E+00 0.00000E+00 0.00000E+00 0.00000E+00
             1     0     0     0     0     0    -1     0     0     0     0
           0.530E-07 0.500E-07 0.730E-06 0.100E-06
HCO3-        1 0.10329E+02 0.00000E+00 0.00000E+00 0.00000E+00 0.00000E+00
             0     0     0     0     1     0     1     0     0     0     0
           0.630E-03 0.630E-03 0.730E-06 0.100E-06
H2CO3aq      1 0.16681E+02 0.00000E+00 0.00000E+00 0.00000E+00 0.00000E+00
             0     0     0     0     1     0     2     0     0     0     0
           0.130E-04 0.730E-06 0.130E-04 0.100E-06
HSO4-        1 0.19880E+01 0.00000E+00 0.00000E+00 0.00000E+00 0.00000E+00
             0     0     0     0     0     1     0     0     0     0     0
           0.130E-08 0.100E-08 0.730E-06 0.100E-06
FeSO4aq      1 0.22500E+01 0.00000E+00 0.00000E+00 0.00000E+00 0.00000E+00
             0     0     0     0     1     0     0     0     0     0     0
           0.830E-05 0.800E-05 0.730E-06 0.100E-06
FeHCO3       1 0.12329E+02 0.00000E+00 0.00000E+00 0.00000E+00 0.00000E+00
             0     0     0     0     1     1     0     0     0     0     0
           0.500E-06 0.500E-06 0.730E-06 0.100E-06
FeCO3        1 0.43800E+01 0.00000E+00 0.00000E+00 0.00000E+00 0.00000E+00
             0     0     0     0     1     1     0     0     0     0     0
           0.300E-06 0.300E-06 0.730E-06 0.100E-06
FeHSO4+      1 0.30680E+01 0.00000E+00 0.00000E+00 0.00000E+00 0.00000E+00
             0     0     0     0     1     0     1     0     0     0     0
           0.800E-05 0.800E-05 0.730E-06 0.100E-06
FeCl         1 0.14000E+00 0.00000E+00 0.00000E+00 0.00000E+00 0.00000E+00
             0     0     0     0     1     0     0     0     0     0     0
           0.200E-05 0.200E-05 0.730E-06 0.100E-06
FeOH        1-0.95000E+01 0.00000E+00 0.00000E+00 0.00000E+00 0.00000E+00
             0     0     0     0     1     0     0    -1     0     0     0
           0.200E-06 0.200E-06 0.730E-06 0.100E-06
NiCl+        1 0.40000E+00 0.00000E+00 0.00000E+00 0.00000E+00 0.00000E+00
             0     0     0     0     0     1     0     0     0     0     0
           0.600E-08 0.200E-15 0.730E-06 0.100E-06
NiCl2        1 0.96000E+00 0.00000E+00 0.00000E+00 0.00000E+00 0.00000E+00
             0     0     0     0     0     2     0     0     0     0     0
           0.200E-08 0.200E-18 0.730E-06 0.100E-06
NiSO4aq      1 0.23100E+01 0.00000E+00 0.00000E+00 0.00000E+00 0.00000E+00
```

```
NiSO4aq      1 0.23100E+01 0.00000E+00 0.00000E+00 0.00000E+00
               0    0    0    0    0    0    0    1    0    0    0    0    1    0    0    0    0    0    0
           0.330E-08 0.800E-16 0.730E-06 0.100E-06
NiSO42       1 0.32000E+01 0.00000E+00 0.00000E+00 0.00000E+00
               0    0    0    0    0    0    0    2    0    0    0    0    1    0    0    0    0    0    0
           0.330E-08 0.800E-16 0.730E-06 0.100E-06
NiCO3        1 0.42000E+01 0.00000E+00 0.00000E+00 0.00000E+00
               0    0    0    0    0    0    1    0    0    0    0    0    1    0    0    0    0    0    0
           0.300E-05 0.300E-06 0.730E-06 0.100E-06
NiCO32       1 0.62000E+01 0.00000E+00 0.00000E+00 0.00000E+00
               0    0    0    0    0    0    2    0    0    0    0    0    1    0    0    0    0    0    0
           0.300E-05 0.300E-06 0.730E-06 0.100E-06
NiHCO3       1 0.11720E+02 0.00000E+00 0.00000E+00 0.00000E+00
               0    0    0    0    0    0    1    0    0    0    0    1    1    0    0    0    0    0    0
           0.300E-05 0.300E-06 0.730E-06 0.100E-06
Ni_sKd       1 0.29090E+01 0.00000E+00 0.00000E+00 0.00000E+00
               0    0    0    0    0    0    0    0    0    0    0    0    0    0    1    0    0    0    0
           0.600E-08 0.200E-15 0.730E-06 0.100E-06
XSOH         1 0.55700E+01 0.00000E+00 0.00000E+00 0.00000E+00
               0    0    0    0    0    0    0    0    1    0    0    1    0    0    0    1    0    0    0
           0.100E-09 0.100E-09 0.100E-09 0.100E-09
XSO          1-0.67400E+01 0.00000E+00 0.00000E+00 0.00000E+00
               1    0    0    0    0    0    0    0    0    0    0   -1    0    0    0    1    0    0    0
           0.500E-09 0.100E-09 0.100E-09 0.100E-09
XSONi        1 0.29600E+00 0.30000E+02 0.00000E+00 0.00000E+00
               0    0    0    0    0    0    0    0    1    0    0   -1    1    0    0    1    0    0    0
           0.200E-15 0.100E-15 0.100E-09 0.100E-09
XSNiOH       1-0.90000E+01 0.00000E+00 0.00000E+00 0.00000E+00
               0    0    0    0    0    0    0    0    0    0    0   -2    1    0    0    1    0    0    0
           0.100E-17 0.100E-17 0.100-180 0.000E+00
XSONi-Na     1-0.17700E+02 0.38000E+03 0.00000E+00 0.00000E+00
               1    0    0    0    0    0    0    0    0    0    0   -3    1    0    0    1    0    0    0
           0.600E-20 0.100E-20 0.100E-09 0.100E-09
XW1OH        1 0.58000E+01 0.00000E+00 0.00000E+00 0.00000E+00
               0    0    0    0    0    0    0    0    1    0    0    1    0    0    0    0    1    0    0
           0.100E-09 0.100E-09 0.100E-09 0.100E-09
XW1O         1-0.63000E+01 0.00000E+00 0.00000E+00 0.00000E+00
               1    0    0    0    0    0    0    0    0    0    0   -1    0    0    0    0    1    0    0
           0.100E-09 0.100E-09 0.100E-09 0.100E-09
K-CE-mon     1 0.11100E+01 0.00000E+00 0.00000E+00 0.00000E+00
              -1    1    0    0    0    0    0    0    0    0    0    0    0    0    0    0    0    0    1
           0.100E-01 0.100E-01 0.100E-09 0.100E-09
Ca-CE-mon    1 0.50300E+01 0.00000E+00 0.00000E+00 0.00000E+00
              -2    0    1    0    0    0    0    0    0    0    0    0    0    0    0    0    0    0    2
           0.100E-02 0.100E-02 0.100E-09 0.100E-09
Mg-CE-mon    1 0.50300E+01 0.00000E+00 0.00000E+00 0.00000E+00
              -2    0    0    1    0    0    0    0    0    0    0    0    0    0    0    0    0    0    2
           0.100E-09 0.100E-03 0.100E-09 0.100E-09
Sr-CE-mon    1 0.50300E+01 0.00000E+00 0.00000E+00 0.00000E+00
```

```
Sr-CE-mon    1 0.50300E+01 0.00000E+00 0.00000E+00 0.00000E+00
            -2          0          1          0          0
     0.100E-09  0.100E-09  0.100E-09  0.100E-09
Ni-CE-mon    1 0.50800E+01 0.00000E+00 0.00000E+00 0.00000E+00
            -2          0          0          0          0
     0.100E-09  0.100E-09  0.100E-09  0.100E-09
Fe-CE-mon    1 0.50800E+01 0.00000E+00 0.00000E+00 0.00000E+00
            -2          0          0          1          0
     0.100E-09  0.100E-09  0.100E-09  0.100E-09
XSOFe        1 0.62000E+00 0.30000E+02 0.00000E+00 0.00000E+00
             0          0          0          1          0
     0.200E-15  0.100E-15  0.100E-09  0.100E-09
XSFeOH       1-0.10440E+02 0.00000E+00 0.00000E+00 0.00000E+00
             0          0          0          0          1
     0.100E-17  0.100-180  0.000E+00
XSOFe-Na     1-0.18630E+02 0.70000E+02 0.00000E+00 0.00000E+00
             1          0          0          0          0
     0.600E-20  0.100E-20  0.100E-09  0.100E-09
Xw1ONi+Cl    1-0.21480E+01 0.00000E+00 0.00000E+00 0.00000E+00
             0          0          0          0          1
     0.100E-17  0.100-180  0.000E+00
Xw1NiOH      1-0.12400E+02 0.20000E+02 0.00000E+00 0.00000E+00
             0          0          0          0          0
     0.100E-17  0.100-180  0.000E+00
Xw1ONi-Na    1-0.21600E+02 0.34000E+03 0.00000E+00 0.00000E+00
             1          0          0          0          0
     0.600E-20  0.100E-20  0.100E-09  0.100E-09
Xw1OFe+Cl    1-0.17900E+01 0.50000E+02 0.00000E+00 0.00000E+00
             0          0          1          0          0
     0.100E-17  0.100E-17  0.100-180  0.000E+00
Xw1FeOH      1-0.13900E+02 0.90000E+02 0.00000E+00 0.00000E+00
             0          0          1          0          0
     0.100E-17  0.100E-17  0.100-180  0.000E+00
Xw1OFe-Na    1-0.22600E+02 0.10000E+02 0.00000E+00 0.00000E+00
             1          0          0          1          0
     0.600E-20  0.100E-20  0.100E-09  0.100E-09
Xw2OH        1 0.70700E+01 0.00000E+00 0.00000E+00 0.00000E+00
             0          0          0          0          1
     0.100E-09  0.100E-09  0.100E-09  0.100E-09
Xw2O         1-0.93300E+01 0.80000E+02 0.00000E+00 0.00000E+00
             1          0          0          0          0
     0.100E-09  0.100E-09  0.100E-09  0.100E-09

63 complexes
      charge      stoichiometry
OH-     -1.    0  0  0  0  0  0  0  0  0  0  0  0  0  0  0  0  0  0
NiOH+    1.    0  0  0  0  0  0  0  0  0  0  0  0  0  0  0  0  0  0
NiOH     0.    0  0  0  0  0  0  0  0  0  0  0  0  0  0  0  0  0  0
NiOH-   -1.    0  0  0  0  0  0  0  0  0  0  0  0  0  0  0  0  0  0
```

NiOH-	-1.	0	0	0	0	0	0	0	0	0	0	0	-3	1	0	0	0	0	0	0
CaHCO3	1.	0	0	1	0	0	0	1	0	0	0	0	1	0	0	0	0	0	0	0
CaSO4aq	0.	0	0	1	0	0	0	0	1	0	0	0	0	0	0	0	0	0	0	0
CaCO3	0.	0	0	1	0	0	0	1	0	0	0	0	0	0	0	0	0	0	0	0
CaOH	1.	0	0	1	0	0	0	0	0	0	0	0	-1	0	0	0	0	0	0	0
MgCO3aq	0.	0	0	0	1	0	0	1	0	0	0	0	0	0	0	0	0	0	0	0
MgSO4aq	0.	0	0	0	1	0	0	0	1	0	0	0	0	0	0	0	0	0	0	0
MgHCO3	1.	0	0	0	1	0	0	1	0	0	0	0	1	0	0	0	0	0	0	0
MgOH-	1.	0	0	0	1	0	0	0	0	0	0	0	-1	0	0	0	0	0	0	0
SrHCO3	1.	0	0	0	0	1	0	1	0	0	0	0	1	0	0	0	0	0	0	0
SrSO4aq	0.	0	0	0	0	1	0	0	1	0	0	0	0	0	0	0	0	0	0	0
SrOH+	1.	0	0	0	0	1	0	0	0	0	0	0	-1	0	0	0	0	0	0	0
SrCO3	0.	0	0	0	0	1	0	1	0	0	0	0	0	0	0	0	0	0	0	0
KOH	0.	0	1	0	0	0	0	0	0	0	0	0	-1	0	0	0	0	0	0	0
KSO4-	-1.	0	1	0	0	0	0	0	1	0	0	0	0	0	0	0	0	0	0	0
NaSO4-	-1.	1	0	0	0	0	0	0	1	0	0	0	0	0	0	0	0	0	0	0
NaCO3-	-1.	1	0	0	0	0	0	1	0	0	0	0	0	0	0	0	0	0	0	0
NaHCO3	0.	1	0	0	0	0	0	1	0	0	0	0	1	0	0	0	0	0	0	0
NaOHaq	0.	1	0	0	0	0	0	0	0	0	0	0	-1	0	0	0	0	0	0	0
HCO3-	-1.	0	0	0	0	0	0	1	0	0	0	0	1	0	0	0	0	0	0	0
H2CO3aq	0.	0	0	0	0	0	0	1	0	0	0	0	2	0	0	0	0	0	0	0
HSO4-	-1.	0	0	0	0	0	0	0	1	0	0	0	1	0	0	0	0	0	0	0
FeSO4aq	0.	0	0	0	0	0	1	0	1	0	0	0	0	0	0	0	0	0	0	0
FeHCO3	1.	0	0	0	0	0	1	1	0	0	0	0	1	0	0	0	0	0	0	0
FeCO3	0.	0	0	0	0	0	1	1	0	0	0	0	0	0	0	0	0	0	0	0
FeHSO4+	1.	0	0	0	0	0	1	0	1	0	0	0	1	0	0	0	0	0	0	0
FeCl	1.	0	0	0	0	0	1	0	0	1	0	0	0	0	0	0	0	0	0	0
FeOH	1.	0	0	0	0	0	1	0	0	0	0	0	-1	0	0	0	0	0	0	0
NiCl+	1.	0	0	0	0	0	0	0	0	1	0	0	0	1	0	0	0	0	0	0
NiCl2	0.	0	0	0	0	0	0	0	0	2	0	0	0	1	0	0	0	0	0	0
NiSO4aq	0.	0	0	0	0	0	0	0	1	0	0	0	0	1	0	0	0	0	0	0
NiSO42	-2.	0	0	0	0	0	0	0	2	0	0	0	0	1	0	0	0	0	0	0
NiCO3	0.	0	0	0	0	0	0	1	0	0	0	0	0	1	0	0	0	0	0	0
NiCO32	-2.	0	0	0	0	0	0	2	0	0	0	0	0	1	0	0	0	0	0	0
NiHCO3	1.	0	0	0	0	0	0	1	0	0	0	0	1	1	0	0	0	0	0	0
Ni_sKd	0.	0	0	0	0	0	0	0	0	0	0	0	0	0	0	1	0	0	0	0
XSOH	0.	0	0	0	0	0	0	0	0	1	0	0	1	0	0	0	1	0	0	0
XSO	0.	1	0	0	0	0	0	0	0	0	0	0	-1	0	0	0	1	0	0	0
XSONi	0.	0	0	0	0	0	0	0	0	1	0	0	-1	1	0	0	1	0	0	0
XSNiOH	0.	0	0	0	0	0	0	0	0	0	0	0	-2	1	0	0	1	0	0	0
XSONi-Na	0.	1	0	0	0	0	0	0	0	0	0	0	-3	1	0	0	1	0	0	0
Xw1OH	0.	0	0	0	0	0	0	0	0	1	0	0	1	0	0	0	0	1	0	0
Xw1O	0.	1	0	0	0	0	0	0	0	0	0	0	-1	0	0	0	0	1	0	0
K-CE-mon	0.	-1	1	0	0	0	0	0	0	0	0	0	0	0	0	0	0	0	0	1
Ca-CE-mon	0.	-2	0	1	0	0	0	0	0	0	0	0	0	0	0	0	0	0	0	2
Mg-CE-mon	0.	-2	0	0	1	0	0	0	0	0	0	0	0	0	0	0	0	0	0	2
Sr-CE-mon	0.	-2	0	0	0	1	0	0	0	0	0	0	0	0	0	0	0	0	0	2
Ni-CE-mon	0.	-2	0	0	0	0	0	0	0	0	0	0	0	1	0	0	0	0	0	2
Fe-CE-mon	0.	-2	0	0	0	0	1	0	0	0	0	0	0	0	0	0	0	0	0	2

```
 Fe-CE-mon    0.      -2   0   0   0   0   1   0   0   0   0   0    0   0   0   0   0   0   0   2
 XSOFe        0.       0   0   0   0   0   1   0   0   1   0   0   -1   0   0   0   1   0   0   0
 XSFeOH       0.       0   0   0   0   0   1   0   0   0   0   0   -2   0   0   0   1   0   0   0
 XSOFe-Na     0.       1   0   0   0   0   1   0   0   0   0   0   -3   0   0   0   1   0   0   0
 Xw1ONi+Cl    0.       0   0   0   0   0   0   0   0   1   0   0   -1   1   0   0   0   1   0   0
 Xw1NiOH      0.       0   0   0   0   0   0   0   0   0   0   0   -2   1   0   0   0   1   0   0
 Xw1ONi-Na    0.       1   0   0   0   0   0   0   0   0   0   0   -3   1   0   0   0   1   0   0
 Xw1OFe+Cl    0.       0   0   0   0   0   1   0   0   1   0   0   -1   0   0   0   0   1   0   0
 Xw1FeOH      0.       0   0   0   0   0   1   0   0   0   0   0   -2   0   0   0   0   1   0   0
 Xw1OFe-Na    0.       1   0   0   0   0   1   0   0   0   0   0   -3   0   0   0   0   1   0   0
 Xw2OH        0.       0   0   0   0   0   0   0   0   1   0   0    1   0   0   0   0   0   1   0
 Xw2O         0.       1   0   0   0   0   0   0   0   0   0   0   -1   0   0   0   0   0   1   0

              boundary or influx conditions
                      temp =  25.00
             ionic strength at index =      2    0.18576719

                    total          basis         activity         sorbed
basis          aqueous conc.   concentration   coefficient
 Na+           -8.5484E-01      9.1345E-02      0.7538        9.8044E-01
 K+             4|.7186E-04     3.8365E-04      0.7538        8.1848E-05
 Ca+2           2.2724E-01      1.2725E-02      0.3229        2.1249E-01
 Mg+2           2.8696E-01      1.6046E-02      0.3229        2.6795E-01
 Sr+2           1.5284E-03      8.5597E-05      0.3229        1.4294E-03
 Fe+2           2.0030E-03      1.6115E-06      0.3229        2.0010E-03
 CO3-2          2.1799E-03      4.6622E-06      0.3229        0.0000E+00
 SO4-2          1.3116E-02      7.2567E-03      0.3229        0.0000E+00
 Cl-            1.1283E-01      1.0933E-01      0.7538        3.4965E-03
 Dummy_F-       1.0000E-10      1.0000E-10      0.7538        0.0000E+00
 DummyH2Si      1.0000E-10      1.0000E-10      0.3229        0.0000E+00
 H+            -1.4727E-02      5.5302E-08      0.7538        2.0065E-02
 trac_Ni        2.8379E-08      4.7175E-11      0.3229        2.8318E-08
 trac_X         1.6890E-07      1.6890E-07      0.3229        0.0000E+00
 Ni_s_kd        8.1196E-08      1.0000E-10       1.000        0.0000E+00
 Ss1_OH         1.8400E-03      2.7382E-04       1.000        1.8400E-03
 Sw1_OH         3.6800E-02      1.9843E-02       1.000        3.6800E-02
 Sw2_OH         3.8338E-02      3.6800E-02       1.000        3.8338E-02
 Na-Mont        9.6539E-01      1.5127E-03       1.000        9.6539E-01
 OH-               -1.          3.1821E-07
 NiOH+              1.          6.6913E-14
 NiOH               0.          8.7653E-16
 NiOH-             -1.          2.7893E-19
 CaHCO3             1.          9.3142E-05
 CaSO4aq            0.          1.9211E-03
 CaCO3              0.          1.0361E-05
 CaOH               1.          2.1700E-08
 MgCO3aq            0.          7.4493E-06
 MgSO4aq            0.          2.8462E-03
 MgHCO3             1.          1.0761E-04
```

MgHCO3	1.	1.0761E-04
MgOH-	1.	5.9864E-07
SrHCO3	1.	7.5153E-07
SrSO4aq	0.	1.2629E-05
SrOH+	1.	4.5108E-11
SrCO3	0.	2.6559E-08
KOH	0.	2.4054E-11
KSO4-	-1.	6.3643E-06
NaSO4-	-1.	1.0728E-03
NaCO3-	-1.	2.5607E-06
NaHCO3	0.	5.1836E-05
NaOHaq	0.	1.0913E-08
HCO3-	-1.	1.7759E-03
H2CO3aq	0.	1.2551E-04
HSO4-	-1.	1.2605E-08
FeSO4aq	0.	2.1683E-07
FeHCO3	1.	9.2410E-08
FeCO3	0.	1.8792E-08
FeHSO4+	1.	7.8862E-14
FeCl	1.	7.8535E-08
FeOH	1.	5.2363E-09
NiCl+	1.	4.1835E-12
NiCl2	0.	9.4370E-13
NiSO4aq	0.	7.2880E-12
NiSO42	-2.	4.1053E-13
NiCO3	0.	3.6346E-13
NiCO32	-2.	1.6946E-16
NiHCO3	1.	6.6558E-13
Ni_sKd	0.	8.1096E-08
XSOH	0.	3.4954E-07
XSO	0.	8.2301E-05
XSONi	0.	2.0553E-08
XSNiOH	0.	2.4001E-09
XSONi-Na	0.	1.4883E-10
Xw1OH	0.	4.3017E-05
Xw1O	0.	1.6427E-02
K-CE-mon	0.	8.1848E-05
Ca-CE-mon	0.	2.1249E-01
Mg-CE-mon	0.	2.6795E-01
Sr-CE-mon	0.	1.4294E-03
Ni-CE-mon	0.	8.8388E-10
Fe-CE-mon	0.	3.0193E-05
XSOFe	0.	1.4805E-03
XSFeOH	0.	2.9768E-06
XSOFe-Na	0.	5.4510E-08
Xw1ONi+Cl	0.	4.2502E-09
Xw1NiOH	0.	8.0808E-11
Xw1ONi-Na	0.	9.9698E-13
Xw1OFe+Cl	0.	4.8711E-04

Xw1OFe+Cl	0.	4.8711E-04
Xw1FeOH	0.	1.4988E-07
Xw1OFe-Na	0.	2.6630E-10
Xw2OH	0.	1.4855E-03
Xw2O	0.	5.2737E-05

A.2.2 Conc3t

This is the record of concentrations corresponding to the location 0.3325 meters for each single species of the model. Only part of it is shown, because it is very long. With these files the breakthrough curves are later plot on a graph. There are 5 files like this corresponding to the 5 nodes or locations of interest.

```
|   time_s     time_y     Na+        K+         Ca+2       Mg+2       Sr+2       Fe+2       CO3-2      SO4-2      Cl-        Dummy_F-   DummyH2Si  H+         trac_Ni
 Dummy_F-   DummyH2Si  H+         trac_Ni    trac_X     Ni_s_kd    Ss1_OH     Sw1_OH     Sw2_OH     Na-Mont    Na+        K+         Ca+2       Mg+2       Sr+2
tc_NiHCO3 dtc_Ni_SKd dtc_XSOH    dtc_XSO    dtc_XSONi  dtc_XSNiOH dtc_XSONi- dtc_Xw1OH  dtc_Xw1O   dtc_K-CE-m dtc_Ca-CE- dtc_Mg-CE- dtc_Sr-CE- dtc_Ni-CE- dtc_Fe-CE- d
  0.316E+08  0.100E+01  0.913E-01  0.384E-03  0.127E-01  0.160E-01  0.856E-04  0.161E-05  0.466E-05  0.726E-02  0.109E+00  0.100E-09  0.100E-09  0.553E-07  0.472E-10
0.100E-09  0.100E-09  0.228E-02  0.611E-10  0.180E-06  0.152E-05  0.184E-02  0.368E-01  0.383E-01  0.965E+00  0.000E+00  0.390E+00  0.208-316  0.741-304  0.229-316
.000E+00  0.000E+00  0.000E+00  0.000E+00  0.000E+00  0.000E+00  0.000E+00  0.876E-13  0.654E-16  0.530E-14  0.668E-14  0.356E-16  0.306E-17 -0.222E-17  0.203E-14 -0
  0.891E+08  0.282E+01  0.913E-01  0.384E-03  0.127E-01  0.160E-01  0.856E-04  0.161E-05  0.466E-05  0.726E-02  0.109E+00  0.100E-09  0.100E-09  0.553E-07  0.472E-10
0.100E-09  0.100E-09  0.228E-02  0.611E-10  0.721E-06  0.986E-05  0.184E-02  0.368E-01  0.383E-01  0.965E+00  0.000E+00  0.390E+00  0.208-316  0.741-304  0.229-316
.000E+00  0.000E+00  0.000E+00  0.000E+00  0.000E+00  0.000E+00  0.000E+00  0.899E-11  0.137E-14  0.399E-12  0.503E-12  0.268E-14  0.330E-15 -0.356E-15  0.377E-13 -0
  0.117E+09  0.370E+01  0.913E-01  0.384E-03  0.127E-01  0.160E-01  0.856E-04  0.161E-05  0.466E-05  0.726E-02  0.109E+00  0.100E-09  0.100E-09  0.553E-07  0.472E-10
0.100E-09  0.100E-09  0.228E-02  0.611E-10  0.114E-05  0.105E-04  0.184E-02  0.368E-01  0.383E-01  0.965E+00  0.000E+00  0.390E+00  0.208-316  0.741-304  0.229-316
.000E+00  0.000E+00  0.000E+00  0.000E+00  0.000E+00  0.000E+00  0.000E+00  0.208E-10  0.249E-14  0.893E-12  0.113E-11  0.601E-14  0.761E-15 -0.831E-15  0.697E-13 -0
  0.146E+09  0.462E+01  0.913E-01  0.384E-03  0.127E-01  0.160E-01  0.856E-04  0.161E-05  0.466E-05  0.726E-02  0.109E+00  0.100E-09  0.100E-09  0.553E-07  0.472E-10
0.100E-09  0.100E-09  0.228E-02  0.611E-10  0.148E-05  0.101E-04  0.184E-02  0.368E-01  0.383E-01  0.965E+00  0.000E+00  0.390E+00  0.208-316  0.741-304  0.229-316
.000E+00  0.000E+00  0.000E+00  0.000E+00  0.000E+00  0.000E+00  0.000E+00  0.364E-10  0.364E-14  0.153E-11  0.193E-11  0.103E-13  0.133E-14 -0.146E-14  0.109E-12 -0
  0.174E+09  0.553E+01  0.913E-01  0.384E-03  0.127E-01  0.160E-01  0.856E-04  0.161E-05  0.466E-05  0.726E-02  0.109E+00  0.100E-09  0.100E-09  0.553E-07  0.472E-10
0.100E-09  0.100E-09  0.228E-02  0.611E-10  0.178E-05  0.963E-05  0.184E-02  0.368E-01  0.383E-01  0.965E+00  0.000E+00  0.390E+00  0.208-316  0.741-304  0.229-316
.000E+00  0.000E+00  0.000E+00  0.000E+00  0.000E+00  0.000E+00  0.000E+00  0.526E-10  0.466E-14  0.220E-11  0.277E-11  0.148E-13  0.192E-14 -0.212E-14  0.148E-12 -0
  0.202E+09  0.641E+01  0.913E-01  0.384E-03  0.127E-01  0.160E-01  0.856E-04  0.161E-05  0.466E-05  0.726E-02  0.109E+00  0.100E-09  0.100E-09  0.553E-07  0.472E-10
0.100E-09  0.100E-09  0.228E-02  0.611E-10  0.229E-05  0.953E-05  0.184E-02  0.368E-01  0.383E-01  0.965E+00  0.000E+00  0.390E+00  0.208-316  0.741-304  0.229-316
.000E+00  0.000E+00  0.000E+00  0.000E+00  0.000E+00  0.000E+00  0.000E+00  0.708E-10  0.569E-14  0.294E-11  0.371E-11  0.198E-13  0.258E-14 -0.286E-14  0.191E-12 -0
  0.231E+09  0.732E+01  0.913E-01  0.384E-03  0.127E-01  0.160E-01  0.856E-04  0.161E-05  0.466E-05  0.726E-02  0.109E+00  0.100E-09  0.100E-09  0.553E-07  0.472E-10
0.100E-09  0.100E-09  0.228E-02  0.611E-10  0.260E-05  0.912E-05  0.184E-02  0.368E-01  0.383E-01  0.965E+00  0.000E+00  0.390E+00  0.208-316  0.741-304  0.229-316
.000E+00  0.000E+00  0.000E+00  0.000E+00  0.000E+00  0.000E+00  0.000E+00  0.932E-10  0.674E-14  0.385E-11  0.485E-11  0.259E-13  0.340E-14 -0.376E-14  0.243E-12 -0
  0.260E+09  0.823E+01  0.913E-01  0.384E-03  0.127E-01  0.160E-01  0.856E-04  0.161E-05  0.466E-05  0.726E-02  0.109E+00  0.100E-09  0.100E-09  0.553E-07  0.472E-10
0.100E-09  0.100E-09  0.228E-02  0.611E-10  0.290E-05  0.886E-05  0.184E-02  0.368E-01  0.383E-01  0.965E+00  0.000E+00  0.390E+00  0.208-316  0.741-304  0.229-316
.000E+00  0.000E+00  0.000E+00  0.000E+00  0.000E+00  0.000E+00  0.000E+00  0.115E-09  0.759E-14  0.471E-11  0.594E-11  0.317E-13  0.418E-14 -0.464E-14  0.294E-12 -0
  0.288E+09  0.911E+01  0.913E-01  0.384E-03  0.127E-01  0.160E-01  0.856E-04  0.161E-05  0.466E-05  0.726E-02  0.109E+00  0.100E-09  0.100E-09  0.553E-07  0.472E-10
0.100E-09  0.100E-09  0.228E-02  0.611E-10  0.305E-05  0.854E-05  0.184E-02  0.368E-01  0.383E-01  0.965E+00  0.000E+00  0.390E+00  0.208-316  0.741-304  0.229-316
.000E+00  0.000E+00  0.000E+00  0.000E+00  0.000E+00  0.000E+00  0.000E+00  0.136E-09  0.832E-14  0.556E-11  0.701E-11  0.374E-13  0.494E-14 -0.548E-14  0.343E-12 -0
  0.316E+09  0.100E+02  0.913E-01  0.384E-03  0.127E-01  0.160E-01  0.856E-04  0.161E-05  0.466E-05  0.726E-02  0.109E+00  0.100E-09  0.100E-09  0.553E-07  0.472E-10
0.100E-09  0.100E-09  0.228E-02  0.611E-10  0.331E-05  0.839E-05  0.184E-02  0.368E-01  0.383E-01  0.965E+00  0.000E+00  0.390E+00  0.208-316  0.741-304  0.229-316
.000E+00  0.000E+00  0.000E+00  0.000E+00  0.000E+00  0.000E+00  0.000E+00  0.157E-09  0.900E-14  0.642E-11  0.810E-11  0.432E-13  0.571E-14 -0.634E-14  0.392E-12 -0
  0.568E+09  0.180E+02  0.913E-01  0.384E-03  0.127E-01  0.160E-01  0.856E-04  0.161E-05  0.466E-05  0.726E-02  0.109E+00  0.100E-09  0.100E-09  0.553E-07  0.472E-10
0.100E-09  0.100E-09  0.228E-02  0.611E-10  0.478E-05  0.804E-05  0.184E-02  0.368E-01  0.383E-01  0.965E+00  0.000E+00  0.390E+00  0.208-316  0.741-304  0.229-316
.000E+00  0.000E+00  0.000E+00  0.000E+00  0.000E+00  0.000E+00  0.000E+00  0.328E-09  0.115E-13  0.134E-10  0.169E-10  0.901E-13  0.119E-13 -0.132E-13  0.795E-12 -0
  0.695E+09  0.220E+02  0.913E-01  0.384E-03  0.127E-01  0.160E-01  0.856E-04  0.161E-05  0.466E-05  0.726E-02  0.109E+00  0.100E-09  0.100E-09  0.553E-07  0.472E-10
0.100E-09  0.100E-09  0.228E-02  0.611E-10  0.543E-05  0.823E-05  0.184E-02  0.368E-01  0.383E-01  0.965E+00  0.000E+00  0.390E+00  0.208-316  0.741-304  0.229-316
.000E+00  0.000E+00  0.000E+00  0.000E+00  0.000E+00  0.000E+00  0.000E+00  0.399E-09  0.112E-13  0.163E-10  0.206E-10  0.110E-12  0.145E-13 -0.161E-13  0.963E-12 -0
  0.821E+09  0.260E+02  0.914E-01  0.384E-03  0.127E-01  0.160E-01  0.856E-04  0.161E-05  0.466E-05  0.726E-02  0.109E+00  0.100E-09  0.100E-09  0.553E-07  0.472E-10
0.100E-09  0.100E-09  0.228E-02  0.611E-10  0.603E-05  0.845E-05  0.184E-02  0.368E-01  0.383E-01  0.965E+00  0.000E+00  0.390E+00  0.208-316  0.741-304  0.229-316
.000E+00  0.000E+00  0.000E+00  0.000E+00  0.000E+00  0.000E+00  0.000E+00  0.466E-09  0.103E-13  0.190E-10  0.241E-10  0.129E-12  0.170E-13 -0.190E-13  0.112E-11 -0
  0.947E+09  0.300E+02  0.914E-01  0.384E-03  0.127E-01  0.160E-01  0.856E-04  0.161E-05  0.466E-05  0.726E-02  0.109E+00  0.100E-09  0.100E-09  0.553E-07  0.472E-10
0.100E-09  0.100E-09  0.228E-02  0.611E-10  0.640E-05  0.859E-05  0.184E-02  0.368E-01  0.383E-01  0.965E+00  0.000E+00  0.390E+00  0.208-316  0.741-304  0.229-316
.000E+00  0.000E+00  0.000E+00  0.000E+00  0.000E+00  0.000E+00  0.000E+00  0.528E-09  0.881E-14  0.215E-10  0.274E-10  0.147E-12  0.194E-13 -0.221E-13  0.126E-11 -0
  0.107E+10  0.340E+02  0.914E-01  0.384E-03  0.127E-01  0.160E-01  0.856E-04  0.161E-05  0.466E-05  0.726E-02  0.109E+00  0.100E-09  0.100E-09  0.553E-07  0.472E-10
0.100E-09  0.100E-09  0.228E-02  0.611E-10  0.681E-05  0.876E-05  0.184E-02  0.368E-01  0.383E-01  0.965E+00  0.000E+00  0.390E+00  0.208-316  0.741-304  0.229-316
.000E+00  0.000E+00  0.000E+00  0.000E+00  0.000E+00  0.000E+00  0.000E+00  0.582E-09  0.704E-14  0.236E-10  0.303E-10  0.162E-12  0.216E-13 -0.257E-13  0.137E-11 -0
  0.120E+10  0.380E+02  0.914E-01  0.384E-03  0.127E-01  0.160E-01  0.856E-04  0.161E-05  0.466E-05  0.726E-02  0.109E+00  0.100E-09  0.100E-09  0.553E-07  0.472E-10
```

(...)

```
0.100E-09  0.100E-09  0.228E-02  0.448E-05  0.100E-04  0.101E-04  0.184E-02  0.368E-01  0.383E-01  0.966E+00  0.000E+00  0.390E+00  0.208-316  0.741-304  0.229-316  0.9
.000E+00  0.000E+00  0.000E+00  0.000E+00  0.000E+00  0.000E+00  0.000E+00 -0.546E-07  0.440E-11 -0.282E-08 -0.264E-08 -0.157E-10  0.513E-08  0.704E-09 -0.437E-08  0.66
  0.133E+12  0.420E+04  0.913E-01  0.384E-03  0.127E-01  0.160E-01  0.856E-04  0.261E-05  0.457E-05  0.726E-02  0.109E+00  0.100E-09  0.100E-09  0.564E-07  0.374E-05  0
0.100E-09  0.100E-09  0.228E-02  0.484E-05  0.100E-04  0.101E-04  0.184E-02  0.368E-01  0.383E-01  0.966E+00  0.000E+00  0.390E+00  0.208-316  0.741-304  0.229-316  0.9
.000E+00  0.000E+00  0.000E+00  0.000E+00  0.000E+00  0.000E+00  0.000E+00 -0.567E-07  0.478E-11 -0.346E-08 -0.323E-08 -0.189E-10  0.374E-08  0.870E-09 -0.474E-08  0.71
  0.145E+12  0.460E+04  0.913E-01  0.384E-03  0.127E-01  0.160E-01  0.856E-04  0.263E-05  0.457E-05  0.726E-02  0.109E+00  0.100E-09  0.100E-09  0.564E-07  0.399E-05  0
0.100E-09  0.100E-09  0.228E-02  0.516E-05  0.100E-04  0.101E-04  0.184E-02  0.368E-01  0.383E-01  0.966E+00  0.000E+00  0.390E+00  0.208-316  0.741-304  0.229-316  0.9
.000E+00  0.000E+00  0.000E+00  0.000E+00  0.000E+00  0.000E+00  0.000E+00 -0.584E-07  0.514E-11 -0.409E-08 -0.381E-08 -0.219E-10  0.218E-08  0.103E-08 -0.506E-08  0.76
  0.158E+12  0.500E+04  0.913E-01  0.384E-03  0.127E-01  0.160E-01  0.856E-04  0.265E-05  0.457E-05  0.726E-02  0.109E+00  0.100E-09  0.100E-09  0.563E-07  0.423E-05  0
0.100E-09  0.100E-09  0.228E-02  0.548E-05  0.100E-04  0.101E-04  0.184E-02  0.368E-01  0.383E-01  0.966E+00  0.000E+00  0.390E+00  0.208-316  0.741-304  0.229-316  0.9
.000E+00  0.000E+00  0.000E+00  0.000E+00  0.000E+00  0.000E+00  0.000E+00 -0.596E-07  0.546E-11 -0.468E-08 -0.437E-08 -0.249E-10  0.488E-09  0.118E-08 -0.536E-08  0.79
  0.183E+12  0.580E+04  0.913E-01  0.384E-03  0.127E-01  0.160E-01  0.856E-04  0.267E-05  0.458E-05  0.726E-02  0.109E+00  0.100E-09  0.100E-09  0.562E-07  0.470E-05  0
0.100E-09  0.100E-09  0.228E-02  0.608E-05  0.100E-04  0.101E-04  0.184E-02  0.368E-01  0.383E-01  0.966E+00  0.000E+00  0.390E+00  0.208-316  0.741-304  0.229-316  0.9
.000E+00  0.000E+00  0.000E+00  0.000E+00  0.000E+00  0.000E+00  0.000E+00 -0.610E-07  0.601E-11 -0.579E-08 -0.539E-08 -0.303E-10 -0.313E-08  0.146E-08 -0.585E-08  0.85
  0.196E+12  0.620E+04  0.913E-01  0.384E-03  0.127E-01  0.160E-01  0.856E-04  0.268E-05  0.459E-05  0.726E-02  0.109E+00  0.100E-09  0.100E-09  0.562E-07  0.490E-05  0
0.100E-09  0.100E-09  0.228E-02  0.635E-05  0.100E-04  0.101E-04  0.184E-02  0.368E-01  0.383E-01  0.966E+00  0.000E+00  0.390E+00  0.208-316  0.741-304  0.229-316  0.9
.000E+00  0.000E+00  0.000E+00  0.000E+00  0.000E+00  0.000E+00  0.000E+00 -0.613E-07  0.623E-11 -0.629E-08 -0.586E-08 -0.328E-10 -0.501E-08  0.158E-08 -0.605E-08  0.88
  0.208E+12  0.660E+04  0.913E-01  0.384E-03  0.127E-01  0.160E-01  0.856E-04  0.268E-05  0.459E-05  0.726E-02  0.109E+00  0.100E-09  0.100E-09  0.561E-07  0.510E-05  0
0.100E-09  0.100E-09  0.228E-02  0.660E-05  0.100E-04  0.101E-04  0.184E-02  0.368E-01  0.383E-01  0.966E+00  0.000E+00  0.390E+00  0.208-316  0.741-304  0.229-316  0.9
.000E+00  0.000E+00  0.000E+00  0.000E+00  0.000E+00  0.000E+00  0.000E+00 -0.614E-07  0.642E-11 -0.675E-08 -0.629E-08 -0.351E-10 -0.690E-08  0.170E-08 -0.623E-08  0.90
  0.221E+12  0.700E+04  0.913E-01  0.384E-03  0.127E-01  0.160E-01  0.856E-04  0.269E-05  0.460E-05  0.726E-02  0.109E+00  0.100E-09  0.100E-09  0.561E-07  0.528E-05  0
0.100E-09  0.100E-09  0.228E-02  0.684E-05  0.100E-04  0.101E-04  0.184E-02  0.368E-01  0.383E-01  0.966E+00  0.000E+00  0.390E+00  0.208-316  0.741-304  0.229-316  0.9
.000E+00  0.000E+00  0.000E+00  0.000E+00  0.000E+00  0.000E+00  0.000E+00 -0.614E-07  0.660E-11 -0.719E-08 -0.670E-08 -0.372E-10 -0.879E-08  0.181E-08 -0.639E-08  0.91
  0.234E+12  0.740E+04  0.913E-01  0.384E-03  0.127E-01  0.160E-01  0.856E-04  0.268E-05  0.460E-05  0.726E-02  0.109E+00  0.100E-09  0.100E-09  0.560E-07  0.546E-05  0
0.100E-09  0.100E-09  0.228E-02  0.707E-05  0.100E-04  0.101E-04  0.184E-02  0.368E-01  0.383E-01  0.966E+00  0.000E+00  0.390E+00  0.208-316  0.741-304  0.229-316  0.9
.000E+00  0.000E+00  0.000E+00  0.000E+00  0.000E+00  0.000E+00  0.000E+00 -0.612E-07  0.675E-11 -0.759E-08 -0.707E-08 -0.392E-10 -0.107E-07  0.191E-08 -0.653E-08  0.93
  0.246E+12  0.780E+04  0.913E-01  0.384E-03  0.127E-01  0.160E-01  0.856E-04  0.268E-05  0.460E-05  0.726E-02  0.109E+00  0.100E-09  0.100E-09  0.560E-07  0.562E-05  0
0.100E-09  0.100E-09  0.228E-02  0.728E-05  0.100E-04  0.101E-04  0.184E-02  0.368E-01  0.383E-01  0.966E+00  0.000E+00  0.390E+00  0.208-316  0.741-304  0.229-316  0.9
.000E+00  0.000E+00  0.000E+00  0.000E+00  0.000E+00  0.000E+00  0.000E+00 -0.609E-07  0.689E-11 -0.797E-08 -0.742E-08 -0.410E-10 -0.125E-07  0.200E-08 -0.665E-08  0.94
  0.259E+12  0.820E+04  0.913E-01  0.384E-03  0.127E-01  0.160E-01  0.856E-04  0.267E-05  0.461E-05  0.726E-02  0.109E+00  0.100E-09  0.100E-09  0.559E-07  0.577E-05  0
0.100E-09  0.100E-09  0.228E-02  0.747E-05  0.100E-04  0.101E-04  0.184E-02  0.368E-01  0.383E-01  0.966E+00  0.000E+00  0.390E+00  0.208-316  0.741-304  0.229-316  0.9
.000E+00  0.000E+00  0.000E+00  0.000E+00  0.000E+00  0.000E+00  0.000E+00 -0.606E-07  0.701E-11 -0.831E-08 -0.774E-08 -0.426E-10 -0.144E-07  0.209E-08 -0.676E-08  0.95
  0.271E+12  0.860E+04  0.913E-01  0.384E-03  0.127E-01  0.160E-01  0.856E-04  0.266E-05  0.461E-05  0.726E-02  0.109E+00  0.100E-09  0.100E-09  0.559E-07  0.591E-05  0
0.100E-09  0.100E-09  0.228E-02  0.765E-05  0.100E-04  0.101E-04  0.184E-02  0.368E-01  0.383E-01  0.966E+00  0.000E+00  0.390E+00  0.208-316  0.741-304  0.229-316  0.9
.000E+00  0.000E+00  0.000E+00  0.000E+00  0.000E+00  0.000E+00  0.000E+00 -0.602E-07  0.711E-11 -0.863E-08 -0.803E-08 -0.442E-10 -0.162E-07  0.217E-08 -0.685E-08  0.96
  0.284E+12  0.900E+04  0.913E-01  0.384E-03  0.127E-01  0.160E-01  0.856E-04  0.265E-05  0.462E-05  0.726E-02  0.109E+00  0.100E-09  0.100E-09  0.558E-07  0.603E-05  0
0.100E-09  0.100E-09  0.228E-02  0.781E-05  0.100E-04  0.101E-04  0.184E-02  0.368E-01  0.383E-01  0.966E+00  0.000E+00  0.390E+00  0.208-316  0.741-304  0.229-316  0.9
.000E+00  0.000E+00  0.000E+00  0.000E+00  0.000E+00  0.000E+00  0.000E+00 -0.597E-07  0.719E-11 -0.891E-08 -0.830E-08 -0.455E-10 -0.180E-07  0.224E-08 -0.693E-08  0.96
  0.297E+12  0.940E+04  0.913E-01  0.384E-03  0.127E-01  0.160E-01  0.856E-04  0.263E-05  0.462E-05  0.726E-02  0.109E+00  0.100E-09  0.100E-09  0.558E-07  0.615E-05  0
0.100E-09  0.100E-09  0.228E-02  0.797E-05  0.100E-04  0.101E-04  0.184E-02  0.368E-01  0.383E-01  0.966E+00  0.000E+00  0.390E+00  0.208-316  0.741-304  0.229-316  0.9
.000E+00  0.000E+00  0.000E+00  0.000E+00  0.000E+00  0.000E+00  0.000E+00 -0.592E-07  0.726E-11 -0.918E-08 -0.854E-08 -0.468E-10 -0.198E-07  0.231E-08 -0.700E-08  0.97
  0.309E+12  0.980E+04  0.913E-01  0.384E-03  0.127E-01  0.160E-01  0.856E-04  0.262E-05  0.462E-05  0.726E-02  0.109E+00  0.100E-09  0.100E-09  0.557E-07  0.626E-05  0
0.100E-09  0.100E-09  0.228E-02  0.811E-05  0.100E-04  0.101E-04  0.184E-02  0.368E-01  0.383E-01  0.966E+00  0.000E+00  0.390E+00  0.208-316  0.741-304  0.229-316  0.9
.000E+00  0.000E+00  0.000E+00  0.000E+00  0.000E+00  0.000E+00  0.000E+00 -0.587E-07  0.733E-11 -0.941E-08 -0.876E-08 -0.479E-10 -0.215E-07  0.237E-08 -0.706E-08  0.97
  0.316E+12  0.100E+05  0.913E-01  0.384E-03  0.127E-01  0.160E-01  0.856E-04  0.261E-05  0.463E-05  0.726E-02  0.109E+00  0.100E-09  0.100E-09  0.557E-07  0.631E-05  0
0.100E-09  0.100E-09  0.228E-02  0.818E-05  0.100E-04  0.101E-04  0.184E-02  0.368E-01  0.383E-01  0.966E+00  0.000E+00  0.390E+00  0.208-316  0.741-304  0.229-316  0.9
.000E+00  0.000E+00  0.000E+00  0.000E+00  0.000E+00  0.000E+00  0.000E+00 -0.584E-07  0.735E-11 -0.953E-08 -0.886E-08 -0.485E-10 -0.223E-07  0.239E-08 -0.708E-08  0.97
 at location     0.3325000000000000      [m]
```

A.2.3 Wa

List of node locations (meters) from the reference boundary.

x
0.175E-01
0.350E-01
0.525E-01
0.700E-01
0.875E-01
0.105E+00
0.123E+00
0.140E+00
0.158E+00
0.175E+00
0.193E+00
0.210E+00
0.228E+00
0.245E+00
0.263E+00
0.280E+00
0.298E+00
0.315E+00
0.333E+00
0.350E+00
0.368E+00
0.385E+00
0.403E+00
0.420E+00
0.438E+00
0.455E+00
0.473E+00
0.490E+00
0.508E+00
0.525E+00
0.543E+00
0.560E+00
0.578E+00
0.595E+00
0.613E+00
0.630E+00
0.647E+00
0.665E+00
0.682E+00
0.700E+00

A.2.4 Conca, concb, etc.

List of concentration of each species in each node at a certain time instant.

x	Na+	K+	Ca+2	Mg+2	Sr+2	Fe+2	CO3-2	SO4-2	Cl-	Dummy_F-	DummyH2Si	H+	trac_Ni
0.000E+00	0.913E-01	0.384E-03	0.127E-01	0.160E-01	0.856E-04	0.161E-05	0.466E-05	0.726E-02	0.109E+00	0.100E-09	0.100E-09	0.553E-07	0.100E-04
0.175E-01	0.913E-01	0.384E-03	0.127E-01	0.160E-01	0.856E-04	0.198E-05	0.464E-05	0.726E-02	0.109E+00	0.100E-09	0.100E-09	0.556E-07	0.595E-05
0.350E-01	0.913E-01	0.384E-03	0.127E-01	0.160E-01	0.856E-04	0.221E-05	0.462E-05	0.726E-02	0.109E+00	0.100E-09	0.100E-09	0.558E-07	0.462E-05
0.525E-01	0.913E-01	0.384E-03	0.127E-01	0.160E-01	0.856E-04	0.236E-05	0.461E-05	0.726E-02	0.109E+00	0.100E-09	0.100E-09	0.559E-07	0.337E-05
0.700E-01	0.913E-01	0.384E-03	0.127E-01	0.160E-01	0.856E-04	0.242E-05	0.460E-05	0.726E-02	0.109E+00	0.100E-09	0.100E-09	0.561E-07	0.230E-05
0.875E-01	0.913E-01	0.384E-03	0.127E-01	0.160E-01	0.856E-04	0.238E-05	0.459E-05	0.726E-02	0.109E+00	0.100E-09	0.100E-09	0.561E-07	0.145E-05
0.105E+00	0.914E-01	0.384E-03	0.127E-01	0.160E-01	0.856E-04	0.225E-05	0.459E-05	0.726E-02	0.109E+00	0.100E-09	0.100E-09	0.562E-07	0.825E-06
0.123E+00	0.914E-01	0.384E-03	0.127E-01	0.160E-01	0.856E-04	0.207E-05	0.459E-05	0.726E-02	0.109E+00	0.100E-09	0.100E-09	0.561E-07	0.421E-06
0.140E+00	0.914E-01	0.384E-03	0.127E-01	0.160E-01	0.856E-04	0.191E-05	0.460E-05	0.726E-02	0.109E+00	0.100E-09	0.100E-09	0.561E-07	0.193E-06
0.158E+00	0.914E-01	0.384E-03	0.127E-01	0.160E-01	0.856E-04	0.178E-05	0.461E-05	0.726E-02	0.109E+00	0.100E-09	0.100E-09	0.560E-07	0.810E-07
0.175E+00	0.914E-01	0.384E-03	0.127E-01	0.160E-01	0.856E-04	0.170E-05	0.462E-05	0.726E-02	0.109E+00	0.100E-09	0.100E-09	0.558E-07	0.315E-07
0.193E+00	0.914E-01	0.384E-03	0.127E-01	0.160E-01	0.856E-04	0.166E-05	0.463E-05	0.726E-02	0.109E+00	0.100E-09	0.100E-09	0.557E-07	0.116E-07
0.210E+00	0.914E-01	0.384E-03	0.127E-01	0.160E-01	0.856E-04	0.163E-05	0.463E-05	0.726E-02	0.109E+00	0.100E-09	0.100E-09	0.556E-07	0.410E-08
0.228E+00	0.914E-01	0.384E-03	0.127E-01	0.160E-01	0.856E-04	0.162E-05	0.464E-05	0.726E-02	0.109E+00	0.100E-09	0.100E-09	0.556E-07	0.141E-08
0.245E+00	0.914E-01	0.384E-03	0.127E-01	0.160E-01	0.856E-04	0.162E-05	0.465E-05	0.726E-02	0.109E+00	0.100E-09	0.100E-09	0.555E-07	0.489E-09
0.263E+00	0.914E-01	0.384E-03	0.127E-01	0.160E-01	0.856E-04	0.162E-05	0.465E-05	0.726E-02	0.109E+00	0.100E-09	0.100E-09	0.554E-07	0.186E-09
0.280E+00	0.914E-01	0.384E-03	0.127E-01	0.160E-01	0.856E-04	0.161E-05	0.465E-05	0.726E-02	0.109E+00	0.100E-09	0.100E-09	0.554E-07	0.892E-10
0.298E+00	0.914E-01	0.384E-03	0.127E-01	0.160E-01	0.856E-04	0.161E-05	0.466E-05	0.726E-02	0.109E+00	0.100E-09	0.100E-09	0.554E-07	0.593E-10
0.315E+00	0.914E-01	0.384E-03	0.127E-01	0.160E-01	0.856E-04	0.161E-05	0.466E-05	0.726E-02	0.109E+00	0.100E-09	0.100E-09	0.554E-07	0.506E-10
0.333E+00	0.914E-01	0.384E-03	0.127E-01	0.160E-01	0.856E-04	0.161E-05	0.466E-05	0.726E-02	0.109E+00	0.100E-09	0.100E-09	0.553E-07	0.482E-10
0.350E+00	0.914E-01	0.384E-03	0.127E-01	0.160E-01	0.856E-04	0.161E-05	0.466E-05	0.726E-02	0.109E+00	0.100E-09	0.100E-09	0.553E-07	0.475E-10
0.368E+00	0.914E-01	0.384E-03	0.127E-01	0.160E-01	0.856E-04	0.161E-05	0.466E-05	0.726E-02	0.109E+00	0.100E-09	0.100E-09	0.553E-07	0.473E-10
0.385E+00	0.914E-01	0.384E-03	0.127E-01	0.160E-01	0.856E-04	0.161E-05	0.466E-05	0.726E-02	0.109E+00	0.100E-09	0.100E-09	0.553E-07	0.472E-10
0.403E+00	0.914E-01	0.384E-03	0.127E-01	0.160E-01	0.856E-04	0.161E-05	0.466E-05	0.726E-02	0.109E+00	0.100E-09	0.100E-09	0.553E-07	0.472E-10
0.420E+00	0.914E-01	0.384E-03	0.127E-01	0.160E-01	0.856E-04	0.161E-05	0.466E-05	0.726E-02	0.109E+00	0.100E-09	0.100E-09	0.553E-07	0.472E-10
0.438E+00	0.914E-01	0.384E-03	0.127E-01	0.160E-01	0.856E-04	0.161E-05	0.466E-05	0.726E-02	0.109E+00	0.100E-09	0.100E-09	0.553E-07	0.472E-10
0.455E+00	0.914E-01	0.384E-03	0.127E-01	0.160E-01	0.856E-04	0.161E-05	0.466E-05	0.726E-02	0.109E+00	0.100E-09	0.100E-09	0.553E-07	0.472E-10
0.473E+00	0.914E-01	0.384E-03	0.127E-01	0.160E-01	0.856E-04	0.161E-05	0.466E-05	0.726E-02	0.109E+00	0.100E-09	0.100E-09	0.553E-07	0.472E-10
0.490E+00	0.914E-01	0.384E-03	0.127E-01	0.160E-01	0.856E-04	0.161E-05	0.466E-05	0.726E-02	0.109E+00	0.100E-09	0.100E-09	0.553E-07	0.472E-10
0.508E+00	0.914E-01	0.384E-03	0.127E-01	0.160E-01	0.856E-04	0.161E-05	0.466E-05	0.726E-02	0.109E+00	0.100E-09	0.100E-09	0.553E-07	0.472E-10
0.525E+00	0.914E-01	0.384E-03	0.127E-01	0.160E-01	0.856E-04	0.161E-05	0.466E-05	0.726E-02	0.109E+00	0.100E-09	0.100E-09	0.553E-07	0.472E-10
0.543E+00	0.914E-01	0.384E-03	0.127E-01	0.160E-01	0.856E-04	0.161E-05	0.466E-05	0.726E-02	0.109E+00	0.100E-09	0.100E-09	0.553E-07	0.472E-10
0.560E+00	0.914E-01	0.384E-03	0.127E-01	0.160E-01	0.856E-04	0.161E-05	0.466E-05	0.726E-02	0.109E+00	0.100E-09	0.100E-09	0.553E-07	0.472E-10
0.578E+00	0.914E-01	0.384E-03	0.127E-01	0.160E-01	0.856E-04	0.161E-05	0.466E-05	0.726E-02	0.109E+00	0.100E-09	0.100E-09	0.553E-07	0.472E-10
0.595E+00	0.914E-01	0.384E-03	0.127E-01	0.160E-01	0.856E-04	0.161E-05	0.466E-05	0.726E-02	0.109E+00	0.100E-09	0.100E-09	0.553E-07	0.472E-10
0.613E+00	0.914E-01	0.384E-03	0.127E-01	0.160E-01	0.856E-04	0.161E-05	0.466E-05	0.726E-02	0.109E+00	0.100E-09	0.100E-09	0.553E-07	0.472E-10
0.630E+00	0.914E-01	0.384E-03	0.127E-01	0.160E-01	0.856E-04	0.161E-05	0.466E-05	0.726E-02	0.109E+00	0.100E-09	0.100E-09	0.553E-07	0.472E-10
0.647E+00	0.914E-01	0.384E-03	0.127E-01	0.160E-01	0.856E-04	0.161E-05	0.466E-05	0.726E-02	0.109E+00	0.100E-09	0.100E-09	0.553E-07	0.472E-10
0.665E+00	0.914E-01	0.384E-03	0.127E-01	0.160E-01	0.856E-04	0.161E-05	0.466E-05	0.726E-02	0.109E+00	0.100E-09	0.100E-09	0.553E-07	0.472E-10
0.682E+00	0.914E-01	0.384E-03	0.127E-01	0.160E-01	0.856E-04	0.161E-05	0.466E-05	0.726E-02	0.109E+00	0.100E-09	0.100E-09	0.553E-07	0.472E-10
0.700E+00	0.914E-01	0.384E-03	0.127E-01	0.160E-01	0.856E-04	0.161E-05	0.466E-05	0.726E-02	0.109E+00	0.100E-09	0.100E-09	0.553E-07	0.472E-10
time =	3155760000.000000	(s)	99.99999999999999	(s)									

Appendix B: MCOTAC code

In this section the most interesting parts of the algorithm of MCOTAC are showed. It would be out of the scope of this project to show the whole algorithm, because this is not a programming-focused project. Nevertheless, from the geochemical point of view it may be interesting to verify what the original algorithm is really doing when running the calculations.

B.1 Walk2_.c

Subprogram responsible for moving particles with already assigned concentrations from time t to dt.

```
/*=============================================================================*
*
*                           Unterprogramm: walk2
*                       Berechnung eines Zeitschritts
*
* Input:
*
*    nxmax        : Anzahl der Knoten in X-Richtung
*    icyc      : Zeitzyklus-Nummer
*    along, aq    : longitudinale bzw. transversale Dispersivit„t
*    de        : Zeitschrittweite =delt
*    vx[i]  : Geschwindigkeitskomponente in X-Richtung
*    dx[i]     : Knotenabst„nde in X-Richtung
*
*    ir[i][j]: ir-Maske - Transportmodell, enth„lt Randbedingungen
*
* Output:
*
*    partx[i]       : Koordinaten des Partikels i
*    npmax        : Anzahl Partikel im Modell
*
* 16.11.92
*=============================================================================*/
#include <stdlib.h>
#include <stdio.h>
#include <math.h>

#include "gwheader.h"

#define SQRT12 3.464101615
#define randinv 1.0/RAND_MAX
float gasdev();

void walk2_(npmax,nxmax,ncyc,along,aquer,dm,texe,dx,vx,partx,partxo,
     xmaxr,xminr,partic,bn,cn,partib,ibpstart,x,bo,co,m1,m2)


double partx[NCPMAX],partxo[NCPMAX],dx[NCNODEX+2],vx[NCNODEX+2],*xmaxr,*xminr, *texe;
double  partic[NCBASIS+NCCOMPL][NCPMAX];
double x[NCNODEX],bn[NCNODEX][NCBASIS],cn[NCNODEX][NCCOMPL] ,bo[NCNODEX][NCBASIS],co[NCNODEX][NCCOMPL] ;
double dm[NCNODEX+2];
double *along,*aquer;
int    *nxmax,  *ncyc ,partib[NCNODEX],*ibpstart,*m1, *m2 ;
int   *npmax;

{
        double  slong,slongy,xlaenge, xxmin, xxmax, xl;
        double dabs(),dpx, A1,A2,A3,A4 ,vpx,z1,vabs;
        register i, ip,ipa;
```

```
/*      float gasdef(idum);*/
        int idum, iknx,iknx_n;
        char dummy;

        idum=1;
        ip = 0;
        ipa =0;
/*      printf("walk c %d %d %d %g %g% %g %g\n",*ibpstart,*nxmax,*ncyc,*along,*texe,*xmaxr, *xminr);
      printf("walk %d %d %d %g %g %g %g %g \n",*ibpstart,*nymax,*ncyc,*along,*dm,*texe,*ymaxr, *yminr);

        for (i=0; i<=(*nxmax)-1; i++) {
              printf("i dx vx %d %f %f \n", i, dx[i], vx[i] );
        }
*/
        xlaenge = *xmaxr - *xminr + 2 * dx[1];
        xxmin = *xminr - dx[1];
        xxmax = *xmaxr + dx[1];     /*  + dx[1]; */

        do  {  /*  teilchenloop  */
           iknx= (int ) ( (partx[ip]+dx[1])  / dx[2])  ;

           dpx=dx[1]-(partx[ip]-x[iknx]);
           vpx=vx[iknx];
           vabs=sqrt(vpx*vpx);
           if(vabs == 0.)  vabs=1.e-50; /* keine division durch 0 */
/* neu 23 05 95 */

           if (*along == 0. && *aquer == 0. && dm[iknx] == 0.)  {              /* disp + diff =0  */
             slong=0.0;
           }
           else {                                                  /* wenigstens eine Dispersivitaet > 0 */

              z1=(double) rand()*randinv -0.5 ;
              slong = 2.*z1* sqrt(6.* (*along*vpx  + dm[iknx]) * *texe);  /* longitu. Weg x' */

           }
           slongy = vpx *  *texe;
/*           xl = partx[ip] + slongy + slong;*/
           partx[ip] +=   vpx *  *texe + slong;  /* neue position der teilchen = konv. Anteil + disp. Anteil x */
/* new reflection option at x=0    */
           iknx_n= (int ) ( (partx[ip]+dx[1])  / dx[2]);

           if(iknx_n == 0 && iknx >= 1 ){
/*         printf("walk c %d %d %d %g %g  %g %g %g\n",ip,iknx,iknx_n,partx[ip],partxo[ip],x[iknx], x[iknx_n],xl);*/
//         partx[ip]= x[1] +(dx[1]-(x[1]+partx[ip]));   /* partx[ip] always < x[1]  */
/*         printf("walk reflect %d %d %d %g %g %g %g %g\n",ip,iknx,iknx_n,partx[ip],partxo[ip],x[iknx], slong,xl);*/
/*           scanf(" %d", idum);*/
           }
```

```
/* new reflection option at x=0    */
        if(partx[ip]  >=   xxmax  ){  /*keine diffusion ueber 'rechten rand' - const. conc   */
                     /*   printf("walkrand ip dx[1] partxo xmaxr xlaenge %d %f %f %f %f\n", ip, dx[1] ,partxo[ip], *xmaxr,xlaenge);*/
                     /* neue Teilchenposition als ob Teilchen "links" im Randgrid neu eingesetztwird, Konzentration dabei egal, da nicht gerechnet */
/*          if(partx[ip]- partxo[ip] > 2*dx[1])printf(">xmax ip  %d %f %f \n", ip,partxo[ip], partx[ip] );*/
          partx[ip] -=  xlaenge ;
          for (ipa=0; ipa< *m1; ipa++) {
             partic[ipa][ip]= bn[0][ipa]/(double)*ibpstart ;/* division durch 50 partikelx in randbox */

          }
          for (ipa=0; ipa< *m2; ipa++) {
            partic[ipa+ *m1][ip]= cn[0][ipa]/(double)*ibpstart;
          }
        }
        if(partx[ip] <= xxmin) {
/*          if(-1.*(partx[ip]- partxo[ip]) > dx[1])printf("< xmin ip  %d %f %f \n", ip,partxo[ip], partx[ip] );*/
          partxo[ip] =  partx[ip] ;
            partx[ip] += xlaenge   ;
            for (ipa=0; ipa< *m1; ipa++) {
               partic[ipa][ip]= bo[*nxmax-1][ipa]/(double)*ibpstart; /* -1 durch -2 ersetzt, 090796 */
            }
            for (ipa=0; ipa< *m2; ipa++) {
               partic[ipa+ *m1][ip]=  co[*nxmax-1][ipa]/(double)*ibpstart; /*   -1 durch -2 ersetzt, 090796 */
            }
         }
 /*       printf("walk11 %d %d  %g %g\n",*ibpstart,ip,partx[ip], partxo[ip]);*/
      ++ip;
/*     scanf(" walk %s \n" , &dummy) ;
    printf("walk11 %d %d  %s\n",*ibpstart,ip,dummy);
*/       }   while (ip<= *npmax-1  );      /* ende teilchenloop */
}



#include <math.h>
#include <stdlib.h>
#define randinv 1.0/RAND_MAX

float gasdev(idum)
int *idum;
/* returns a normally distributed deviate with  zero mean and unit variance */

{
       int iset=0;
       float gset;
       float fac,r,v1,v2;
```

```
        if (iset ==0) {
                do {
                        v1=2.0*rand()*randinv - 1.0;
                        v2=2.0*rand()*randinv - 1.0;
                        r=v1*v1+v2*v2;
                } while( r >= 1.0 || r ==0 );
                fac = sqrt(-2.0*log(r)/r);
                gset=v1*fac;
                iset=1;
                return v2*fac;
        } else {
                iset=1;
                return gset;
        }
}
```

B.2 Setpar_.c

File containing the routines or subprograms responsible of counting particles in each cell at time t, assigning concentration to particles at time t, and recalculating concentrations in each cell.

```
/*
*                           Unterprogramm: setpar
*                        Aussetzen von Partikeln
* Input:
*
*    npmax          :  Anzahl neu zu setzender Partikel
*    xmin, xmax     :  min und max -werte von x
*    ymin, ymax     :  min und max -werte von y
* Output:
*    partx[n]| : Partikel coordinaten
*    party[n] : Partikel coordinaten
*
* 18.04.95
*=============================================================================*/

#include <stdlib.h>
#include <math.h>
#include "gwheader.h"

void setpar_(npmax,xmin,xmax,partx,nbox)
double *xmin, *xmax;
double  partx[NCPMAX];
int *nbox;
int *npmax  ;

{
        register i ;
        double xco ;

        xco= (*xmax-*xmin) / (double) *npmax ;
        partx[0] = *xmin + xco/2.0;
        printf("setpar nbox  npmax %d %d xco  %f  %f \n",*nbox,*npmax,xco,partx[0]);
        for (i=1; i<=*npmax-1; i++)  {
                partx[i] =partx[i-1] + xco;
        }
}


/*****************************************************************************
*                             Unterprogramm: partid
*                           Partikeln in welcher box
* Input:
*
*    npmax          :  Anzahl neu zu setzender Partikel
*    nbox            :  Anzahl box zwischen xmin und xmax
*    partx[n]       :     Partikel coordinaten
* Output:
*     partb(nb)    : Anz Partikel in box nb
* 28.10.92
```

```
#include <stdlib.h>
#include <math.h>
#include "gwheader.h"

void partid_(npmax,nbox,xmin,xmax,partib,dx,partx)
double  partx[NCPMAX],dx[NCNODEX+2], *xmin, *xmax;
int *nbox,partib[NCNODEX];
int *npmax;

{
        register i, j;
        int iknx;

        for(i=0; i<= *nbox ; i++)   {

                partib[i]=0;
        }
        for (i=0; i<=*npmax-1; i++)  {

                if(partx[i] > *xmin && partx[i] < *xmax)   {

                        iknx= (int ) ( (partx[i]+dx[1])  / dx[2])  ;
                        partib[iknx] += 1 ;
                  }
                  else {
                      printf(" partibx %d %f  %d %d  \n",i,partx[i],iknx,partib[iknx]);
                }
        }
}

/*****************************************************************************
*                            Unterprogramm: concver
*                          Partikelconcentration festlegen
* Input:
*
*    npmax          :  Anzahl neu zu setzender Partikel
*    nbox           :  Anzahl box zwischen xmin und xmax
*    partx[n]       :     Partikel coordinaten
*    partib[ib]    :
* Output:
*    partic[n,nspec]: partikel n mit speciesconcentrationen nspec
* 28.10.92
*===========================================================================*/

#include <stdlib.h>
#include <math.h>
#include "gwheader.h"
```

```
void concver_(npmax,nbox,dx,bn,cn,partib,partx,partic,ismooth,m1,m2)
double  bn[NCNODEX][NCBASIS],cn[NCNODEX][NCCOMPL],partx[NCPMAX], partic[NCBASIS+NCCOMPL][NCPMAX],dx[NCNODEX+2];
int *nbox, partib[NCNODEX], *ismooth, *m1, *m2 ;
int *npmax;

{
        double dxinv, partiv[NCNODEX];
        register i,j,i1,i2,j2;
        int iknx;

        for(i2=0;i2<=*nbox; i2++)   {
           if(*ismooth ==1) {
              partiv[i2]=1. ;
           }
           else {
              if(partib[i2]!=0.)partiv[i2]=1./(double) partib[i2];
           }
         }

        for (i=0; i<=*npmax-1; i++)  {
              iknx= (int )(( partx[i]+dx[1])  / dx[2] );

              for(j=0; j< *m1;j++) {
                   partic[j][i]= bn[iknx][j] * partiv[iknx];
              }
              for(j=0; j< *m2;j++) { /*new 050494*/
                   partic[j+ *m1][i]=cn[iknx][j] *partiv[iknx];
              }
        }

}


/*****************************************************************************
*                            Unterprogramm: concneu
*                          Partikelconcentration festlegen fuer t+dt
* Input:
*
*    npmax          :  Anzahl neu zu setzender Partikel
*    nbox           :  Anzahl box zwischen xmin und xmax
*    partx[n]       :     Partikel coordinaten
*    partib[ib]    :
* Output:
*    partic[n,nspec]: partikel n mit speciesconcentrationen nspec
* 28.10.92
*===========================================================================*/
```

```
#include <stdlib.h>
#include <math.h>
#include "gwheader.h"


void concneu_(npmax,nbox,nxmax,xminr,xmaxr,dx,bn,cn,partib,partx,partxo,partic,bo,
              co,por,ismooth,m1,m2)
double  bn[NCNODEX][NCBASIS],bo[NCNODEX][NCBASIS],cn[NCNODEX][NCCOMPL]
       ,co[NCNODEX][NCCOMPL];
double  partx[NCPMAX],partxo[NCPMAX], partic[NCBASIS+NCCOMPL][NCPMAX];
double dx[NCNODEX+2],por[NCNODEX+2];
double *xminr, *xmaxr;
int *nbox,*nxmax ,partib[NCNODEX], *ismooth,*m1, *m2 ;
int *npmax;

{
        register i,j,k,ky,i1,n;
        int iknx;
        double dxinv ;

/* set new concentrations at t +dt equal zero and sum over particles to get the new ones */
        for(i=0; i< *nxmax-1; i++) {
                partib[i]=0;
        }
        for(i=1; i< *nxmax-2; i++) {   /* cal_dol 1 durch 0 ersetzt */
/*                partib[i]=0; */
                for(j=0; j< *m1;j++) {
                        bn[i][j] = 0.0;
                }
                for(j=0; j< *m2;j++) {
                       cn[i][j] =  0.0;
                }
/*                        printf("boooooo i j %d %d %e \n",i,j,bo[i][j]); */
        }

        for (i=0; i<=*npmax-1; i++)  {

           if(partx[i] > *xminr && partx[i] < *xmaxr) {  /*+dx[2]*/

                  iknx= (int ) (( partx[i]+dx[1]) /dx[2] ) ;
                  if( iknx > 0  ) {
                        partib[iknx] += 1 ;
                        for(j=0; j< *m1;j++) {
                                bn[iknx][j] += partic[j][i];
                        }
                        for(j=0; j< *m2;j++) {
                              cn[iknx][j] += partic[j+ *m1][i] ;
                        }
```

```
                  }
          }
        }
/*   printf("i  j bn partic partib  %d %d %e  %e %d  \n",i,j,bn[iknx][j],partic[j][i],partib[iknx]); */


/* new part of particle concentration in a box  */

       if( *ismooth ==1) {
            for(n=0; n<= *nxmax-1 ;n++) {  /* cal_dol 1 durch 0 ersetzt */
                for(j=0; j< *m1;j++) {
                   if(partib[n]!=0) bn[n][j]=bn[n][j]/(double)partib[n];
                }
                for(j=0; j< *m2;j++) {
                   if(partib[n]!=0) cn[n][j]=cn[n][j]/(double)partib[n];
                }
             }
       }
/*  constant concentration at x=0   */
            for(j=0; j< *m1;j++) {
/*              bn[0][j] = bo[0][j] ;    inlet = const. concentration */
            }
            for(j=0; j< *m2;j++) {
/*              cn[0][j] = co[0][j] ;     inlet = const. concentration */
            }
/*  const conc right side */


/*          for(j=0; j< *m1;j++) {
                bn[*nxmax-1][j] = bo[*nxmax-1][j] ;
               }
            for(j=0; j< *m2;j++) {
                cn[*nxmax-1][j] = co[*nxmax-1][j] ;
               }
*/
//    printf("boooooo i j %d %d %e %e\n",i,j,bn[1][11],bo[1][11]);
//    printf("boooooo i j %d %d %e %e\n",i,j,bn[2][11],bo[2][11]);
//    printf("boooooo i j %d %d %e %e\n",i,j,bn[3][11],bo[3][11]);

            for(j=0; j< *m1;j++) {
                  bn[*nxmax -2][j] = bn[*nxmax -3][j] ;
                  bn[*nxmax -1][j] = bn[*nxmax -2][j] ;
                  bn[*nxmax][j] = bn[*nxmax -1][j] ;
                  bn[*nxmax+1][j] = bn[*nxmax][j] ;
//                  bo[*nxmax -2][j] = bn[*nxmax -3][j] ;
//                  bo[*nxmax -1][j] = bn[*nxmax -2][j] ;
//                  bo[*nxmax][j] = bn[*nxmax -1][j] ;
```

```
                }
                for(j=0; j< *m2;j++) {
                     cn[*nxmax -2][j] = cn[*nxmax -3][j] ;
                     cn[*nxmax -1][j] = cn[*nxmax -2][j] ;
                     cn[*nxmax][j] = cn[*nxmax -1][j] ;
                     cn[*nxmax+1][j] = cn[*nxmax][j] ;
//                     co[*nxmax -2][j] = cn[*nxmax -3][j] ;
//                     co[*nxmax -1][j] = cn[*nxmax -2][j] ;
//                     co[*nxmax][j] = cn[*nxmax -1][j] ;
                }

}
```

B.3 mcotac1d

Main algorithm calling the mentioned routines or subprograms. Partly shown.

```
c   assign concentration at time t to particles
c   1. nuber of particles in each grid cell
c      write (*,*) npmax, nbox,xmin,xmax
       call partid(npmax, nbox,xmin,xmax,partib,dx,partx)
c      write(*,*)'partid hinter'

c   2. "concentrations of species" assigned to particles
       call concver(npmax,nbox,dx,bn,cn,partib,partx,partic,ismooth
     * ,m1,m2)

c       write(*,*)'conver'

       do 1329 ib=1,npmax
       partxo(ib)=partx(ib)

c      do 1329 ic =1,35
c      write(*,'(a6,1x,2i8,3(1x,e10.4))')'conver',ib,ic,partic(ib,ic),
c     * partx(ib),party(ib)
 1329 continue
c
c  ************************************************************
c  calculate new values of conc. and temp. as functions of time
c  ************************************************************
c
c   move particles during dt
c      write (*,*) 'walk time:  treal texe', treal, texe
       call walk2(npmax,nxmax,ncyc,along,aquer,dm,texe,dx,vx
     *  ,partx,partxo, xmaxr,xminr,partic,bn,cn,partib,
     *  ibpstart,x,bo,co,m1,m2)

c**assign concentrations at t+dt to grid  (including boundary conditions)
c**particle in which nbox

c      write (*,*)'xminr xmaxr',xminr,xmaxr
c      write(*,'(6(e10.4,1x))')(bn(i,1),i=1,m1)
c      write(*,'(6(e10.4,1x))')(bn(i,2),i=1,m1)
c      write(*,'(6(e10.4,1x))')(bn(i,3),i=1,m1)
c      write(*,'(6(e10.4,1x))')(bn(i,11),i=1,m1)
c       pause
c**new concentration in each box
       call concneu(npmax,nbox,nxmax,xminr,xmaxr,dx,bn,cn
     * ,partib,partx,partxo,partic,bo,co,por,ismooth,m1,m2)
c>>>>>02-2003 modified boundary on the right side
c      if(imodbound.gt.0)then
       do 1328, nspezx=1,nxmax+1
ccc       if (nspezx.ge.45)then

        do 1428 mm=1,m1
```